12-20-2023

A Dynamic Duo: Investigating the Interactions between Xanthomonas citri pv. malvacearum and Pseudomonas syringae

Taylor Harris
Washington University in St. Louis

WASHINGTON UNIVERSITY IN ST. LOUIS

Division of Biology and Biomedical Sciences
Plant and Microbial Biosciences

Dissertation Examination Committee:
Rebecca Bart, Chair
Barbara Kunkel
Blake Meyers
Rachel Penczykowski
Christina Stallings

A Dynamic Duo: Investigating the Interactions between *Xanthomonas citri* pv. *malvacearum* and *Pseudomonas syringae*

by
Taylor M. Harris

A dissertation presented to
Washington University in St. Louis
in partial fulfillment of the
requirements for the degree
of Doctor of Philosophy

December 2023
St. Louis, Missouri

Table of Contents

List of Figures ..... **iv**
List of Tables ..... **v**
Acknowledgements ..... **vi**
Abstract of the Dissertation ..... **viii**
Chapter 1: Introduction **1**
1.1 A potential disease complex in cotton 1
1.2 Xanthomonas and Pseudomonas, two household names in plant-microbe interactions 2
1.3 An overview of plant-pathogen interactions 4
1.4 Bacteria-bacteria interactions 6
1.5 Chapter summary, significant, and scope 8
1.6 References 9
Chapter 2: *Pseudomonas syringae* strains isolated from cotton, migrate towards *Xanthomonas* strains in vitro and this response is negatively regulated by iron **13**
2.1 Abstract 13
2.2 Importance 14
2.3 Introduction 14
2.4 Results 17
2.4.1 Xcm prompts movement in Ps183 but not Ps236 17
2.4.2 Flagella and Type-4 pili are not necessary for Ps183 movement response to Xcm 19
2.4.3 Transcriptome analysis of Ps183-Xcm interaction 22
2.4.4 Iron negatively regulates Ps183 movement towards Xcm 25
2.5 Discussion 27
2.6 Methods 31
2.6.1 **Bacterial strains and culture conditions** 31
2.6.2 **Motility Assays** 31
2.6.3 De novo reference genome assemblies 31
2.6.4 Transmission electron microscopy 32
2.6.5 RNA extraction and sequencing 32
2.6.6 Read mapping and differential gene expression analysis 33
2.6.7 Bacterial mutant generation 34
2.7 Acknowledgments 34
2.8 References 34
Chapter 3: Assessment of Xcm and Ps in cotton and in the laboratory 38
3.1 Abstract 38
3.2 Introduction 38
3.3 Results 41
3.3.1 Generating Ps mutants 41
3.3.1.a Transformation efficiency of Ps 41

3.3.1b Using Tn5 in Ps 42
3.3.2 *Xanthomonas-Pseudomonas in vitro* interactions 43
3.3.2a Crude extracts from Xcm do not prompt movement in Ps 43
3.3.2b Cooperative biofilm formation is not a mode of interaction between Xcm and Ps....44
3.3.3 *Xanthomonas-Pseudomonas in planta* interactions....44
3.3.3a Xcm induced HR in cotton prevent Ps spreading necrosis....45
3.3.3b Fluorescent strains of Xcm and Ps can be visualized in cotton....46
3.4 Discussion....49
3.5 Materials and methods....51
3.5.1 Bacterial strains and culture conditions....51
3.5.2 Plant growth conditions and inoculations....51
3.5.3 Biofilm assays 52
3.5.4 Crude extractions....52
3.5.5 Microscopy 53
3.5.6 Calculating transformation efficiency 53
3.5.7 Transposon mutagenesis....54
3.6 References 55
Chapter 4: Contemporary look at CBB and its pathogens....57
4.1 Abstract....57
4.2 Introduction 58
4.3 Results 59
4.3.1 Xanthomonas resistance in RILs 59
4.3.2 Pseudomonas resistance in RILs 60
4.4 Discussion....61
4.5 Materials and methods....63
4.5.1 Strains used....63
4.5.2 Screening RILs and Diversity Panel....63
4.5.3 Infiltrating cotton diversity panel and RILs 63
4.5.4 Phenotyping 64
4.6 References 64
Chapter 5: Discussion and Future Directions....66
5.1 Introduction 66
5.2 Investigating disease complexes in plants 67
5.3 Volatile signaling between bacteria....69
5.4 The future of cotton bacterial blight resistance 72
5.5 Conclusion of the thesis....73
5.6 References 74

List of Figures

Figure 1.1: Xcm and P. syringae symptoms in cotton 2
Figure 1.2: Different viewpoints to consider in multi-pathogen infections in plants 7
Figure 2.1: Ps moves towards Xcm 18
Figure 2.2: Flagella is not necessary for Ps movement response to Xcm 20
Figure 2.3: RNA-seq experimental setup and principal component analysis 21
Figure 2.4: Expression patterns of genes related to motility, iron and alginate synthesis in Ps183 when exposed to Xcm 23
Figure 2.5: Iron affects *Pseudomonas* movement 26
Figure 3.1: Ps480 does not respond to Xcm supernatant extracts or cell-washes 43
Figure 3.2: Ps480 and Xcm do not produce biofilm together 45
Figure 3.3: Xcm-induced resistance response to cotton prevent Ps disease 47
Figure 3.4: Ps480 and Xcm can form mixed microcolonies in cotton leaves 48
Figure 4.1: Working model for Ps and Xcm interact in a disease complex 72
Figure S2.1: Cotton isolates Ps183 and Ps480 migrate toward Xcm, while cotton isolates Ps236 and model strain DC3000 do not 77
Figure S2.2: Ps183 flagella mutant confirmation and motility 78
Figure S2.3: Ps183 Type-4 pili mutant confirmation and motility assay 79
Figure S2.4: Xcm principal component analysis and upregulated genes when exposed to Ps183 80
Figure S2.5: Additional iron tests 81
Figure S3.1: Nanopore EZ-Tn5 <R6Kyori/KAN-2> insertion sequencing alignment with Ps480 genome 91
Figure S3.2: EZ-Tn5 <R6Kyori/KAN-2> alignment with Ps480 23S sequence 92
Figure S3.3: Symptoms of Ps480-mCitrine and Xcm-cyan 92

List of Tables

Table S2.1: Strains used in this study 82
Table S2.2: Genome assembly statistics of *P. syringae* cotton pathogens 82
Table S2.3: Ps183 day 3 upregulated differentially expressed genes 84
Table S2.4: Ps236 day 3 upregulated differentially expressed genes 87
Table S2.5: Xcm differentially expressed genes with annotations 88
Table S2.6: Ps183 GO enrichment analysis results 89
Table S2.7: Ps236 GO enrichment analysis results 90
Table S3.1: List of strains used in this study 93
Table S3.2: Transformation efficiency of Ps480 94
Table S3.3: BLAST results of mini-Tn5 insertion mutants 94
Table S3.4: BLAST results of EZ-Tn5 <R6Kyori/KAN-2> insertion mutants in Ps480 genome 95

Acknowledgements

Thank you to all my lab mates, committee members, family, and friends for helping me bring this thesis to life. I appreciate my thesis advisor, Dr. Becky Bart, for supporting me throughout this project and helping me learn to give myself grace when learning new things. I'm thankful to all my lab mates and committee members for their generosity in time, feedback, and support in developing my project, planning experiments, presenting, and having an all-around fun time both outside and at work. I am forever thankful for my family for being my cheerleaders. They've continued to be positive beacons of light during this journey and for that I'm extremely grateful. I want to thank my best friend, Terisha, for being so loving and for aways being a listening ear. I am so grateful for my loving husband, Winston, for his unwavering support and for falling asleep every time I practiced my lab meeting presentations. He witnessed my evolution first-hand and there is no telling how I would have completed this work without his commitment to our relationship and for pushing me to believe in myself. Finally, I want to thank my spirit team for the countless sleepless nights and persistent urges to explore myself and my place in this world. I heard their call and answering it catapulted me into an endless abyss of self-realization that has since then, opened my eyes and helped me gain tremendous clarity. Everyone mentioned here has helped me along a very intense, transformative period of my life that was packaged within a Ph.D. Without you all, I would not have achieved this or even recognize my place in this world. Thank you!

Sincerely, Taylor M. Harris

Washington University in St. Louis

December 2023

Dedicated to my family and those on a life-long journey of learning.

ABSTRACT OF THE DISSERTATION

A dynamic Duo: Investigating the interactions between *Xanthomonas citri* pv. *malvacearum* and *Pseudomonas syringae*

For Arts & Sciences Graduate Students

by

Taylor M. Harris

Doctor of Philosophy in Biology and Biomedical Sciences

Plant and Microbial Biosciences

Washington University in St. Louis, 2023

Professor Rebecca Bart, Chair

Bacterial pathogens threaten crop production worldwide, which highlights the need to understand plant and pathogen interactions. Studies on plant-pathogen interactions typically focus on a single host and pathogen. However, bacteria exist in complex microbial communities, not alone. There are few studies that examine the mechanisms behind multi-pathogen infections which renders a gap in our understanding of the subsequent implications on agriculture. In this dissertation, I use *in vitro* plate assays with RNA-sequencing and *in planta* assays to investigate the interactions between two cotton bacterial pathogens, *Xanthomonas citri* pv. *malvaearum* (Xcm) and *Pseudomonas syringae* (Ps). *In vitro* plate assays demonstrate that the bacteria can interact outside their host and that Xcm can prompt directional movement in Ps. RNA-sequencing along with studying genetic mutants revealed that iron-sensing in Ps plays a role in this interaction, and that the movement is independent of typical movement appendages, flagella and Type-4 pili. For *in planta* interactions, sequential infiltrations and microscopy suggest that both bacteria can

colocalize in cotton and that a cotton defense response, once initiated by Xcm first, is effective against Ps. I also explore the presence of genetic resistance to either pathogen in cotton by screening a diversity panel of 253 accessions. This screen revealed that cotton lacks resistance to Ps. Sixty-one accessions showed strong resistance responses to Xcm. This work expands our broad understanding of how bacteria can interact and, more specifically, the interaction dynamics between Ps and Xcm and the potential implications in cotton.

Chapter 1: Introduction

1.1 A potential disease complex in cotton

Cotton bacterial blight (CBB) is a detrimental disease of cotton caused by the bacterial pathogen *Xanthomonas citri* pv. *malvacearum* (Xcm). For the past several decades, the disease had not been an issue because farmers grew cotton varieties with strong genetic resistance; however, CBB reemerged between 2011-2016 in the US because farmers switched to growing susceptible varieties (Anne Z. Phillips et al. 2017). After discovering this and informing farmers, resistant varieties were once again prioritized, but there were still multiple reports of foliar disease in resistant cotton varieties. Bacteria isolations from these diseased cotton samples yielded two species, Xcm and *Pseudomonas syringae* (Ps). Afterwards, Ps was co-isolated with Xcm multiple times from CBB-resistant cotton (A. Z. Phillips et al. 2018). In the laboratory, Ps causes severe spreading necrosis in the leaves of both Xcm -resistant and -susceptible cotton when inoculated alone or with Xcm (Fig 1.1). The observations that *P. syringae* could cause disease alone, at least in a lab setting, but was always co-isolated with Xcm from diseased fields, led to the hypothesis that, in the field, the bacteria form a disease complex where they collaborate to block cotton resistance and cause disease.

As the evolutionary arms race between plants and their bacterial pathogens persists, it would be advantageous to explore how bacteria influence each other and their subsequent implications in plant diseases. To explore the hypothesis that Xcm and *P. syringae* form a disease complex, I investigated how *P. syringae* and Xcm interact with each other separately.

In this dissertation, I focus on

1) identifying the interaction mechanisms between *P. syringae* and Xcm *in vitro*, with some exploration on their *in planta* behavior;

2) screening cotton for resistance to Xcm and *P. syringae*

This work informs our basic understanding of how two prominent and environmentally relevant bacteria interact and their potential implications in cotton.

1.2 *Xanthomonas* and *Pseudomonas*, two household names in plant-microbe interactions

Xanthomonas and *Pseudomonas* are two major groups of phytopathogenic bacteria. Here I highlight well-established traits of both genera. Though they are similar, some traits vary and can help us understand ways they may collaborate.

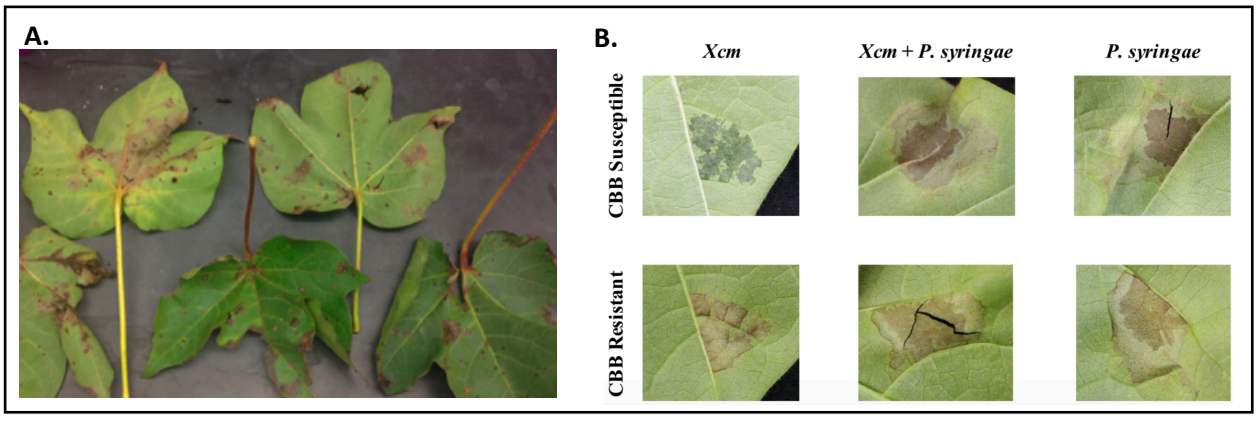

Fig 1.1: Xcm and *P. syringae* symptoms in cotton. A) Samples of diseased CBB-resistant cotton. Samples were sent to the Bart lab from Terry Wheeler. Image was taken by Anne Phillips. B) Symptoms from Xcm, *P. syringae* isolate Ps480, and both in susceptible (top) and resistant (bottom) cotton. Top left: watersoaking; bottom left: hypersensitive response; Ps480 spreading necrosis symptom middle and right columns. Image from Phillips et al. 2018.

Xanthomonas

The genus *Xanthomonas* is one of the most environmentally and agriculturally relevant bacteria and infects over 400 different types of plants, including important crops like cassava, wheat, rice, and many others (Ryan et al. 2011). These gram-negative bacteria are aerobic, contain single polar flagellum, and are typically yellow-pigmented (Jalloul et al. 2015; He, Cao, and Poplawsky 2020). The optimal growth temperature for *Xanthomonas* is 25-30°C (He, Cao, and Poplawsky 2020). Host range and tissue specificity varies based on pathovar. For example, the rice pathogen *Xanthomonas oryzae* pv. *oryzicola* infects leaf parenchyma cells, while *Xanthomonas oryzae* pv. *oryzae* infects parenchyma cells and the vascular system (Jacques et al. 2016). *Xanthomonas citri* pv. *malvacearum*, or Xcm, is the causal agent of bacterial blight and is a systemic pathogen, capable of infecting both parenchyma tissues and vasculature of cotton. Its symptoms include cotton boll rot, black arm, and water-soaking (Innes 1983). Twenty-two races are known to infect cotton, and race 18 is the most common infectious strain in the US (Delannoy et al. 2005).

Pseudomonas

Pseudomonas syringae is a commonly studied species regarding host-microbe interactions, with over 50 pathovars infecting important crops. This gram-negative bacterium is rod-shaped, with polar flagella. *P. syringae* pv. *tomato* DC3000, the causal agent of bacterial speck in tomato, is the model organism for understanding host-microbe interactions because it is a pathogen of the model plant *Arabidopsis thaliana*. In nature, Pseudomonads are seed borne and like other bacteria, spread by wind and rainfall (Lamichhane, Messéan, and Morris 2015). Disease symptoms occur at cooler temperatures ranging from 13-25°C (Preston 2000). Pseudomonads typically cause

localized symptoms in parenchyma tissues, causing foliar symptoms like leaf spots, blight, speck, and wilting (Lamichhane, Messéan, and Morris 2015).

Several disease outbreaks caused by *P. syringae* have occurred in recent years. In the early 2010's *P. syringae* pv. *actinidiae* re-emerged causing severe kiwifruit canker in New Zealand and Europe (O'Brien, Thakur, and Guttman 2011). In 2016, *P. syringae* was isolated from diseased raspberry and blackberry fields in Serbia (Ivanović et al. 2023). As mentioned earlier, *P. syringae* also re-emerged in cotton fields of Texas in 2016 (Anne Z. Phillips et al. 2017). In this case, *P. syringae* was co-isolated with Xcm, the causal agent of cotton bacterial blight. *Pseudomonas* was first reported in cotton in the 60's by Texas A&M (Lewis 1960). Though different strains have been isolated infrequently from cotton since 1996, there are no bona-fide *P. syringae* pathovars that infect cotton exclusively.

1.3 An overview of plant-pathogen interactions

During the phytopathogenic bacterial infection cycle, bacteria transition from living on plant surfaces such as leaves (epiphytic stage) to the inside of the plant through natural openings and wounds (Leben 1974). Cell-to-cell communication between bacteria helps facilitate infection. For example, quorum sensing (QS) (explained in section 1.4) plays an important role in bacteria persistence on leaf surfaces and virulence (Loh et al. 2002; Von Bodman, Bauer, and Coplin 2003). Xanthomonads have QS-like systems where structurally variant diffusible signaling factors, which are derivatives of *cis*-2-unsaturated fatty acids, control traits important for virulence like prevention of stomatal closing, biofilm formation, as well as extracellular polysaccharide and extracellular enzyme production (Gudesblat, Torres, and Vojnov 2009; Torres et al. 2007; Vojnov et al. 2001). Motility is also a virulence trait important for disease progression. Loss of motility

genes related to flagella and Type-4 pili in some phytopathogenic bacteria lessens virulence (Dunger et al. 2014; Ichinose, Taguchi, and Mukaihara 2013; Pfeilmeier, Caly, and Malone 2016).

Once inside the host, during the endophytic stage, pathogens deliver virulence molecules known as effectors to overcome initial immune responses from the host. Effector proteins are injected into host cells by the bacterial Type-3-secretion system (T3SS), an important virulence factor in most Gram-negative phytopathogenic bacteria, including *Pseudomonas spp*. and *Xanthomonas spp*. (Alfano and Collmer 1997). The T3SS is encoded by the *hrp*/*hrc* gene cluster and loss of genes involved in its assembly and function lessens pathogen virulence (Ichinose, Taguchi, and Mukaihara 2013; Büttner and Bonas 2010). Both *Xanthomonas spp*. and *Pseudomonas spp*. carry effectors. Some Xanthomonads have distinct effector proteins known as transcription-activator like (TAL) effectors that can upregulate host susceptibility genes to promote virulence (Cox et al. 2017; Anne Z. Phillips et al. 2017; Timilsina et al. 2020). Pseudomonads also harbor specific Type-3 effectors that have various enzymatic functions that are often redundant (Block and Alfano 2011; Bundalovic-Torma et al. 2022).

Plants have a two-layered innate immune system for detection and defense against pathogens: Pattern Triggered Immunity (PTI) and Effector-Triggered Immunity (ETI) (Dodds and Rathjen 2010; J. D. G. Jones and Dangl 2006). During PTI, conserved molecular patterns of microbes like bacterial flagella are recognized by pattern recognition receptors, which activates defense gene expression and other well-studied events such as oxidative burst, and deposition of callose and lignin into the plant cell wall. Successful pathogens can overcome PTI through secreted effector proteins that block this initial immune response. To overcome this method of virulence, however, plants have evolved resistance genes, or R genes, capable of recognizing specific effectors or their actions within plant cells (J. D. G. Jones and Dangl 2006). Effector recognition

leads to ETI, which results in a hypersensitive response (HR), a localized cell death capable of keeping pathogens from spreading beyond the infection sites.

1.4 Bacteria-bacteria interactions

There are several reports of plant infection by multiple pathogens, however the interaction mechanisms among the infecting microbes are not fully understood (Buonaurio et al. 2015; Dandve et al. 2019; Mahuku et al. 2015; Tran et al. 2014; Le May et al. 2009). The disease complex investigated in olive knot it one example of multi-bacterial infection. *P. savastanoi* pv. *savastanoi* causes olive knot. Its co-inoculation with non-pathogens *Erwinia toletana*, *Pantoaea agglaomeran*, and *Erwinia oleae*, which all cohabit in the olive knots, results in larger knots and better colonization (Buonaurio et al. 2015).

Investigating coinfections in plants can be complex and difficult because there are multiple viewpoints to consider: 1) interaction between pathogen A and the host; 2) interactions between pathogen B and the host; and 3) interaction between pathogen A and B (Fig. 1.2). While it's only part of the entire picture, understanding how bacteria interact with each other, separate from their environment or host, can provide us clues for how they may influence each other in nature. Interactions within microbial communities can lead to various outcomes: antagonism, where microbes benefit at the expense of other microbes and behave competitively for nutritional resources; coexistence, where the presence of other organisms does not impact the microbe of interest; and synergism, where microbes are mutualistic and each benefit from the polymicrobial environment (Abdullah et al. 2017). Some bacteria can interact within and between species through direct contact with nearby cells or by communicating with signals such as volatile organic compounds or diffusible molecules. Communication in this way can lead to changes in gene

expression, growth, antibiotic resistance, motility, and biofilm production. (Westhoff, van Wezel, and Rozen 2017; Konovalova and Søgaard-Andersen 2011).

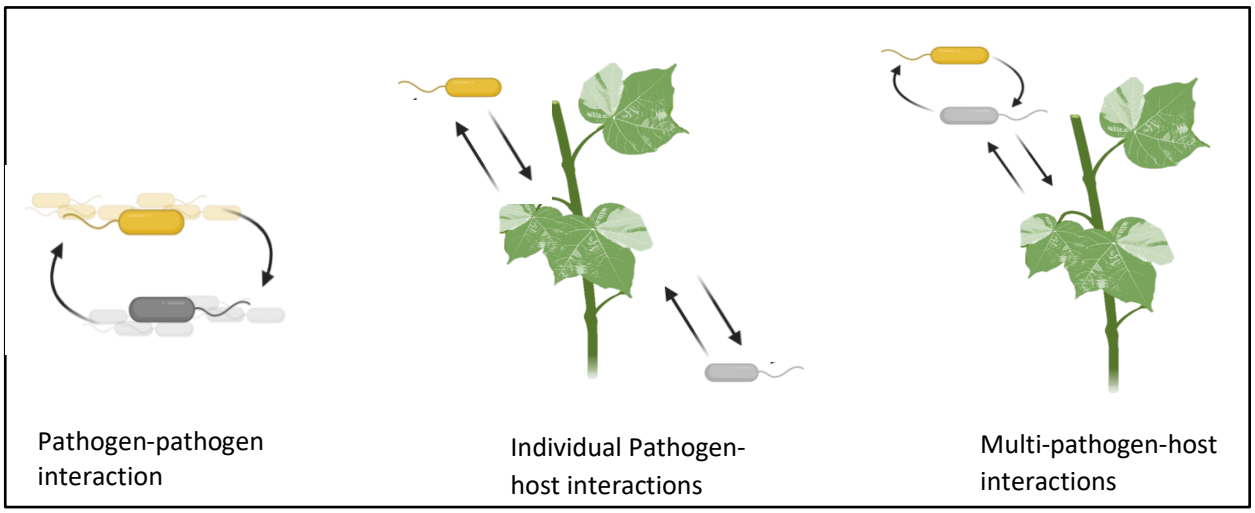

Fig 1.2: Different viewpoints to consider in multi-pathogen infections in plants. Left: Interactions can exist between pathogens directly. Middle: Interactions may exist between the host and individual pathogens. Right: Interactions may exist among all pathogens and the host.

It is well-established that bacteria can interact through direct cell-to-cell contact. These close-knit interactions can be facilitated by specialized secretion systems that connect one cell to another. For example, the Type-4 secretion system (which is distinguished from the Type-4 pilus that helps bacteria move) allows for exchange of DNA from one cell to another. Additionally, some Gram-negative bacteria utilize the type-6 secretion system in antagonistic interactions to target and kill other competing bacteria (Cianfanelli, Monlezun, and Coulthurst 2016). Antibiotics also play a role in antagonistic interactions. For example, *Vibrio cholera* increases its swimming speed, turning rate, and run lengths while moving away from *Vibrio* species SWAT3, a producer of the antibiotic andrimid (Graff et al. 2013).

Quorum sensing is an example of communication where bacteria emit a signaling molecule to assess cell density and collectively respond once the signal has reached a certain concentration

(Fuqua, Winans, and Greenberg 1994). As mentioned earlier, Xanthomonads produce QS-like signals called diffusible signaling factors. DSF signals have also been found to participate in interspecies and cross- kingdom cell-cell communication (Wang et al. 2004; Ryan et al. 2011). Bacteria release chemically diverse volatile compounds that can have effects on the producers and receivers even from a distance. For example, when cocultured separately, the volatiles 2,3-butanedione and glyoxylic acid produced by *Bacillus subtilis* influence *Escherichia coli* antibiotic- and motility-related gene expression (Kim, Lee, and Ryu 2013). In this case, both species were cultured in two compartment plates for 24 hours and microarray analysis was used to monitor *E. coli* gene expression changes. In another report, *Streptomyces venezuelae* explorer cells can produce volatile trimethylamine, which decreases growth of *Bacillus subtilis* and *M. luteus*. Trimethylamine caused an increase in the environment pH, which in turn reduced available iron and affected growth of the nearby bacteria (S. E. Jones et al. 2019). In all, these examples demonstrate that bacteria can participate in both intra- and interspecies interactions in various ways.

1.5 Chapter summary, significance, and scope

Pathogens and pests threaten agriculture production globally. Crop losses due to diseases are large, ranging from 10-40% (Savary et al. 2019). With this, understanding pathogen virulence and their interactions with plants is extremely important for disease prevention strategies. To date, most plant-pathogen interaction studies focus on a single host and a single pathogen. In nature, however, the onset of disease can be complicated, as disease development relies on the host, the environment, and the microbial community as a whole. Concrete mechanisms behind multi-pathogen infections have not been studied extensively. Thus, studying the occurrence of multi-

pathogen systems can further our understanding of pathogen interactions and the subsequent implications on agriculture.

Xcm and Ps cotton isolates provide a biologically relevant pathosystem to study multi-species interactions. Here, I examine the interactions between the two pathogens exclusively and their interactions in their plant host, and I investigate whether resistance to Ps exists in cotton. I explore the interactions between both pathogens in chapters 2 and 3. I first approached this by examining how Ps and Xcm behave when infected in cotton at different time points and by monitoring their localization in cotton. I examined their *in vitro* interactions by studying their behaviors in different plate assays, and by using RNA-sequencing to monitor their gene expression changes when cocultured. In chapter 4, I discuss the development of the screening method used to examine whether cotton has resistance to Ps. This research provides a glimpse into how Ps and Xcm interact in cotton and deepens our understanding on how the two can impact each other's behavior, both phenotypically and transcriptionally. This expands our understanding of multi-pathogen infection mechanisms more broadly and can inform how we approach disease prevention strategies.

1.6 References

Abdullah, Araz S., Caroline S. Moffat, Francisco J. Lopez-Ruiz, Mark R. Gibberd, John Hamblin, and Ayalsew Zerihun. 2017. "Host–Multi-Pathogen Warfare: Pathogen Interactions in Co-Infected Plants." *Frontiers in Plant Science* 8. https://doi.org/10.3389/fpls.2017.01806.

Alfano, J. R., and A. Collmer. 1997. "The Type III (Hrp) Secretion Pathway of Plant Pathogenic Bacteria: Trafficking Harpins, Avr Proteins, and Death." *Journal of Bacteriology* 179 (18): 5655–62.

Block, Anna, and James R. Alfano. 2011. "Plant Targets for Pseudomonas Syringae Type III Effectors: Virulence Targets or Guarded Decoys?" *Current Opinion in Microbiology* 14 (1): 39–46.

Bundalovic-Torma, Cedoljub, Fabien Lonjon, Darrell Desveaux, and David S. Guttman. 2022. "Diversity, Evolution, and Function of Pseudomonas Syringae Effectoromes." *Annual Review of Phytopathology* 60 (August): 211–36.

Buonaurio, Roberto, Chiaraluce Moretti, Daniel Passos da Silva, Chiara Cortese, Cayo Ramos, and Vittorio Venturi. 2015. "The Olive Knot Disease as a Model to Study the Role of Interspecies Bacterial Communities in Plant Disease." *Frontiers in Plant Science* 6 (June): 434.

Büttner, Daniela, and Ulla Bonas. 2010. "Regulation and Secretion of Xanthomonas Virulence Factors." *FEMS Microbiology Reviews* 34 (2): 107–33.

Cianfanelli, Francesca R., Laura Monlezun, and Sarah J. Coulthurst. 2016. "Aim, Load, Fire: The Type VI Secretion System, a Bacterial Nanoweapon." *Trends in Microbiology* 24 (1): 51–62.

Cox, Kevin L., Fanhong Meng, Katherine E. Wilkins, Fangjun Li, Ping Wang, Nicholas J. Booher, Sara C. D. Carpenter, et al. 2017. "TAL Effector Driven Induction of a SWEET Gene Confers Susceptibility to Bacterial Blight of Cotton." *Nature Communications* 8 (May): 15588.

Dandve, Minal S., Sopan Ganpatrao Wagh, Prachi R. Bhagat, Kiran Pawar, Sarika A. Timake, Abhijeet A. Daspute, and Manoj Baliram Pohare. 2019. "Bacterial and Fungal Pathogen Synergetics after Co-Infection in the Wheat (Triticum Aestivum L.)." *Biotechnology Journal International* 23 (4): 1–9.

Delannoy, E., B. R. Lyon, P. Marmey, A. Jalloul, J. F. Daniel, J. L. Montillet, M. Essenberg, and M. Nicole. 2005. "Resistance of Cotton towards Xanthomonas Campestris Pv. Malvacearum." *Annual Review of Phytopathology* 43: 63–82.

Dodds, Peter N., and John P. Rathjen. 2010. "Plant Immunity: Towards an Integrated View of Plant–Pathogen Interactions." *Nature Reviews. Genetics* 11 (8): 539–48.

Dunger, German, Cristiane R. Guzzo, Maxuel O. Andrade, Jeffrey B. Jones, and Chuck S. Farah. 2014. "Xanthomonas Citri Subsp. Citri Type-4 Pilus Is Required for Twitching Motility, Biofilm Development, and Adherence." *Molecular Plant-Microbe Interactions: MPMI* 27 (10): 1132–47.

Fuqua, W. C., S. C. Winans, and E. P. Greenberg. 1994. "Quorum Sensing in Bacteria: The LuxR-LuxI Family of Cell Density-Responsive Transcriptional Regulators." *Journal of Bacteriology* 176 (2): 269–75.

Graff, Jason R., Stephanie R. Forschner-Dancause, Susanne Menden-Deuer, Richard A. Long, and David C. Rowley. 2013. "Vibrio Cholerae Exploits Sub-Lethal Concentrations of a Competitor-Produced Antibiotic to Avoid Toxic Interactions." *Frontiers in Microbiology* 4 (January): 8.

Gudesblat, Gustavo E., Pablo S. Torres, and Adrián A. Vojnov. 2009. "Xanthomonas Campestris Overcomes Arabidopsis Stomatal Innate Immunity through a DSF Cell-to-Cell Signal-Regulated Virulence Factor." *Plant Physiology* 149 (2): 1017–27.

He, Ya-Wen, Xue-Qiang Cao, and Alan R. Poplawsky. 2020. "Chemical Structure, Biological Roles, Biosynthesis and Regulation of the Yellow Xanthomonadin Pigments in the Phytopathogenic Genus Xanthomonas." *Molecular Plant-Microbe Interactions: MPMI* 33 (5): 705–14.

Ichinose, Yuki, Fumiko Taguchi, and Takafumi Mukaihara. 2013. "Pathogenicity and Virulence Factors of Pseudomonas Syringae." *Journal of General Plant Pathology: JGPP* 79 (5): 285–96.

Innes, N. L. 1983. “Bacterial Blight of Cotton.” *Biol. Rev*. 58: 157–76.
Ivanović, Milan, Anđelka Prokić, Katarina Gašić, Jelena Menković, Nemanja Kuzmanović, Nevena Zlatković, and Aleksa Obradović. 2023. “Characterization of Pseudomonas Syringae Strains Associated with Shoot Blight of Raspberry and Blackberry in Serbia.” *Plant Disease* 107 (3): 826–33.
Jacques, Marie-Agnès, Matthieu Arlat, Alice Boulanger, Tristan Boureau, Sébastien Carrère, Sophie Cesbron, Nicolas W. G. Chen, et al. 2016. “Using Ecology, Physiology, and Genomics to Understand Host Specificity in Xanthomonas.” *Annual Review of Phytopathology* 54 (August): 163–87.
Jalloul, Aïda, Majd Sayegh, Antony Champion, and Michel Nicole. 2015. “Bacterial Blight of Cotton.” *Phytopathologia Mediterranea* 54 (1): 3–20.
Jones, Jonathan D. G., and Jeffery L. Dangl. 2006. “The Plant Immune System.” *Nature* 444 (7117): 323–29.
Jones, Stephanie E., Christine A. Pham, Matthew P. Zambri, Joseph McKillip, Erin E. Carlson, and Marie A. Elliot. 2019. “Streptomyces Volatile Compounds Influence Exploration and Microbial Community Dynamics by Altering Iron Availability.” *MBio* 10 (2). https://doi.org/10.1128/mBio.00171-19.
Kim, Kwang-Sun, Soohyun Lee, and Choong-Min Ryu. 2013. “Interspecific Bacterial Sensing through Airborne Signals Modulates Locomotion and Drug Resistance.” *Nature Communications* 4: 1809.
Konovalova, Anna, and Lotte Søgaard-Andersen. 2011. “Close Encounters: Contact-Dependent Interactions in Bacteria.” *Molecular Microbiology*. Wiley.
Lamichhane, Jay Ram, Antoine Messéan, and Cindy E. Morris. 2015. “Insights into Epidemiology and Control of Diseases of Annual Plants Caused by the Pseudomonas Syringae Species Complex.” *Journal of General Plant Pathology: JGPP* 81 (5): 331–50.
Le May, Christophe, Gael Potage, Didier Andrivon, Bernard Tivoli, and Yannick Outreman. 2009. “Plant Disease Complex: Antagonism and Synergism between Pathogens of the Ascochyta Blight Complex on Pea.” *Phytopathologische Zeitschrift. Journal of Phytopathology* 157 (11–12): 715–21.
Leben, Curt. 1974. *Survival of Plant Pathogenic Bacteria*. Ohio Agricultural Research and Development Center.
Lewis, R. D. 1960. “Pseudomonas Wilt of Cotton.”
Loh, John, Elizabeth A. Pierson, Leland S. Pierson 3rd, Gary Stacey, and Arun Chatterjee. 2002. “Quorum Sensing in Plant-Associated Bacteria.” *Current Opinion in Plant Biology* 5 (4): 285–90.
Mahuku, George, Benham E. Lockhart, Bramwel Wanjala, Mark W. Jones, Janet Njeri Kimunye, Lucy R. Stewart, Bryan J. Cassone, et al. 2015. “Maize Lethal Necrosis (MLN), an Emerging Threat to Maize-Based Food Security in Sub-Saharan Africa.” *Phytopathology* 105 (7): 956–65.
O’Brien, Heath E., Shalabh Thakur, and David S. Guttman. 2011. “Evolution of Plant Pathogenesis in Pseudomonas Syringae: A Genomics Perspective.” *Annual Review of Phytopathology* 49: 269–89.
Pfeilmeier, Sebastian, Delphine L. Caly, and Jacob G. Malone. 2016. “Bacterial Pathogenesis of Plants: Future Challenges from a Microbial Perspective: Challenges in Bacterial Molecular Plant Pathology.” *Molecular Plant Pathology* 17 (8): 1298–1313.

Phillips, A. Z., T. Wheeler, J. Woodward, and R. S. Bart. 2018. "Pseudomonas Syringae Pathogen Causes Foliar Disease of Upland Cotton in Texas." *Plant Disease* 102 (6): 1171–1171.

Phillips, Anne Z., Jeffrey C. Berry, Mark C. Wilson, Anupama Vijayaraghavan, Jillian Burke, J. Imani Bunn, Tom W. Allen, Terry Wheeler, and Rebecca S. Bart. 2017. "Genomics-Enabled Analysis of the Emergent Disease Cotton Bacterial Blight." *PLoS Genetics* 13 (9): e1007003.

Preston, G. M. 2000. "Pseudomonas Syringae Pv. Tomato: The Right Pathogen, of the Right Plant, at the Right Time." *Molecular Plant Pathology* 1 (5): 263–75.

Ryan, Robert P., Frank-Jörg Vorhölter, Neha Potnis, Jeffrey B. Jones, Marie-Anne Van Sluys, Adam J. Bogdanove, and J. Maxwell Dow. 2011. "Pathogenomics of Xanthomonas: Understanding Bacterium–Plant Interactions." *Nature Reviews. Microbiology* 9 (5): 344–55.

Savary, Serge, Laetitia Willocquet, Sarah Jane Pethybridge, Paul Esker, Neil McRoberts, and Andy Nelson. 2019. "The Global Burden of Pathogens and Pests on Major Food Crops." *Nature Ecology & Evolution* 3 (3): 430–39.

Timilsina, Sujan, Neha Potnis, Eric A. Newberry, Prabha Liyanapathiranage, Fernanda Iruegas-Bocardo, Frank F. White, Erica M. Goss, and Jeffrey B. Jones. 2020. "Xanthomonas Diversity, Virulence and Plant–Pathogen Interactions." *Nature Reviews. Microbiology* 18 (8): 415–27.

Torres, Pablo S., Florencia Malamud, Luciano A. Rigano, Daniela M. Russo, María Rosa Marano, Atilio P. Castagnaro, Angeles Zorreguieta, Kamal Bouarab, John Maxwell Dow, and Adrián A. Vojnov. 2007. "Controlled Synthesis of the DSF Cell-Cell Signal Is Required for Biofilm Formation and Virulence in Xanthomonas Campestris." *Environmental Microbiology* 9 (8): 2101–9.

Tran, Hieu Sy, Yu Pin Li, Ming Pei You, Tanveer N. Khan, Ian Pritchard, and Martin J. Barbetti. 2014. "Temporal and Spatial Changes in the Pea Black Spot Disease Complex in Western Australia." *Plant Disease* 98 (6): 790–96.

Vojnov, A. A., H. Slater, M. J. Daniels, and J. M. Dow. 2001. "Expression of the Gum Operon Directing Xanthan Biosynthesis in Xanthomonas Campestris and Its Regulation in Planta." *Molecular Plant-Microbe Interactions: MPMI* 14 (6): 768–74.

Von Bodman, Susanne B., W. Dietz Bauer, and David L. Coplin. 2003. "Quorum Sensing in Plant-Pathogenic Bacteria." *Annual Review of Phytopathology* 41 (April): 455–82.

Wang, Lian-Hui, Yawen He, Yunfeng Gao, Ji En Wu, Yi-Hu Dong, Chaozu He, Su Xing Wang, et al. 2004. "A Bacterial Cell-Cell Communication Signal with Cross-Kingdom Structural Analogues." *Molecular Microbiology* 51 (3): 903–12.

Westhoff, Sanne, Gilles P. van Wezel, and Daniel E. Rozen. 2017. "Distance-Dependent Danger Responses in Bacteria." *Current Opinion in Microbiology* 36 (April): 95–101.

Chapter 2: *Pseudomonas syringae* strains isolated from cotton migrate towards *Xanthomonas* strains in vitro and this response is negatively regulated by iron.

2.1 Abstract

Plant-pathogens cause significant crop losses. Most previous research has considered a single pathogen instead of the more intricate dynamics that might occur if multiple pathogens coexist. Two bacterial pathogens, *Xanthomonas citri* pv. *malvacearum* (Xcm) and *Pseudomonas syringae* (Ps), were co-isolated multiple times from Texas cotton fields. Here, we investigated the interactions between these bacteria *in vitro*. Soft agar assays revealed that specific strains of Ps exhibit a unique motility phenotype that we define as 'directional spread'. Specifically, Ps spreads towards Xcm, likely sensing an Xcm-derived volatile. RNA-sequencing was used to monitor gene expression in Ps and Xcm when grown in isolation or together. We find that Ps responds transcriptionally to the presence of Xcm. In Ps, motility-related genes were downregulated during spread. Further, flagella or Type-4 pilus mutants still display directional spread towards Xcm, demonstrating that these appendages are dispensable for the phenotype. Several iron related genes were upregulated during directional spread. Adding ferrozine, an iron chelator, to the soft agar media induced non-directional spread in Ps in the absence of Xcm. Conversely, addition of $FeSO_4$ to the soft agar plates inhibited the Ps directional spread toward Xcm. This work demonstrates that two co-occurring bacterial pathogens of cotton sense and respond to each other and reveals a link to iron perception. Whether the interaction reflects simple competition for limited resources or

more nuanced dynamics in planta, is yet to be revealed. This work opens the doors for additional investigations into multi-pathogen dynamics during disease.

2.2 Importance

Traditionally, research on host-pathogen interactions has focused on a single pathogen. However multiple pathogens can infect a host simultaneously. Here, we report on the interactions between two bacterial pathogens of cotton, *Xanthomonas citri* pv. *malvacearum* and *Pseudomonas syringae*. We find that both bacteria sense the presence of the other, prompting directional spread of *Pseudomonas* towards *Xanthomonas*. The movement behavior in *Pseudomonas* is connected to the presence of iron in the environment. Understanding interactions among multiple co-occurring pathogens may prove critical for effective disease management strategies.

2.3 Introduction

Plant-pathogen interactions play a significant role in shaping the health and productivity of agricultural crops. Traditionally, research on these interactions has focused on understanding the dynamics between a single pathogen and its plant host. However, in natural environments, pathogens are embedded within a complex microbiome that can affect disease outcomes (Stone, Weingarten, and Jackson 2018; Leveau 2019). Similarly, multiple pathogens may, in theory, co-occur and affect one another. For example, many plant viral pathogens exist as disease complexes (Mansoor et al. 2003; Hull 1996). Similarly, interactions between some nematodes and fungi have been described as mutually beneficial (Bergeson 1972; Back, Haydock, and Jenkinson 2002).

More generally, the prevalence of multiple pathogen co-infections and implications on disease is less well understood.

Previous examples of bacterial co-infections are particularly scarce within the plant pathology field. Yet, it is well established that bacteria employ various mechanisms to facilitate intra- and interspecies interactions. These include production of volatile organic compounds (VOCs) and other signaling molecules that lead to important outcomes such as quorum sensing, biofilm production, and changes in motility (Fuqua, Winans, and Greenberg 1994; Schauder and Bassler 2001; Straight and Kolter 2009; Schmidt et al. 2015). While investigations into bacterial pathogen co-infections are lacking, a few previous reports on bacterial interactions more generally provide clues into the types of interactions that may occur between co-occurring pathogens. For example, two common bacteria, *P. aeruginosa* and *Agrobacterium tumefaciens*, were shown to coexist in biofilm communities, with *A. tumefaciens* able to persist for long periods of time even though *P. aeruginosa* quickly dominated the community (An et al. 2006). Induced changes in movement appear to be a common theme in interspecies bacterial interactions. When cocultured separately within two-compartment petri dishes, volatiles produced by *Bacillus subtilis* were found to influence *Escherichia coli* gene expression and induce movement (Kim, Lee, and Ryu 2013). Similarly, *P. fluorescens* Pf0-1 and *Pedobacter* sp. strain V48 exhibited coordinated movement when cocultured on hard surfaces, despite their lack of motility individually (McCully et al. 2019). The plant pathogen *X. perforans* was observed hitchhiking with *Paenibacillus vortex* on hard surfaces *in vitro* and on the surface of tomato leaves (Hagai et al. 2014). Here again, an airborne signal from *X. perforans* was implicated in inducing motility in *P. vortex.* Taken together, these previous studies demonstrate various modes of interspecies bacterial interactions and highlight changes in movement phenotypes as a particularly common outcome.

Swarming, swimming, twitching, sliding, and gliding are all forms of bacteria movement that can be vital for establishment and survival in certain environments (Kearns 2010; Harshey 2003; Wadhwa and Berg 2022). Swarming and swimming both require flagella, which are rotating appendages that propel cells in a certain direction. These two movements are distinguished by the location of movement; Swarming occurs on the surface while swimming occurs within media. Experimentally, flagella-mediated movements can be distinguished using specific agar concentrations: swimming occurs in low agar concentration (<0.3%), while swarming occurs when cultures are grown on moderate concentrations (0.3-1%) (Kearns 2010). Twitching motility occurs at the surface and is mediated by Type-4 pili which extends and retracts, pulling cells forward (Craig, Forest, and Maier 2019). Bacterial movement is also possible without the aid of flagella or pili. For example, gliding motility requires adhesins on the cell surface that move across the length of the bacterium, pulling it forward, like the tread on a tire (Wadhwa and Berg 2022). Sliding motility is a passive movement that occurs when cells multiply causing pressure to move outward from the origin point (Kearns 2010). Types of bacterial motility that do not strictly fall into these defined buckets have also been described but are not well understood (Wadhwa and Berg 2022).

Two bacterial pathogens, *Xanthomonas citri* pv. *malvacearum* (Xcm) and *Pseudomonas syringae* (Ps), were identified in diseased cotton fields in Texas (Phillips et al. 2018). Xcm is a known pathogen of cotton, responsible for cotton bacterial blight (CBB), and able to cause severe losses in susceptible cultivars (Hillocks 1992). Ps is not considered a major pathogen of cotton. Mysteriously, in at least some cases, Xcm and Ps were co-isolated from cotton cultivars known to be resistant to Xcm. Isolation of each strain and re-inoculation into CBB- resistant cotton varieties confirmed that in isolation, Xcm triggered a resistance response and Ps produced necrotic disease symptoms (Phillips et al. 2018). This consistent co-isolation led to the hypothesis that Ps and Xcm

may interact to the benefit of at least one of the organisms. As a first step towards investigating this hypothesis, we characterized bacterial-bacterial interactions through *in vitro* plate assays. We report that Ps moves towards Xcm and this movement is likely triggered by an Xcm-derived volatile. RNA-seq revealed that motility-related genes like flagella were downregulated in Ps, when exposed to Xcm. Flagella or pili mutants maintained the directional spread towards Xcm. The RNAseq data revealed that genes related to iron storage were highly induced in the presence of Xcm. Addition of iron to the *in vitro* plate assay negatively regulated the movement response in Ps while addition of an iron chelator induced Ps motility even in the absence of Xcm. In summary, this work establishes a direct interaction between two bacterial pathogens of cotton that often co-occur in cotton fields and reveals a role for iron in this interaction.

2.4 Results

2.4.1 Xcm prompts movement in Ps183 but not Ps236

We previously isolated several strains of Ps from diseased cotton leaves (Fig. S2.1, Table S2.1) (Phillips et al. 2018). As a starting point to explore potential interspecies bacterial interactions, we tested Ps strains in an *in vitro* system with Xcm. Ps and Xcm were spotted approximately 1 cm apart on soft agar (0.4%) and monitored over the course of 5 days (Fig 2.1A, Fig. S2.1). Two strains, Ps183 and Ps480, both migrated in the direction of Xcm. In contrast, Ps236, which was also isolated from diseased cotton leaves, did not migrate towards Xcm. The model strain of *P. s.* pv. *syringae* DC3000 did not display the movement phenotype (Fig. S2.1). However, diverse isolates of *Xanthomonas* did induce movement in the newly isolated strains of Ps (Fig. S2.1). To further understand this striking phenotype, we focused on a single strain of Xcm (Xcm Fm2007-

GLT) and two Ps strains, Ps183 which migrates towards Xcm and Ps236 which does not. Previous examples of bacterial-induced movement have been linked to volatiles (Schmidt et al. 2015; Kim,

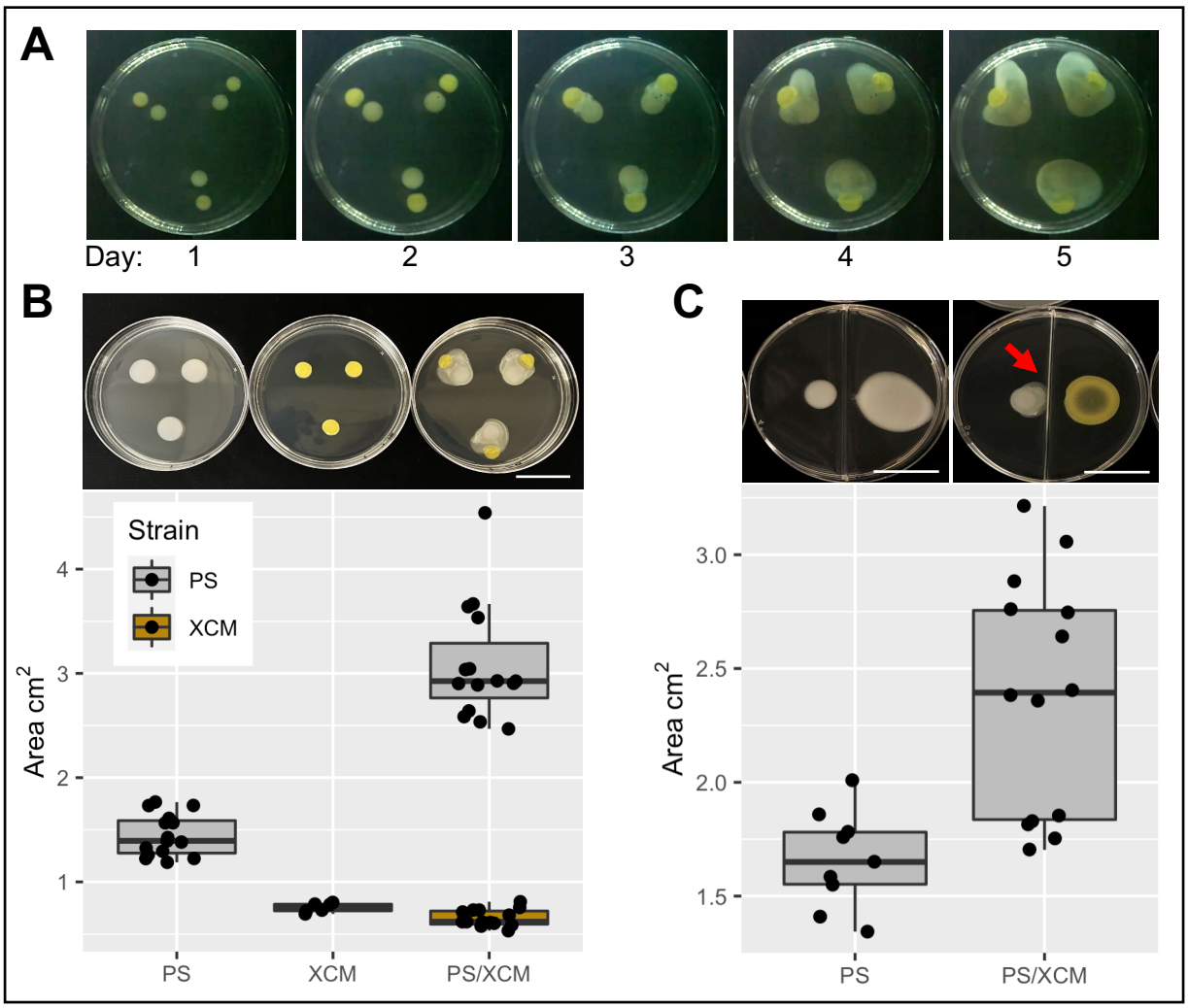

Fig 2.1. Ps moves towards Xcm. (A) Xcm and Ps183 were spotted (5μl of OD600 = 0.1) 1cm apart on NYGA soft agar (0.4%) plates, 3 replicates per plate, with Ps towards the center of the plate and Xcm on the outside. Plates were imaged every hour for 5 days using a raspberry pi micro computer and attached camera. Representative photos from each day are shown. **(B)** Ps and Xcm when grown in isolation or together and spot size at day 5 was calculated (cm^2). In the presence of Xcm, Ps spread was significantly greater than when Ps was grown in isolation ([T-Test] p-value = 1.70E-11). **(C)** I-plates were used to create a physical barrier in the media while allowing air exchange. On the left of each plate, 5μl of Ps was spotted as in A and B. On the right side of the plate, 100μl of Ps or Xcm was spotted. Red arrow shows area of directional spread. Images and area measurements were done at day 5, as in B. In the presence of Xcm, the Ps spot size was significantly larger than when Ps was grown in isolation ([T-Test] p-value = 0.0007). In all assays, area was determined from at least 3 replicates of at least two separate experiments. Each replicate represents one colony spot measurement. 3cm scale.

Lee, and Ryu 2013). Thus, we hypothesized that Xcm may produce a volatile that is sensed by

Ps183. As previously described (Kim, Lee, and Ryu 2013), I-plate assays were used to separate both bacteria and their phenotypes were monitored. The I-plates contain a plastic partition that serves as a physical barrier in the agar medium, while still allowing gas exchange throughout the plate. Xcm and Ps183 were drop-inoculated separately on either side of the plate and co-cultured up to 5 days. In the I-plate assay, the movement phenotype was less obvious. However, when the amount of Xcm was increased 20-fold, clear directional movement was observed in Ps183 when plated opposite of Xcm (Fig. 2.1C), suggesting that signaling occurs through a volatile.

2.4.2 Flagella and Type-4 pili are not necessary for Ps183 movement response to Xcm

The flagellum has been established as an important motility factor under specific culture conditions (0.4% agar), thus it was hypothesized that flagella function is necessary for Ps183 movement response. To address this, *flagella hook-associated protein 1* (*flgK)* mutants were generated (Fig S2.2). Approximately 500bp flanking regions located up and downstream of the *flgK* coding sequence were amplified using polymerase chain reaction (PCR) and cloned into a suicide vector with SacBR counter selection. Ex-conjugates were obtained, and PCR was used to confirm that the *flgK* coding sequence had been removed. Surprisingly, the Ps183Δ*flgK* mutant maintained the directional spread phenotype when plated next to Xcm, spreading even more than the Ps183 WT strain (Fig. 2.2). However, we note that a difference in motility between Ps183 WT and the Ps183Δ*flgK* mutant was also not observed. This assay was conducted at 30°C and previous reports indicate that flagellar-mediate movement is suppressed at higher temperatures (Hockett, Burch, and Lindow 2013). Thus, we tested Ps183 WT and the Ps183Δ*flgK* mutant on soft agar at

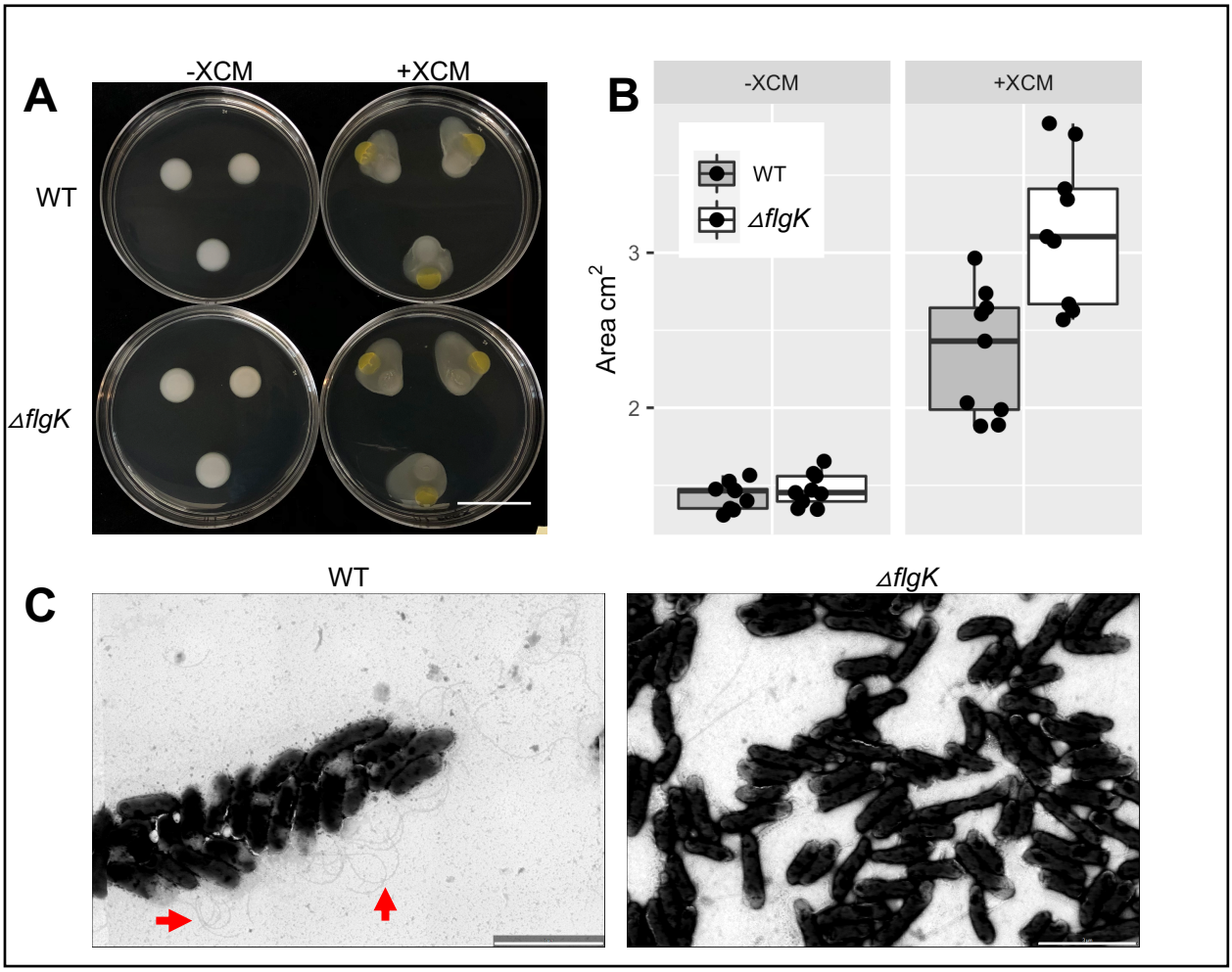

Fig 2.2. Flagella is not necessary for Ps movement response to Xcm. A) Ps183 wildtype (WT), Ps183 flagella mutant (*ΔflgK*), and Xcm were spotted (5μl of OD600 = 0.1) 1cm apart on NYGA soft agar (0.4%) plates, 3 replicates per plate, with Ps strains towards the center of the plate and Xcm on the outside. Top: Wildtype alone (left) and with Xcm (right). Bottom: *ΔflgK* alone (left) and with Xcm (right). B) Area measurement of Ps183 WT and *ΔflgK*. In the presence of Xcm, both WT (T-Test p-value = 7.53E-06) and *ΔflgK* (T-Test p-value = 1.62E-08) spread was significantly greater than when grown in isolation. *ΔflgK* and WT areas were similar when exposed to Xcm (T-Test p-value 0.0015). Spot size (cm^2) was calculated on day 5. Measurements were determined from 9 replicates from three separate experiments. Each replicate represents one colony spot measurement. 3cm scale. C) Transmission electron microscopy images of 2% phosphotungstic acid negatively stained Ps183 WT (left) and *ΔflgK* (right) cultured for 5 days at 30°C. Red arrows point toward flagella. 3μm scale.

25°C and at that temperature observed a clear motility defect in the Ps183Δ*flgK* mutant (Fig. S2.2). Ps183 WT and the Ps183D*flgK* mutant were viewed using negative staining and transmission electron microscopy (TEM). Flagella were clearly visible on the wildtype cells at 30°C, indicating that temperature blocks motility, not assembly of the appendage. TEM showed that the wildtype

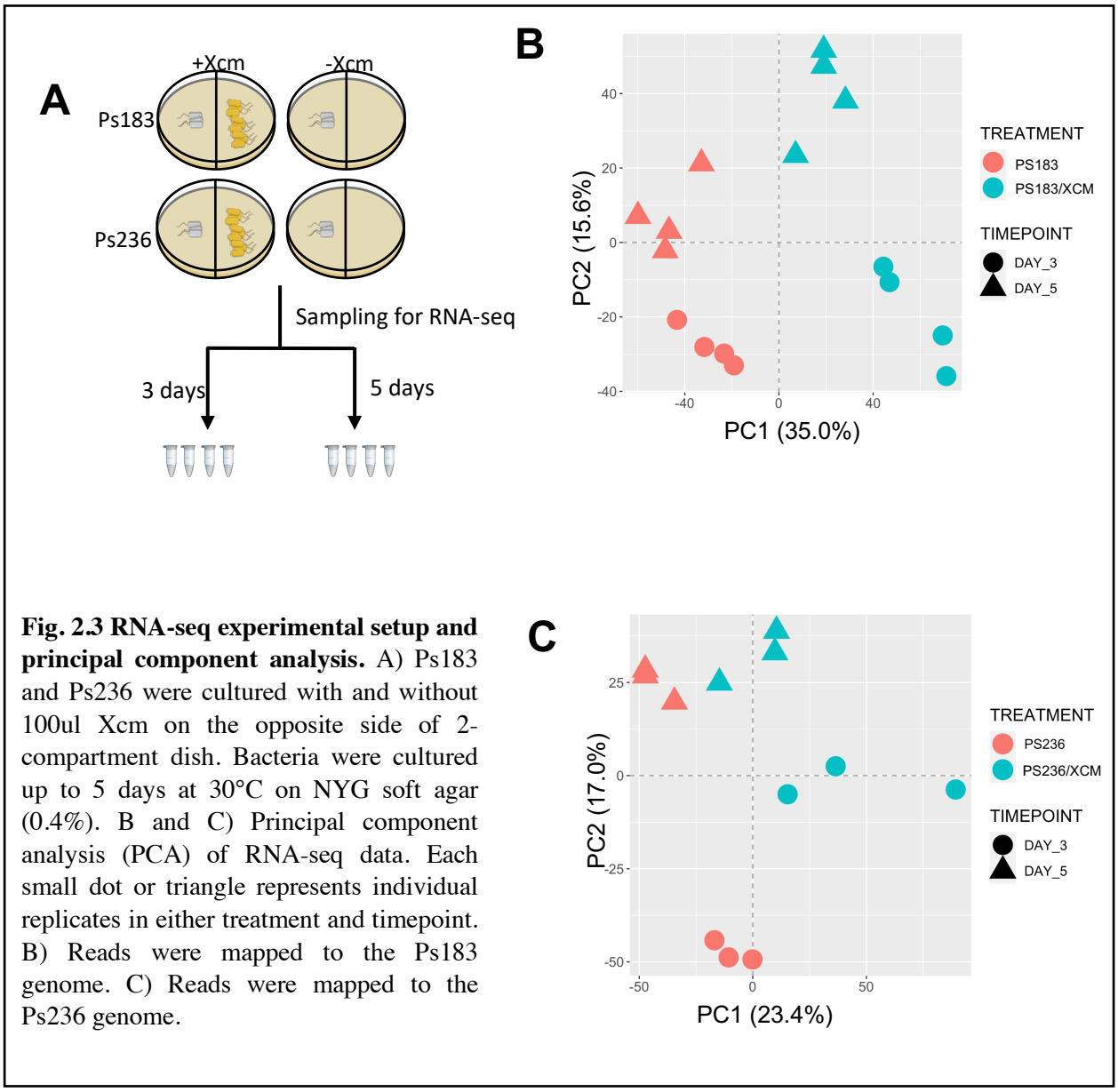

Fig. 2.3 RNA-seq experimental setup and principal component analysis. A) Ps183 and Ps236 were cultured with and without 100ul Xcm on the opposite side of 2-compartment dish. Bacteria were cultured up to 5 days at 30°C on NYG soft agar (0.4%). B and C) Principal component analysis (PCA) of RNA-seq data. Each small dot or triangle represents individual replicates in either treatment and timepoint. B) Reads were mapped to the Ps183 genome. C) Reads were mapped to the Ps236 genome.

cells were more aggregated, forming clumps within the sample, compared to the Ps183Δ*flgK* mutant cells which were relatively dispersed (Fig 2.2C). These observations suggest that at 30°C, flagella present in the wildtype cells are associated with bacterial aggregation. This may inhibit spread in the absence of Xcm, though additional work would be required to investigate this hypothesis. In addition to flagella, many bacteria use Type-4 pili to move (Craig, Forest, and Maier 2019). However, we found that a Ps183Δ*pilBCD* mutant responded similarly to wildtype Ps183

when plated next to Xcm, suggesting that the Type-4 pilus is not necessary for the movement phenotype (Fig. S2.3).

2.4.3 Transcriptome analysis of Ps183-Xcm interaction

Since neither flagella nor Type-4 pili were required for the Ps directional spread phenotype, we adopted a transcriptomics approach to shed light on the molecular mechanism that governs the Ps183 and Xcm interaction. This experiment was designed to reveal gene expression changes in Ps183 and Xcm before movement occurred (day 3) and during movement (day 5) (Fig 2.3A). Ps236 was included as a control as it does not exhibit the motility response to Xcm (Fig S2.1). I-plates were used to separate the bacteria on either side of a petri dish. Xcm and Ps183 or Ps236 were drop-inoculated separately on opposite sides of the plate and co-cultured for up to 5 days. Ps183 and Ps236 cells were collected directly off the plates and RNA was extracted, followed by library preparation and sequencing. Reference genomes were constructed for Ps183 and Ps236 using a combination of Nanopore and Illumina sequencing reads and annotated using Prokka (Table S2.2). A principal component analysis (PCA) was performed on the *Pseudomonas* data and confirmed that replicates clustered together (Fig 2.3B, C). For Ps183, replicates clustered by treatment and time point. Ps183 alone versus Ps183 with Xcm showed clear separation across PC1. Samples also clustered by day across PC2. These results suggest Ps183 gene expression is altered between time points and that there is a transcriptional response when Xcm is present. Replicate samples for Ps236 also displayed clear clustering but were less well separated based on the presence or absence of Xcm. The transcriptome of Xcm was also profiled and PCA suggests that Xcm responds transcriptionally to the presence of Ps (Fig. S2.4). In all, these data demonstrate that

Ps183 and Ps236 both respond transcriptionally to Xcm, with the strongest response occurring at day 3 and between Ps183 and Xcm.

To further explore the specific transcriptional impacts of coculturing Ps with Xcm, differentially expressed genes (DEGs) (FDR adjusted $p < 0.05$; log2 fold change > 1) were identified (Tables S2.3, S2.4, S2.5). Consistent with the PCA analysis, the most DEGs (n = 431) were observed in Ps183, when exposed to Xcm, at day 3. Of these, 144 were upregulated in response to Xcm. At day 5, we observed 219 DEGs, 134 of which were upregulated. In Ps236, at day 3, we observed only 131 DEGs when exposed to Xcm and of these, 61 were upregulated. At day 5, in Ps236 there were 83 DEGs, 42 of which were upregulated. Examining the DEGs in Xcm,

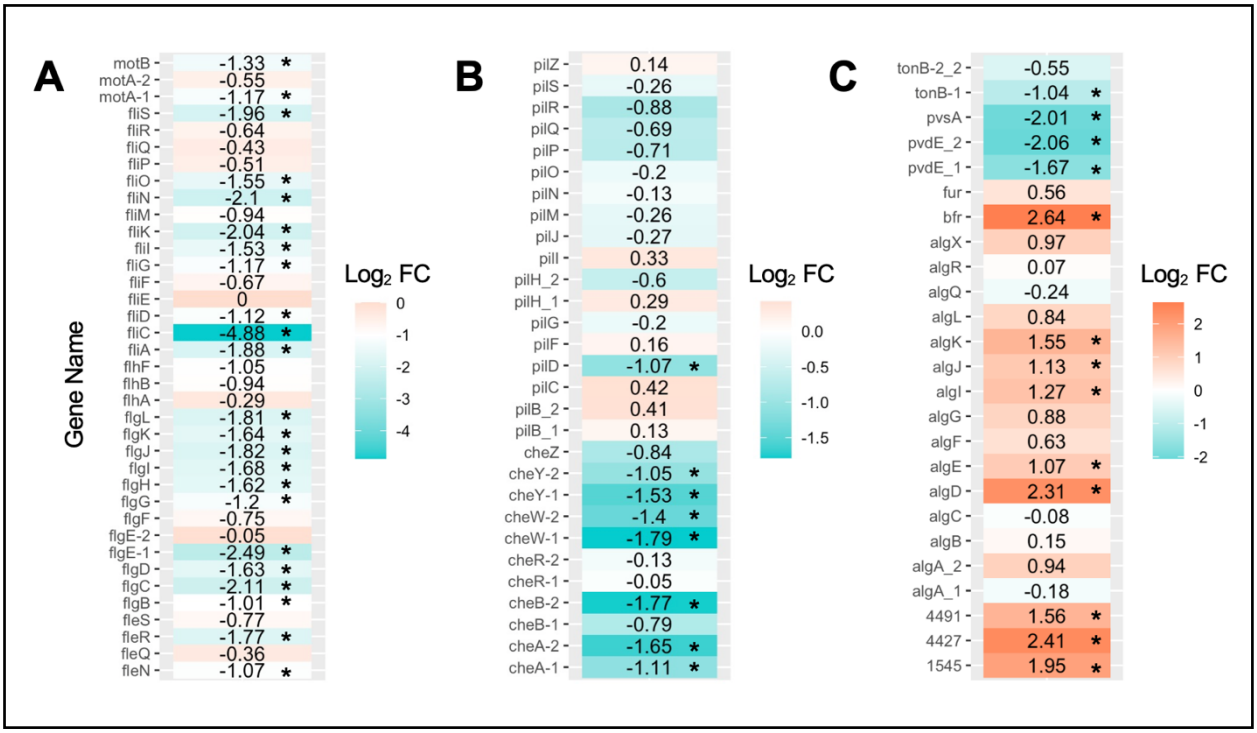

Fig. 2.4 Expression patterns of genes related to motility, iron and alginate synthesis in Ps183 when exposed to Xcm. A) Heatmap showing the differential expression of flagella-related genes in *Pseudomonas*. B) Heatmap showing the expression of Type-4 pili and chemotaxis related genes. C) Heatmap showing differential expression profiles of genes related to iron and alginate synthesis. 4491 and 4427 genes BLAST results matched bacterioferritin and 1545 gene BLAST matched ferritin-like domain containing protein. Values represent the average RPKM (reads per kilobase per million reads mapped) of four replicates. Asterisks indicate significant differential expression (FDR adjusted p-value < 0.05 and $\log_2$ fold change ≥≤ 1).

we found 46 differentially expressed genes, most of which were annotated as "hypothetical proteins." The biological importance of this transcriptional response is not yet clear; therefore, we deprioritized the Xcm dataset and focused our analysis on Ps183 at day 3.

Gene expression differences were explored using Gene Ontology (GO) enrichment analysis. When comparing Ps183 with and without coculturing with Xcm, we found that 'Cellular carbohydrate metabolic process' and 'iron ion transport' were among the upregulated GO terms while 'bacterial-type flagellum-dependent cell motility', 'chemotaxis' and 'iron ion transport' were among the downregulated GO terms (Table S2.6). Similar to Ps183, GO enrichment analysis for Ps236 revealed 'chemotaxis' and 'bacterial-type flagellum-dependent cellular process' were downregulated GO terms, however 'iron ion transport' and 'cellular carbohydrate metabolic process' were not present (Table S2.7).

Given the surprising result that flagella and Type-4 pilus mutants maintain the movement phenotype and that motility related GO terms were downregulated, we took a closer look at the expression of genes related to these appendages. Consistent with the data presented above, genes related to flagella, pili and chemotaxis were either downregulated or not differentially expressed in Ps183 at day 3 after exposure to Xcm (Fig 2.4A, B). However, many genes related to iron were upregulated in Ps183 at day 3 after exposure to Xcm (Fig 2.4C). Specifically, the siderophore pyoverdine synthesis genes, *pvsA* and *pvdE,* and the iron transport gene, *tonB* (Noinaj et al. 2010; Fujita et al. 2019; Poole et al. 1996)*,* were down regulated, suggesting negative regulation of iron acquisition and import. Conversely, the bacterioferritin gene, *bfr* (Rivera 2017), and several *bfr*-like genes (gene IDs 4491, 4427 and 1545) which function as iron-storage proteins, were upregulated. The observation that iron import genes were downregulated, and iron storage genes

were upregulated, is consistent with the 'iron ion transport' GO term being observed in both the up- and down- regulated lists from the GO term analysis.

In addition to genes related to iron, six alginate biosynthesis genes (Hay et al. 2013) were upregulated in response to Xcm (Fig. 2.4). Alginate has been linked to bacterial movement previously (Keith et al. 2003; Yu et al. 1999; Whitchurch, Alm, and Mattick 1996) so may contribute to the Xcm-induced Ps surface spread. In Ps236, which does not move in response to Ps, alginate biosynthesis genes were not upregulated, however, like Ps183, flagella-related genes were downregulated.

2.4.4 Iron negatively regulates Ps183 movement towards Xcm

Four copies of bacterioferritin or bacterioferritin-like genes were upregulated in Ps183 in response to Xcm. Bacterioferritins are iron-storage proteins that serve as iron-reservoirs in low-iron conditions and function to protect cells from iron-toxicity (Rivera 2017; Andrews 2010). To test if iron affects Ps183 movement, motility assays were performed on soft agar plates with varying concentrations of $FeSO_4$. These assays revealed that Ps183 motility was negatively correlated with iron concentration (Fig 2.5A, S2.5). Iron impact on Ps183 movement was further investigated by adding the iron-chelator ferrozine to nutrient-rich medium and measuring spread. Ps183 spread was greater in plates with higher concentrations of ferrozine (Fig 2.5B, S2.5), suggesting that reducing iron availability promotes movement in Ps183. These results demonstrate that iron negatively regulates Ps movement. To test whether the effect of iron on Ps183 movement would block the Xcm induced movement, we returned to the I-plate assays and compared Ps183 movement with and without iron ($FeSO_4$) supplemented media and/or Xcm. As expected, Ps183 movement was observed in low iron conditions when exposed to Xcm. When iron was added to

the media, the movement was blocked (Fig 2.5). We note that in this experiment the spreading

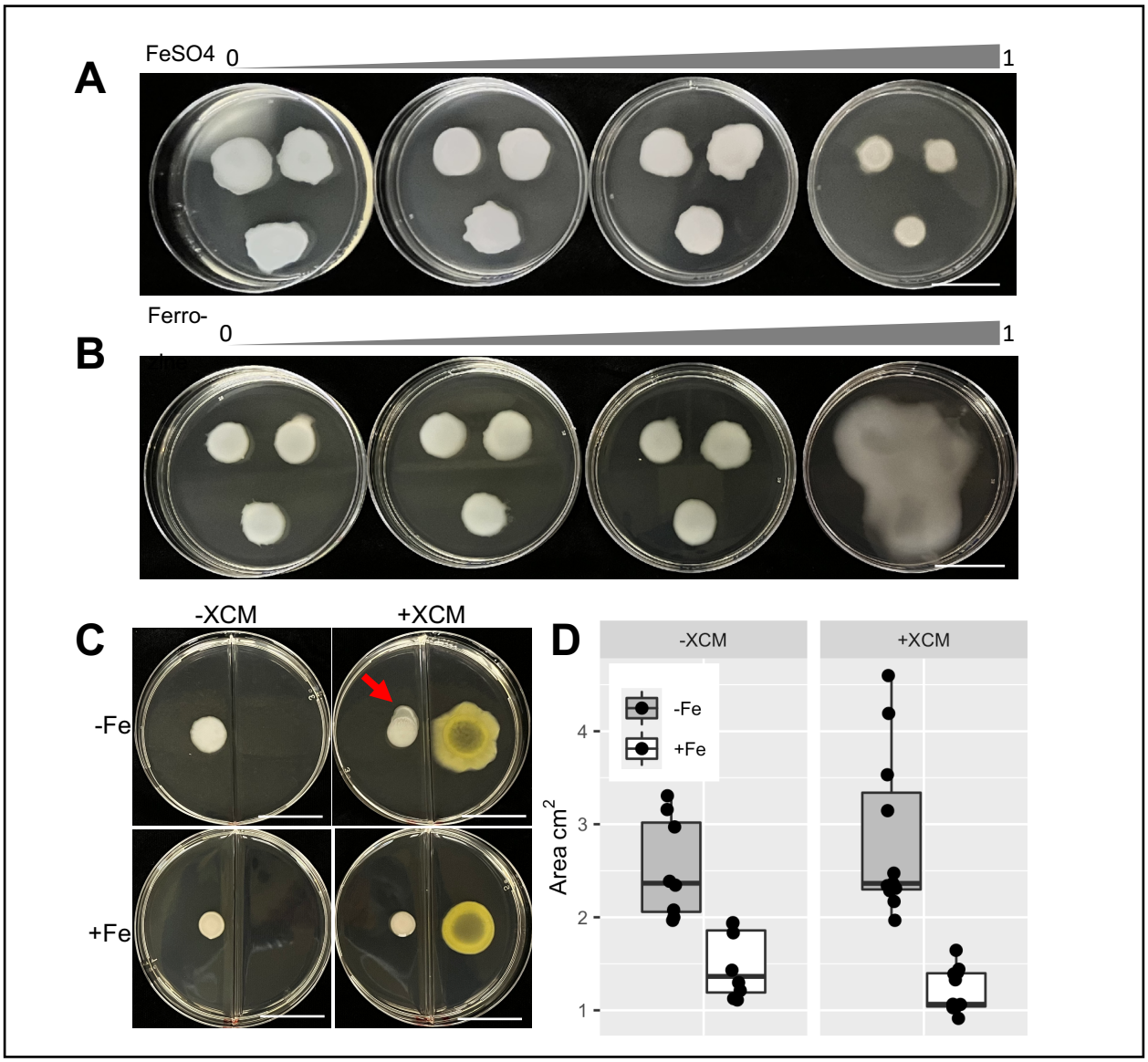

Fig 2.5. Iron affects *Pseudomonas* movement. A) Ps183 spread on iron deficient King's Broth agar (0.4%). From left to right: plates were supplemented with 0, 0.01, 0.1, 1 mM FeSO4. B) Ps183 spread on nutrient rich media (NYGA soft agar 0.4%) with addition of iron-chelator ferrozine. From left to right: 0, 0.01, 0.1, 1 mM ferrozine was added to the plates. C) Ps183 spread in response to Xcm with and without additional 0.6mM FeSO4. Ps183 (5μl of OD_{600} = 0.1) and Xcm (100μl of OD_{600} = 0.1) were spotted 1cm apart on NYGA soft agar (0.4%) plates. D) Area measurement of Ps183 +/- 0.6mM FeSO4 with and without Xcm. Without Xcm, Ps -Fe spread was greater than +Fe conditions (T-Test p-value = 0.0004); with Xcm Ps spread was greater in –Fe condition compared to +Fe (T-Test = 8.77E-06). In these experiments, a clear Ps movement phenotype was observed in –Fe conditions with Xcm (red arrow) but not in +Fe conditions. However, total area measurements did not always capture this phenotype (Ps with and without Xcm in –Fe condition (T-Test p-value = 0.3715) and in +Fe condition (T-Test p-value = 0.0625)). Spot size (cm^2) was calculated on day 5. Measurements were determined from at least 3 replicates from 2-3 separate experiments. Each replicate represents one colony spot measurement. 3cm scale.

phenotype was visually obvious but was not captured through area measurements, highlighting the limitation of our image analysis method of measuring the entire area of bacterial spread. In summary, these data demonstrate that iron negatively regulates the Xcm-induced movement in Ps183.

2.5 Discussion

In this study, the molecular interactions between *Pseudomonas syringae* (Ps) and *Xanthomonas citri* pv. *malvacearum* (Xcm) were investigated. While Xcm is a common cotton pathogen, Ps has rarely been reported as causing disease on cotton (Phillips et al. 2018). However, in 2016, Xcm and Ps were co-isolated from several diseased cotton fields, including varieties that are reported to be resistant to Xcm. This prompted the hypothesis that these two pathogens may interact. Initial work with the bacteria revealed a striking phenotype, *in vitro*. When plated together, Ps migrates towards Xcm; Characterization of this phenotype is the primary focus of this manuscript.

Based on previous reports of similar interaction phenotypes in other bacteria (Kim, Lee, and Ryu 2013; McCully et al. 2019; Hagai et al. 2014), we first tested whether an Xcm-induced volatile signal might trigger Ps movement. Indeed, I-plate assays revealed that Ps183 moves towards Xcm, even when the two bacteria are physically separated, allowing only air exchange suggesting that volatiles produced by Xcm mediate this movement. The identity of the hypothesized volatile is not yet known. *B. subtilis* and *E. coli* engage in a volatile-mediated interaction. In this case, 2,3-butanedione and glyoxylic acid modulate *E. coli* motility-related gene expression (Kim, Lee, and Ryu 2013). Metabolite profiling in *Xanthomonas citri* pv. *vesicatoria* 85-10 revealed several volatiles emitted by the bacteria, the majority being decan-2-one, undecan-

2-one, dodecan-2-one, and 10-methyl-undecan-2-one (Weise et al. 2012). The emission profiles varied based on growth media used, however some individual volatiles were found to either enhance or inhibit growth of fungus *Rhizoctonia solani*. Further testing of Xcm and Ps183 might involve metabolite profiling through gas chromatography, for instance, to better understand what volatile signals Xcm produces and which prompt Ps183 movement.

We initially assumed that the Xcm-induced movement in Ps183 was a form of swimming or swarming mediated by flagella or pili (Kearns 2010). However, flagella and pili mutants maintained the movement phenotype. These experiments were initially confusing in that neither wildtype nor the flagella mutant moved in soft agar assays. Previous reports suggest that flagella-based movement and gene expression is reduced at higher temperatures (Hockett, Burch, and Lindow 2013); Our assays were conducted at 30°C. When we repeated the motility assay at 25°C, a clear difference in movement was observed between wildtype Ps and the flagella mutant. These observations highlight that bacterial movement is a complex trait, involving multiple different mechanisms and influenced by environmental conditions such as temperature. We have performed these assays hundreds of times over the course of several years and can report confidently that Ps183 moves towards Xcm. However, the phenotype is highly variable and likely affected by environmental conditions other than just temperature. In some cases, clear directional spread was observed but only for a few millimeters; in other experiments, Ps183 quickly spread across the plate completely engulfing Xcm. The Ps and Xcm strains used in this study are 'wild' strains compared to strains such as Ps DC3000 that have been domesticated through laboratory use. The variability observed within these assays complicated the image analysis used to quantify spread. For example, in Figures 1 and 2, Image J was used to trace the area occupied by Ps and this area was quantified as a proxy for movement. In other assays, for example in Figure 5, directional

movement was observed but represented a relatively small percentage of the total spot area and therefore comparing area sizes across conditions did not appropriately capture the phenotype. Future studies might build upon the time course assay shown in Figure 1A to quantify the increase of area over time, instead of a single time point.

To further understand the movement phenotype, we employed RNA sequencing as a hypothesis generating activity into the molecular explanations for the Ps183-Xcm interaction. Consistent with the mutational analysis, genes related to flagella and pili were either downregulated or not differentially expressed in Ps183 after exposure to Xcm. Opposed to the swimming and swarming movement mediated by flagella and pili, sliding motility is a passive form of movement displayed by some bacteria where cells are pushed outward due to cellular division (Kearns 2010). We observed several genes related to alginate biosynthesis upregulated in Ps183 after exposure to Xcm. Alginate is a polysaccharide produced in Pseudomonads and has been reported to promote virulence *in planta*(Keith et al. 2003; Yu et al. 1999). It is possible that alginate production eases surface tension between the cells and the media surface and contributes to Ps183 movement. Collectively, our data suggest that Ps183 movement is likely a form of sliding, potentially involving alginate, though the exact genes governing this movement are yet to be identified.

Along with alginate biosynthesis genes, bacterioferritins were upregulated in response to Xcm, suggesting a role for iron and/or iron perception in the Ps-Xcm interaction. Iron is an essential nutrient for many cellular processes and, as such, in low iron conditions, may cause competition among bacteria (Gu et al. 2020; Raines et al. 2016). On the other hand, excess iron is toxic to cells because of the formation of Fenton reaction hydroxyl radicals (Touati 2000; Frawley and Fang 2014; Braun 1997; Andrews, Robinson, and Rodríguez-Quiñones 2003).

Bacterioferritins serve as iron-storage proteins and protect the cells from iron toxicity (Rivera 2017). We report that iron negatively regulates movement in Ps183 and conversely, adding the iron chelator ferrozine to the media induces Ps183 movement. However, iron-acquisition related genes were found to be downregulated in Ps183. It is possible that Ps183 initially senses Xcm as a competitor and so scavenges iron. Then at the time of sampling, three days after initial exposure to Xcm, intracellular iron concentration has increased to potentially toxic levels. In this case, bacterioferritin would be required to store excess iron and protect cells from iron toxicity and genes related to iron acquisition and import would be downregulated. Further study is needed to ascertain the full role of bacterioferritins in this phenotype. The observed gene expression changes in alginate biosynthesis and iron related genes may be part of a connected mechanism. In a previous case, alginate production was found to increase under iron-limiting conditions in *P. aeruginosa* (Wiens et al. 2014).

The final aspect of this paper interrogated the intersection of iron and Xcm on Ps movement. We observed that iron suppressed the Xcm-induced movement phenotype in Ps183. It is possible that the Xcm-Ps interaction directly relates to iron. For example, Ps may sense the presence of Xcm as a competitor and rapidly move to scavenge available iron. However, in this case, the *directional* movement phenotype is perplexing as iron is likely to be found in all directions. Alternatively, the movement phenotype may indirectly relate to iron. In other words, Ps may sense Xcm and move in its direction, for an unknown reason, and trigger an iron related pathway to achieve this outcome. In this latter explanation, it is tempting to return to potential interactions *in planta*. For example, Ps may derive benefit from co-localization with Xcm in a cotton plant. This and many other questions will be topics for future exploration.

2.6 Methods

2.6.1 Bacterial strains and culture conditions

Pseudomonas syringae (Ps) strains Ps183 and Ps236, and *Xanthomonas citri* pv. *malvacearum* (Xcm) race 18 (supplementary Table S2.1) were used in plate assays and RNA-sequencing. Bacteria were routinely grown on nutrient agar (5g bacteriological peptone, 3g yeast extract, 20mL of glycerol) at 30°C with appropriate antibiotics: Ps (rifampicin) and Xcm (streptomycin).

2.6.2 Motility Assays

Petri plates were prepared with NYG with 0.4% agar. Ps183 and Xcm (5ul volume, OD_{600}= 0.1) were spotted ~1cm apart and incubated at 30°C for up to 5 days and imaged. For I-plate (Nest Scientific USA Inc., NSTF80137) motility assays, plates were prepared similarly with equal volume of NYG agar on both sides of the I-plate. Ps183 (20ul) and Xcm (100ul) were spotted onto either side of the plate. For iron assays, FeSO4 was added at increasing concentrations to either King's Broth (mixed peptone, dipotassium hydrogen phosphate, magnesium sulfate) or NYG media. For ferrozine assays, ferrozine was added at increasing concentrations to NYG media.

2.6.3 De novo reference genome assemblies

DNA with high molecular weight was extracted using a standard CTAB DNA preparation. DNA was sequenced using a nanopore MinION R9 flow cell and SQK-RAD004 Rapid Sequencing kit. The Ps isolates were first sequenced using Nanopore technology. We obtained 214,343-586,120 reads per isolate with a mean read length of 8,474-18,652bp. These reads were assembled using Canu (Koren et al. 2017) and then polished with Nanopolish (Loman, Quick, and Simpson

2015). The genomes were circularized, and chromosomes were reoriented to *DnaA* and plasmids were reoriented to *RepA*.

Shotgun Illumina MiSeq library prep, 2x250 paired-end sequencing, and trimming was performed at the Roy J. Carver Biotechnology Center at the University of Illinois at Urbana-Champaign. Bacterial genomes were then polished again with Pilon using the paired-end reads (Walker et al. 2014). In total, two rounds of Nanopolish and three rounds of Pilon were performed. This resulted in genomes with gammaproteobacteria BUSCO scores >98% (Sup. Fig. S2.6) (Simão et al. 2015). Chromosome sizes range from 5,936,430bp to 6,087,715bp. Genomes Ps236 and Ps480 contained a 68kb plasmid. Genomes were annotated using prokka and a database of T3Es, as described previously (Bart et al. 2012).

2.6.4 Transmission electron microscopy

For negative staining, 300 mesh copper grids (#FCFFT300-CU; EMS Diasum, Hatfield, PA, USA) were touched directly to the bacterial colonies (grown for 5 days at 30°C on NYG media) for 1 second, washed on 3X on drops of 2% phosphotungstic acid (PTA) @ pH 8.0, blotted and air dried. Samples were imaged with a Thermo ScientificTM Talos L 120C G2 at 120kV with a CETA 16M 4K X 4K CMOS camera at 4096x4096 pixel resolution and 2 second exposure. Large grid areas were tile mapped and stitched using Thermo ScientificTM MAPS 3 software to ensure a representative perspective of bacterial phenotypes were documented.

2.6.5 RNA extraction and sequencing

Bacteria were set up in I-plates with 100ul Xcm spotted on one side and 20ul of Ps spotted on the opposite side. Volumes were switched for Xcm sample collection. Plates incubated at 30°C for 5 days. Total RNA was extracted with Invitrogen TRIzol reagent. Six replicates for each condition were stopped by adding TRIzol directly to the plate. Solutions were transferred to vials, separated with chloroform, the aqueous phase was mixed with 70% ethanol, and transferred to Qiagen RNEasy spin columns following the manufacturer's protocol. DNase treatment was performed on columns following the NEB Dnase treatment protocol. RNA quality was checked using Bioanalyzer. Samples were sequenced by Novogene Corporation, California using NovaSeq 6000 PE150 platform sequencing strategy.

2.6.6 Read mapping and differential gene expression analysis

Qiagen CLC Genomics Workbench 22.0.2 was used for read mapping and differential expression analyses. Briefly, paired reads and bacteria genomes were imported, and RNA-sequencing analysis was performed using the RNA-seq function with the following mapping parameters: read alignment mismatch cost = 2, insertion cost = 3, deletion cost = 3, length fraction = 0.8. Principal Component Analysis was performed in CLC and replotted using ggplot2. Genes that were significantly expressed were those with FDR (Benjamini and Hochberg 1995) adjusted $p < 0.05$; $\log_2$ fold change ≥ 1. Heatmaps were generated with ggplot2 in the R environment using the average transcripts per million (TPM). Enriched Gene Ontology (GO) terms were identified using topGO (Alexa, Rahnenführer, and Lengauer 2006; Mansfeld et al. 2017). The GO term database for Ps was derived from *Pseudomonas syringae* pv. *tomato* DC3000 (www.pseudomonas.com). Ps protein sequences were compared by protein BLAST to PstDC3000 proteins. GO terms for the best protein hits (top 25%, based on bit score) were extracted. Additional GO terms were identified

using InterProScan5 (Jones et al. 2014). Significant GO terms were selected using Fisher test with the topGO *"weight01"* algorithm, node size = 20, and p-value < 0.05.

2.6.7 Bacterial mutant generation

A two-step allelic exchange strategy was used as previously described was used with some modification (Hmelo et al. 2015). Sequences both upstream and downstream of the target gene were cloned into sucrose counter-selection allelic exchange vector pDEST2T18ms using the In-Fusion Cloning strategy. Subsequent plasmids were confirmed by Sanger sequencing and conjugated or electroporated into Ps183.

2.7 Acknowledgments

Thanks to all Bart Lab members who provided useful discussion and feedback for this work. Funding for this research was provided by the National Science Foundation (NSF) to RSB (Award ID: 1928344). Additional support for TMH is from the Washington University in St. Louis Chancellor's Graduate Fellowship and the NIGMS-funded IMSD Grant (GM103757). We acknowledge imaging support from the Advanced Bioimaging Laboratory (RRID:SCR_018951) at the Danforth Plant Science Center and usage of the ThermoFisher Scientific Talos L120C TEM acquired through generous donor support to the Donald Danforth Plant Science Center.

2.8 References

Alexa, Adrian, Jörg Rahnenführer, and Thomas Lengauer. 2006. “Improved Scoring of Functional Groups from Gene Expression Data by Decorrelating GO Graph Structure.” *Bioinformatics* 22 (13): 1600–1607.

An, Dingding, Thomas Danhorn, Clay Fuqua, and Matthew R. Parsek. 2006. “Quorum Sensing and Motility Mediate Interactions between Pseudomonas Aeruginosa and Agrobacterium Tumefaciens in Biofilm Cocultures.” *Proceedings of the National Academy of Sciences of the United States of America* 103 (10): 3828–33.

Andrews, Simon C. 2010. “The Ferritin-like Superfamily: Evolution of the Biological Iron Storeman from a Rubrerythrin-like Ancestor.” *Biochimica et Biophysica Acta* 1800 (8): 691–705.

Andrews, Simon C., Andrea K. Robinson, and Francisco Rodríguez-Quiñones. 2003. “Bacterial Iron Homeostasis.” *FEMS Microbiology Reviews* 27 (2–3): 215–37.

Back, M. A., P. P. J. Haydock, and P. Jenkinson. 2002. “Disease Complexes Involving Plant Parasitic Nematodes and Soilborne Pathogens.” *Plant Pathology* 51 (6): 683–97.

Bart, Rebecca, Megan Cohn, Andrew Kassen, Emily J. McCallum, Mikel Shybut, Annalise Petriello, Ksenia Krasileva, et al. 2012. “High-Throughput Genomic Sequencing of Cassava Bacterial Blight Strains Identifies Conserved Effectors to Target for Durable Resistance.” *Proceedings of the National Academy of Sciences of the United States of America* 109 (28): E1972-9.

Benjamini, Yoav, and Yosef Hochberg. 1995. “Controlling the False Discovery Rate: A Practical and Powerful Approach to Multiple Testing.” *Journal of the Royal Statistical Society* 57 (1): 289–300.

Bergeson, Glenn B. 1972. “Concepts of Nematode—Fungus Associations in Plant Disease Complexes: A Review.” *Experimental Parasitology* 32 (2): 301–14.

Braun, V. 1997. “Avoidance of Iron Toxicity through Regulation of Bacterial Iron Transport.” *Biological Chemistry* 378 (8): 779–86.

Craig, Lisa, Katrina T. Forest, and Berenike Maier. 2019. “Type IV Pili: Dynamics, Biophysics and Functional Consequences.” *Nature Reviews. Microbiology* 17 (7): 429–40.

Frawley, Elaine R., and Ferric C. Fang. 2014. “The Ins and Outs of Bacterial Iron Metabolism.” *Molecular Microbiology* 93 (4): 609–16.

Fujita, Masaya, Kosuke Mori, Hirofumi Hara, Shojiro Hishiyama, Naofumi Kamimura, and Eiji Masai. 2019. “Erratum: Publisher Correction: A TonB-Dependent Receptor Constitutes the Outer Membrane Transport System for a Lignin-Derived Aromatic Compound.” *Communications Biology* 2 (December): 476.

Fuqua, W. C., S. C. Winans, and E. P. Greenberg. 1994. “Quorum Sensing in Bacteria: The LuxR-LuxI Family of Cell Density-Responsive Transcriptional Regulators.” *Journal of Bacteriology* 176 (2): 269–75.

Gu, Shaohua, Zhong Wei, Zhengying Shao, Ville-Petri Friman, Kehao Cao, Tianjie Yang, Jos Kramer, et al. 2020. “Competition for Iron Drives Phytopathogen Control by Natural Rhizosphere Microbiomes.” *Nature Microbiology* 5 (8): 1002–10.

Hagai, Efrat, Reut Dvora, Tal Havkin-Blank, Einat Zelinger, Ziv Porat, Stefan Schulz, and Yael Helman. 2014. “Surface-Motility Induction, Attraction and Hitchhiking between Bacterial Species Promote Dispersal on Solid Surfaces.” *The ISME Journal* 8 (5): 1147–51.

Harshey, Rasika M. 2003. “Bacterial Motility on a Surface: Many Ways to a Common Goal.” *Annual Review of Microbiology* 57: 249–73.

Hay, Iain D., Zahid Ur Rehman, M. Fata Moradali, Yajie Wang, and Bernd H. A. Rehm. 2013. "Microbial Alginate Production, Modification and Its Applications." *Microbial Biotechnology* 6 (6): 637–50.

Hillocks, R. J. 1992. "Bacterial Blight." In *Cotton Diseases*, 39–85.

Hmelo, Laura R., Bradley R. Borlee, Henrik Almblad, Michelle E. Love, Trevor E. Randall, Boo Shan Tseng, Chuyang Lin, et al. 2015. "Precision-Engineering the Pseudomonas Aeruginosa Genome with Two-Step Allelic Exchange." *Nature Protocols* 10 (11): 1820–41.

Hockett, Kevin L., Adrien Y. Burch, and Steven E. Lindow. 2013. "Thermo-Regulation of Genes Mediating Motility and Plant Interactions in Pseudomonas Syringae." *PloS One* 8 (3): e59850.

Hull, R. 1996. "Molecular Biology of Rice Tungro Viruses." *Annual Review of Phytopathology* 34: 275–97.

Jones, Philip, David Binns, Hsin-Yu Chang, Matthew Fraser, Weizhong Li, Craig McAnulla, Hamish McWilliam, et al. 2014. "InterProScan 5: Genome-Scale Protein Function Classification." *Bioinformatics* 30 (9): 1236–40.

Kearns, Daniel B. 2010. "A Field Guide to Bacterial Swarming Motility." *Nature Reviews. Microbiology* 8 (9): 634–44.

Keith, Ronald C., Lisa M. W. Keith, Gustavo Hernández-Guzmán, Srinivasa R. Uppalapati, and Carol L. Bender. 2003. "Alginate Gene Expression by Pseudomonas Syringae Pv. Tomato DC3000 in Host and Non-Host Plants." *Microbiology* 149 (Pt 5): 1127–38.

Kim, Kwang-Sun, Soohyun Lee, and Choong-Min Ryu. 2013. "Interspecific Bacterial Sensing through Airborne Signals Modulates Locomotion and Drug Resistance." *Nature Communications* 4: 1809.

Koren, Sergey, Brian P. Walenz, Konstantin Berlin, Jason R. Miller, Nicholas H. Bergman, and Adam M. Phillippy. 2017. "Canu: Scalable and Accurate Long-Read Assembly via Adaptive k-Mer Weighting and Repeat Separation." *Genome Research* 27 (5): 722–36.

Leveau, Johan Hj. 2019. "A Brief from the Leaf: Latest Research to Inform Our Understanding of the Phyllosphere Microbiome." *Current Opinion in Microbiology* 49 (June): 41–49.

Loman, Nicholas J., Joshua Quick, and Jared T. Simpson. 2015. "A Complete Bacterial Genome Assembled de Novo Using Only Nanopore Sequencing Data." *Nature Methods* 12 (8): 733–35.

Mansfeld, Ben N., Marivi Colle, Yunyan Kang, A. Daniel Jones, and Rebecca Grumet. 2017. "Transcriptomic and Metabolomic Analyses of Cucumber Fruit Peels Reveal a Developmental Increase in Terpenoid Glycosides Associated with Age-Related Resistance to Phytophthora Capsici." *Horticulture Research* 4 (May): 17022.

Mansoor, Shahid, Rob W. Briddon, Yusuf Zafar, and John Stanley. 2003. "Geminivirus Disease Complexes: An Emerging Threat." *Trends in Plant Science* 8 (3): 128–34.

McCully, Lucy M., Adam S. Bitzer, Sarah C. Seaton, Leah M. Smith, and Mark W. Silby. 2019. "Interspecies Social Spreading: Interaction between Two Sessile Soil Bacteria Leads to Emergence of Surface Motility." *MSphere* 4 (1). https://doi.org/10.1128/mSphere.00696-18.

Noinaj, Nicholas, Maude Guillier, Travis J. Barnard, and Susan K. Buchanan. 2010. "TonB-Dependent Transporters: Regulation, Structure, and Function." *Annual Review of Microbiology* 64: 43–60.

Phillips, A. Z., T. Wheeler, J. Woodward, and R. S. Bart. 2018. “Pseudomonas Syringae Pathogen Causes Foliar Disease of Upland Cotton in Texas.” *Plant Disease* 102 (6): 1171–1171.

Poole, Keith, Qixun Zhao, Shádi Neshat, David E. Heinrichs, and Charles R. Dean. 1996. “The Pseudomonas Aeruginosa TonB Gene Encodes a Novel TonB Protein.” *Microbiology* 142 (Pt 6) (June): 1449–58.

Raines, Daniel J., Olga V. Moroz, Elena V. Blagova, Johan P. Turkenburg, Keith S. Wilson, and Anne-K Duhme-Klair. 2016. “Bacteria in an Intense Competition for Iron: Key Component of the Campylobacter Jejuni Iron Uptake System Scavenges Enterobactin Hydrolysis Product.” *Proceedings of the National Academy of Sciences of the United States of America* 113 (21): 5850–55.

Rivera, Mario. 2017. “Bacterioferritin: Structure, Dynamics, and Protein–Protein Interactions at Play in Iron Storage and Mobilization.” *Accounts of Chemical Research* 50 (2): 331–40.

Schauder, S., and B. L. Bassler. 2001. “The Languages of Bacteria.” *Genes & Development* 15 (12): 1468–80.

Schmidt, Ruth, Viviane Cordovez, Wietse de Boer, Jos Raaijmakers, and Paolina Garbeva. 2015. “Volatile Affairs in Microbial Interactions.” *The ISME Journal* 9 (11): 2329–35.

Simão, Felipe A., Robert M. Waterhouse, Panagiotis Ioannidis, Evgenia V. Kriventseva, and Evgeny M. Zdobnov. 2015. “BUSCO: Assessing Genome Assembly and Annotation Completeness with Single-Copy Orthologs.” *Bioinformatics* 31 (19): 3210–12.

Stone, Bram W. G., Eric A. Weingarten, and Colin R. Jackson. 2018. “The Role of the Phyllosphere Microbiome in Plant Health and Function.” *Annual Plant Reviews Online*. Wiley. https://doi.org/10.1002/9781119312994.apr0614.

Straight, Paul D., and Roberto Kolter. 2009. “Interspecies Chemical Communication in Bacterial Development.” *Annual Review of Microbiology* 63: 99–118.

Touati, D. 2000. “Iron and Oxidative Stress in Bacteria.” *Archives of Biochemistry and Biophysics* 373 (1): 1–6.

Wadhwa, Navish, and Howard C. Berg. 2022. “Bacterial Motility: Machinery and Mechanisms.” *Nature Reviews. Microbiology* 20 (3): 161–73.

Walker, Bruce J., Thomas Abeel, Terrance Shea, Margaret Priest, Amr Abouelliel, Sharadha Sakthikumar, Christina A. Cuomo, et al. 2014. “Pilon: An Integrated Tool for Comprehensive Microbial Variant Detection and Genome Assembly Improvement.” *PloS One* 9 (11): e112963.

Weise, Teresa, Marco Kai, Anja Gummesson, Armin Troeger, Stephan von Reuß, Silvia Piepenborn, Francine Kosterka, et al. 2012. “Volatile Organic Compounds Produced by the Phytopathogenic Bacterium Xanthomonas Campestris Pv. Vesicatoria 85-10.” *Beilstein Journal of Organic Chemistry* 8 (April): 579–96.

Whitchurch, C. B., R. A. Alm, and J. S. Mattick. 1996. “The Alginate Regulator AlgR and an Associated Sensor FimS Are Required for Twitching Motility in Pseudomonas Aeruginosa.” *Proceedings of the National Academy of Sciences of the United States of America* 93 (18): 9839–43.

Wiens, Jacinta R., Adriana I. Vasil, Michael J. Schurr, and Michael L. Vasil. 2014. “Iron-Regulated Expression of Alginate Production, Mucoid Phenotype, and Biofilm Formation by Pseudomonas Aeruginosa.” *MBio* 5 (1): e01010-13.

Yu, J., A. Peñaloza-Vázquez, A. M. Chakrabarty, and C. L. Bender. 1999. “Involvement of the Exopolysaccharide Alginate in the Virulence and Epiphytic Fitness of Pseudomonas Syringae Pv. Syringae.” *Molecular Microbiology* 33 (4): 712–20.

Chapter 3: Assessment of Xcm and Ps in cotton and in the laboratory

3.1 Abstract

Xanthomonas citri pv. *malvacearum* (Xcm) and *P. syringae* (Ps) were identified in diseased cotton fields of Texas in 2016. The observation of Xcm is less surprising as it is a pathogen of cotton known to cause bacterial blight, however little is known about why Ps is cohabitating cotton with Xcm. To better understand this, I sought to investigate how Ps and Xcm interact in cotton and *in vitro*. Here we show that the Xcm-induced HR in cotton can suppress Ps disease and that both bacteria can colocalize in leaves. For interactions outside the plant host, it was found that Ps and Xcm do not develop biofilms together and though they exhibit a motility interaction, as described in Chapter 2, the signaling cue from Xcm is likely not secreted based on extractions of Xcm supernatants. These observations help our understanding of Ps virulence strategy and its behavior with Xcm. Transposon mutagenesis of Ps was also performed to identify genes involved in Ps/Xcm interactions. It was found that Ps has a low transformation efficiency and that Tn5 has a high affinity for ribosomal RNA sequences in its genome.

3.2 Introduction

With recent advances in sequencing technologies, we are now starting to recognize and appreciate that multi-microbial communities exist. Even more so, recent advances in bacterial ecology work have demonstrated that bacteria do not operate exclusively, but rather exist and interact with other microorganisms. With this, disease complexes in plants can be prioritized as a

topic of discussion as we learn that bacteria can participate in multi-pathogen infections. Understanding how bacteria influence each other can provide insight into how they operate in disease complexes.

We can use what we know about bacterial infections in plants to dissect how interactions within a disease complex play out. Bacteria can live on the surface of plants as epiphytes or within plants either in the leaf apoplasts or dispersed throughout the plant vasculature. Biofilms are microbial aggregates that are attached to a surface and surrounded by an extracellular matrix (Flemming and Wingender 2010). Formation of biofilms can help bacteria persist under harsh conditions and is a strategy for colonization and infection in plants. For example, *X. axonopodis* pv. *citri* can form biofilms both *in vitro* and on citrus leaf surfaces (Rigano et al. 2007). The development of biofilms in this case was contingent on the production of xanthan gum, an extracellular polysaccharide produced by Xanthomonads. Additionally, it has become more evident that bacteria produce molecules (metabolites, volatiles, diffusible signals, etc) that can be exchanged within and between different species, and this exchange of molecules can influence various behaviors. Let's consider quorum sensing, a cell-to-cell signaling mechanism important for virulence in plant-pathogenic bacteria (Von Bodman, Bauer, and Coplin 2003), in the olive knot disease complex. *Pseudomonas savastanoi* pv. *savastanoi* (Psv) causes olive knot tumors in olive trees, which is also cohabited by two nonpathogenic bacteria, *Pantoea agglomerans* and *Erwinia toletana*. Coinfection of each bacteria results in larger olive knots. This community collaborates by sharing the same quorum sensing signals, and the virulence of Psv QS mutants is restored when coinfected with *E. toletana* (Hosni et al. 2011; Buonaurio et al. 2015). Taken together, looking at common bacterial behaviors and probing the chemical exchange between bacteria can provide clues on how they influence each other.

How each bacterium within a disease complex interacts with the host should be considered as well. Bacterial pathogens have many other virulence factors that help establish disease in plants. Effector proteins, for example, are a major virulence determinant in plant-associated bacteria, and function to block basal level immunity in plants. Over time, plants have evolved more robust immunity mechanisms wherein the plant can recognize certain bacterial effector proteins and illicit a hypersensitive response (HR), or rapid localized cell death, which is a strong form of resistance. Rental et al. found that an Arabidopsis HR triggered by fungal effectors can restrict *P. syringae* pv. *tomato* DC3000 growth, demonstrating that an HR caused by one pathogen is effective against others (Rentel et al. 2008).

Two bacterial species, *Pseudomonas syringae* (Ps) and *Xanthomonas citri* pv. *malvacearum* (Xcm) were isolated from disease inflicted cotton in Texas in 2016. Xcm is a known pathogen of cotton and is the causal agent of cotton bacterial blight (CBB). Ps is not established as a cotton pathogen but has been co-isolated with Xcm multiple times from CBB-resistant cotton (A. Z. Phillips et al. 2018), which begs the question of whether Ps can block the resistance response. How and why these bacteria have been closely associated in cotton is not yet understood, thus we hypothesized that both bacteria collaborate in a disease complex to infect CBB-resistant cotton. To examine this, I investigated their behavior *in planta* and *in vitro*. In chapter 2, I explored how Ps and Xcm interact in I-plate assays where they were cocultured separately and discovered that Ps moves in the direction of Xcm. Xcm likely produces a volatile signal capable of attracting Ps, however the nature of the signal remains unknown. Here, I present adjacent work employed to better understand 1) additional modes of interaction between Ps and Xcm, 2) the nature of the signal cue from Xcm, and 3) coinfection strategy and behavior of both bacteria in cotton.

3.3 Results

3.3.1 Generating Ps mutants

3.3.1a Transformation efficiency of Ps

The Pseudomonads used in this study are wild field strains, so the methods and/or parameters needed to introduce mutations or plasmids may be different compared to well-established laboratory strains like *E. coli* or *P. syringae* pv. *tomato* (Pst) DC3000. Genetic mutations and/or alterations would be useful to assess certain questions about Ps. Thus, I measured its transformation efficiency to determine if Ps could be transformed with plasmid DNA. These experiments focused on a single strain of Ps, Ps480.

To begin, I tested the transformation efficiency using green fluorescent protein (GFP) plasmids pHC60 and pDGW4M. Approximately 100ng of plasmid DNA (pDNA) was transformed into Ps and yielded a transformation efficiency of 1.4 cfu/ng for pHC60 and 0.2 cfu/ng for pDGW4M. I then tested varying concentrations of plasmid to see if an increase in total plasmid used could increase the transformation efficiency. I tested 10, 100, and 1000 ng of pHC60 and pDGW4M. Using pDGW4M, the transformation efficiency was below 10 cfu/ng for each concentration. For pHC60, the transformation efficiency was 87 cfu/ng using 10ng plasmid, 40 cfu/ng using 100ng, and 6 cfu/ng using 1000ng (Table S3.2). This suggests that for Ps480, a higher transformation efficiency is achieved using smaller concentrations of plasmid, although more colonies were formed the higher the concentration. For reference, *P. syringae* pv. *syringae* is documented to have a transformation efficiency of 240 transformants/ng using 500ng DNA (Wendt-Potthoff, Niepold, and Backhaus 1992). Taken together, these observations demonstrate that Ps can be transformed using electroporation, albeit at low efficiency.

3.3.1b Using Tn5 in Ps

Two transposon mutagenesis methods were attempted to produce mutants in Ps480: (1) a mini-Tn5 triparental mating conjugation system (de Lorenzo et al. 1990; Kloek, Brooks, and Kunkel 2000) and (2) a commercial EZ-Tn5 transformation kit method. The first approach uses an *E. coli* donor harboring a mini-Tn5 cassette on a suicide plasmid (miniTn5<KanR/Gus>). Only 32 mutants were generated using this method, compared to the 1-2 thousand mutants that are produced in the model pathogen, PstDC3000. Ten of the mutants were randomly selected to confirm that independent mutants could be generated using this method. Out of 10, I found 2 sets of identical insertions: 3 mutants had disruptions upstream an *hdtS* gene, 2 mutants were disrupted in 16S/23S rRNA genes (Table S3.3). The rest of the mutants had independent mutations located in various regions of the genome. These results suggest that this system can produce some frequency of random insertion mutants with low conjugation efficiency.

The second approach involved electroporating a commercial transposome (transposon bound to transposase) into Ps480. This transposon, EZ-Tn5<R6Kyori/KAN-2>, contains Kan resistance and an origin of replication specific to pi-expressing *E. coli*, useful for rescue cloning. This method was performed three times. The first attempt yielded approximately 400 mutants. Of these, 9 were selected for sequencing to identify transposon location and to confirm that independent mutants could be generated using this method. Results revealed that each of the selected mutants had disruptions in the 16S/23S rRNA genes (Fig. S3.1, Table S3.4). A second and third transformation using this system was performed, this time competent cells were frozen away at early log and late log phase. Late log phase cell transformation results in an estimated 3,800 mutants. The early log phase cell transformation resulted in only 256 total mutants. Three mutants from both these batches were selected to identify insertion sites. Only one mutant had

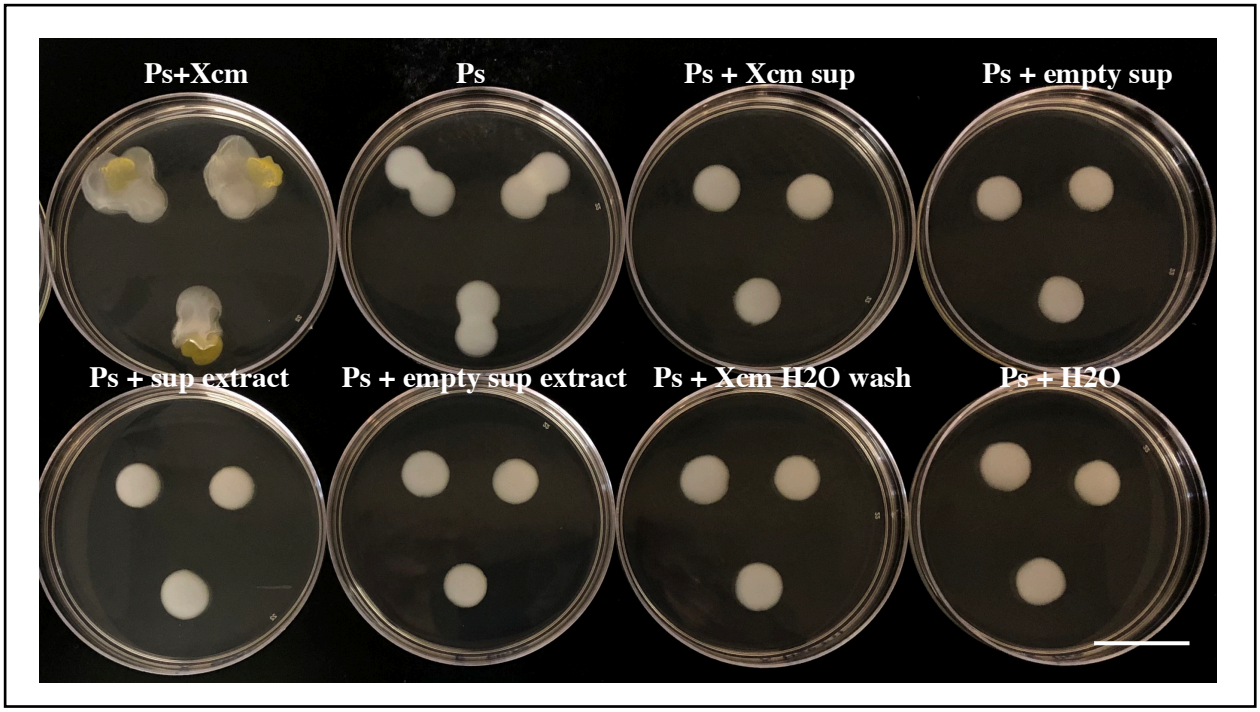

Fig 3.1 – Ps480 does not respond to Xcm supernatant extracts or cell-washes. Ps480 was spotted (5µl of OD_{600} = 0.1) alone or next to Xcm and its supernatant extractions. Top row, from left to right: Ps cultured with Xcm (5µl of OD_{600} = 0.1), alone, filtered Xcm supernatant, empty supernatant. Bottom row, from left to right: Ps cultured with ethyl acetate extraction of Xcm supernatant, ethyl acetate extraction of empty supernatant, H_2O wash of Xcm cells, and empty H_2O. Plates were cultured for 5

insertion in a separate location from 16S/23S rRNA region (Table S3.3) Blasting the transposon sequence against Ps480 genome resulted in no hits, and no contigs were found when mapping the transposon to Ps480 genome. Aligning the transposon sequence with 23S/16S region resulted in a low consensus identity (Fig. S3.2). Taken together, these results suggest EZ-Tn5 <R6Kyori/KAN-2> can yield a high number of clones but has a high affinity for the 16S/23S region of Ps480 genome.

3.3.2 Xcm-Ps *in vitro* interactions

3.3.2a Crude extracts from Xcm do not prompt movement in Ps

In chapter 2, we learned that Xcm can attract Ps isolates Ps183 and Ps480, and that this attraction is likely due to a signal that is, at least partially, a volatile. To further explore the molecular nature of the possible signal cue from Xcm, I investigated whether the cue was secreted. With this, ethyl acetate extractions of Xcm supernatants were performed using a modified approach from Gudesblat et. al. Additionally, filtered supernatant and cell washes from Xcm cultures were used to assess if the cues could be obtained from cells directly. Subsequently, whether the extracts and cell-washes could attract Ps480 was investigated by performing the motility assays and using the sample to spot directly next to Ps480. I found that neither the ethyl acetate extraction, filtered supernatant, or cells washes prompted Ps480 movement (Fig. 3.1). With this, I hypothesize that the signal from Xcm is exclusively volatile, however it is possible that methods used failed to capture the signal.

3.3.2b Cooperative biofilm formation is not a mode of interaction between Xcm and Ps

In addition to exploring the motility interaction between Ps and Xcm, I asked if they could produce biofilm together. Using a modified approach from a biofilm assay protocol by Mingsheng Qi (2019), pure cultures of both strains and a 1:1 coculture were arranged in 96 well plates. Biofilm formation was quantified by using three separate medias (M9 minimal media, M3F media, and NYG media) to culture the cells in, after which, crystal violet was used to stain surface-bound biofilm. The positive control, a strain of *Arthrobacter* previously shown to be a biofilm producer, produced biofilm in each of the different medias. No biofilm was detected in the 1:1 cocultures for any media used (Fig 3.2). Xcm produced biofilm in M3F media only. Ps480 did not produce any biofilm in any the media types when cultured alone. These observations suggest that, at least under these conditions, Ps and Xcm do not cooperate to produce biofilm together.

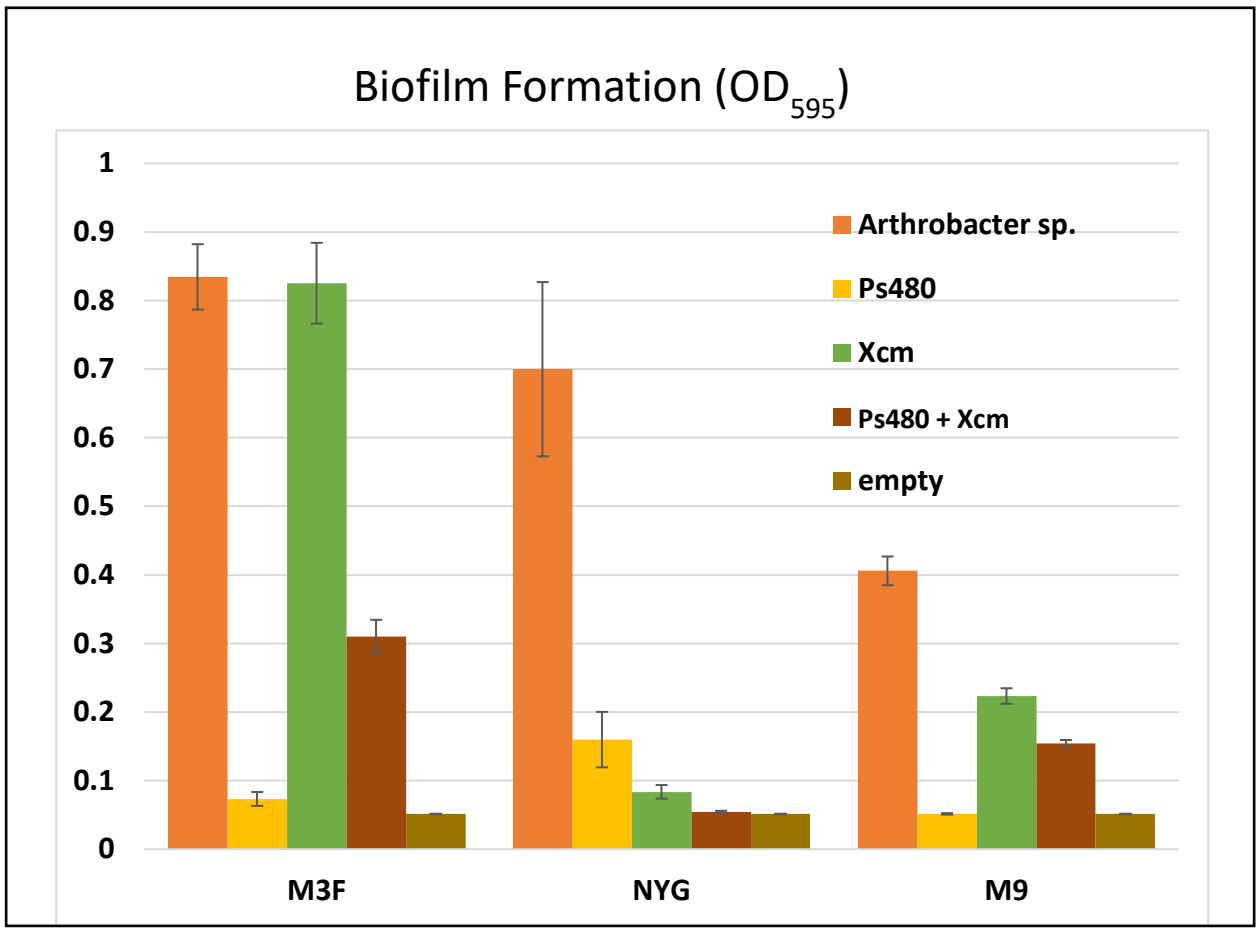

Fig 3.2 – Ps480 and Xcm do not produce biofilm together. Ps480 and Xcm were cultured in 96-well plates together and separately in M3F (left), NYG (middle), and M9 (right) medias. *Arthrobacter* sp. was used as a biofilm producing control. Cultures were grown in 30°C for two days. Biofilm was detected by first staining the wells with crystal violet then OD_{595} reading. Data represents one experiment with 5 replicates.

3.3.3 *Xanthomonas-Pseudomonas in planta* interactions

3.3.3a Xcm induced HR in cotton prevents Ps spreading necrosis

Ps480 causes spreading necrosis symptoms in CBB susceptible and resistant cotton. Even more, it produces these disease symptoms when infiltrated with Xcm and when infiltrated alone (A. Z. Phillips et al. 2018) (Fig. 1.1). Before this study, it was unknown whether CBB-resistance in cotton would be effective against Ps. Work in Arabidopsis has shown that an effector-triggered resistance response for one pathogen is effective against other pathogens (Rentel et al. 2008).

Because Ps produces severe disease symptoms when co-infecting with Xcm, we hypothesized that Ps can block the HR in cotton. To investigate whether the cotton HR is effective against Ps, I performed sequential inoculations where I infiltrated Xcm in CBB-resistant cotton seedlings 24 hours before infiltrating Ps480 in the same area (Fig. 3.1A). The hypersensitive response is rapid and is usually visible within 24 hours of infection. While Ps480 produced spreading necrosis symptoms when infiltrated 24 hours after the mock $MgCl_2$ sample, little to no spreading symptoms were observed in cases where it was infiltrated after Xcm (Fig. 3.1B). This suggests that an Xcm-induced resistance response can prevent Ps spreading necrosis. When Xcm was infected into CBB-susceptible seedlings first, Ps480 produced the spreading necrosis symptoms when infiltrated afterwards although there was some variability as shown in Fig 3.3.

3.3.3b Fluorescent strains of Xcm and Ps can be visualized in cotton

To track the spread and colonization of Ps480 and Xcm in cotton, fluorescently labelled derivatives of each strain were generated (Table 3.1). Cyan fluorescent protein and citrine fluorescent protein were selected because they are easily distinguishable from each other and chloroplast red autofluorescence. Bacterial fitness was monitored for each derivative and its wildtype by infiltrating each into cotton separately and visually comparing symptom development. Ps480-mCitrine produced spreading necrosis symptoms like the wildtype in susceptible cotton. Xcm-cyan induced an HR in CBB resistant cotton. In susceptible cotton Xcm-cyan produced water-soaking, though it appeared lighter than the wildtype (Fig S3.1).

Cotton leaves were inoculated with a mixed 1:1 suspension of both Ps480-mCitrine and Xcm-cyan or with either strain separately. Ps480-mCitrine grew rapidly in cotton as indicated by the large microcolonies that formed in both CBB susceptible and resistant cotton. Xcm-cyan, on the other

hand, formed smaller, less dense colonies. As expected, no cyan signal was observed in CBB-

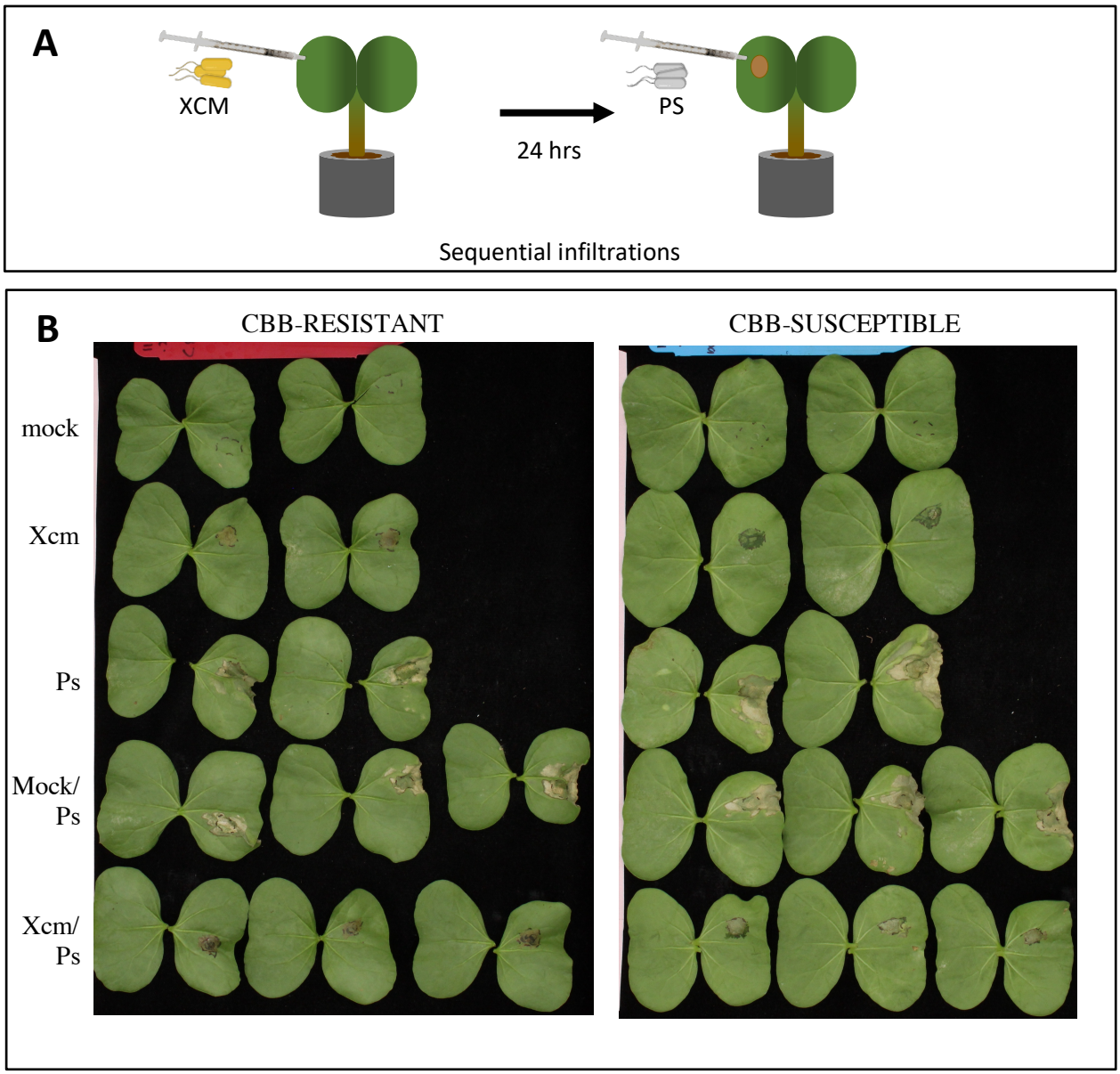

Fig 3.3 – Xcm-induced resistance response in cotton prevents Ps disease. A) Experimental flow for sequential infiltrations. Xcm was infiltrated into cotyledons first. Ps was infiltrated into the same area 24 hours later. B) Symptoms in CBB-resistant (left) and CBB-susceptible (right) cotyledons 7 days after infiltration. $MgCl_2$ was used as a mock infiltration. Bacteria were infiltrated at OD_{600} 0.01 (Ps) and OD_{600} 0.1 (Xcm).

resistant leaves. The bacteria formed mixed colonies in susceptible cotton and Xcm-cyan colonies were observed in resistant cotton, though they remained separate from Ps480 (Fig 3.2).

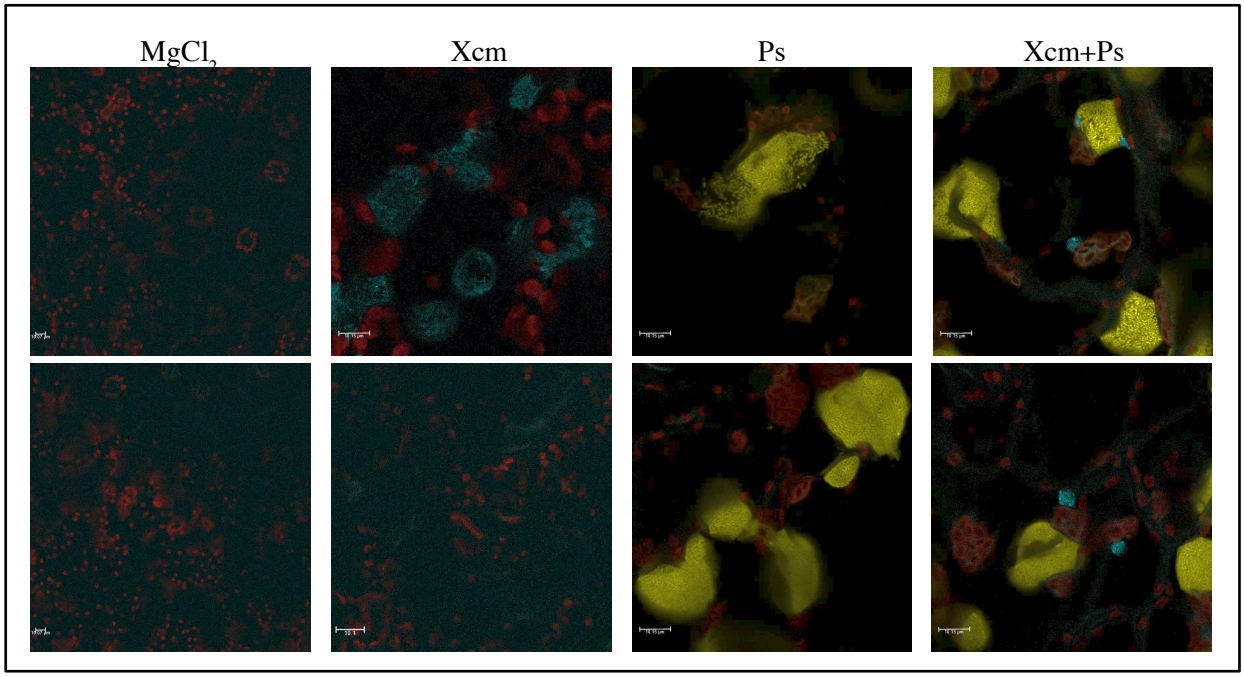

Fig 3.4 – Ps480 and Xcm can form mixed microcolonies in cotton leaves. Fluorescent strains of Ps480 and Xcm were infiltrated (OD_{600} 0.05) either together or separately into CBB-susceptible (top row) and CBB-resistant (bottom row) cotton leaves. Images were taken at 3 dpi. Images are 63x, 10uM

3.4 Discussion

Here, we took the initial steps in understanding how Ps and Xcm interact with each other *in vitro* and in cotton. It was found that an Xcm-induced HR can stop Ps from forming severe disease symptoms in cotton. This observation supports the hypothesis that Ps blocks the HR when coinfecting cotton at the same time as Xcm. Genomic analysis of several cotton associated *P. syringae* isolates revealed that some conserved effector proteins were absent in some isolates, but conserved toxin biosynthetic clusters were present in all isolates (Phillips 2018 dissertation). This begs the question of how Ps can produce such severe spreading necrosis in cotton during coinfection with Xcm, but not if an HR is induced first. It is possible that Ps produces the toxins quickly once inside the host, killing the plant tissue before the HR begins.

Confocal fluorescence microscopy was used to determine whether fluorescent derivatives of Ps and Xcm could be seen *in planta* and to analyze their distribution when co-infiltrated. This report represents the first visual demonstration of *Xanthomonas* and *Pseudomonas* cohabiting *in planta*. Ps480-miCitrine and Xcm-cyan produced bright signals within the leaves and can be used to investigate in planta interactions. Further, presence of mixed colonies revealed that both bacteria were able to colocalize in apoplasts, even in CBB-resistant cotton. Microscopy also revealed that Ps480-miCitrine produces larger colonies than Xcm *in planta* which aligns with its quicker growth time in culture.

To investigate whether Ps and Xcm interact outside the plant host, *in vitro* plate assays were performed. It was found that under the conditions used for this experiment, biofilm formation is not a mechanism of interaction. Most work done investigating *Xanthomonas* biofilm production has been done on *X. citri* pv. *citri,* which is now known to produce biofilms as a virulence strategy in citrus (Marta Sena-Vélez et al. 2016; M. Sena-Vélez et al. 2015; Rigano et al. 2007). Before

this report, there were no records of *X. citri* pv. *malvacearum* biofilm production. Xanthomonads produce xanthan, a major extracellular polysaccharide that is necessary for biofilm development, thus it was no surprise that, at least in M3F media, Xcm produced considerable biofilm. Ps480, on the other hand is not a biofilm producer. Pseudomonads also produce a specific extracellular polysaccharide, alginate, that serves a biofilm constituent, however not all species produce biofilm. Human pathogen *P. aeruginosa* is the most-studied biofilm-forming *Pseudomonas* species, and can colonize and form biofilms on Arabidopsis and sweet basil (Walker et al. 2004). In one study investigating several *Pseudomonas* species, *P. syringae* B728A was the only species that did produce excess amounts of biofilm *in vitro* (Ueda and Saneoka 2015).

Xcm and Ps did not demonstrate biofilm-related interactions, however they were found to have a distinct motility interaction. Here, I tested the hypothesis that Xcm produces a secreted signal that attracts Ps480. Neither the ethyl acetate extractions, supernatants or cell-washes were able to prompt movement or attract Ps480. This suggests that the signal is either not secreted into the media or could not be isolated using these methods. In the future, large volumes of cultures could be used to accumulate more signal.

Lastly, I set out to investigate the ability of Ps480 to be transformed with plasmid DNA and to use a Tn5 transposition system in Ps480 to create a mutant library that could be used to investigate genes that might be involved in interactions with Xcm. Ps480 was successfully transformed though the transformation efficiencies were lower than those reported in other *Pseudomonas* species (Diver, Bryan, and Sokol 1990; Bassett and Janisiewicz 2003). This might be due to not using sucrose as a washing and buffering agent during electroporation. Some studies report using sucrose which is used to support osmotic pressure. Ps480 was able to be transformed with the EZ-Tn5 <R6Kyori/KAN-2> plasmid, however the transposon had a high affinity for 16s

rRNA regions throughout the genome. The cause of this occurrence is still unknown. It's possible that the origin of replication can influence where the transposon lands in the genome. More simplified Tn5 incorporate only an antibiotic resistant cassette. In this case, the origin of replication served to make identifying the insertion location easier by rescue cloning, wherein the Tn5 integrated genome is digested, sheared and self-ligated and transformed into *E. coli*.

3.5 Materials and methods

3.5.1 Bacterial Strains and culture conditions

Pseudomonas syringae (Ps480), and *Xanthomonas citri* pv. *malvacearum* (Xcm) (Table S3.1) were used for cotton experiments and for in vitro plate assays. *Arthrobacter* sp. UNCCL28 was used as a control in the biofilm assays. Ps480-mCitrine and Xcm-cyan (Table S3.1) were used in confocal microscopy experiments. Bacteria were routinely grown on nutrient agar (NYG) (5g bacteriological peptone, 3g yeast extract, 30mL glycerol) at 30°C with appropriate antibiotics: Ps480 (rifampicin), Ps480-mCitrine (rifampicin/spectinomycin), Xcm (streptomycin), Xcm-cyan (streptomycin/spectinomycin), Arthrobacter (none).

3.5.2 Plant growth conditions and inoculations

Cotton varieties DES56 (CBB-susceptible) and C8 (CBB-resistant) were grown in BRK-20 with mycorrhizae in greenhouse conditions (28°C, 50% humidity, 16hr light/8h dark). Adult plants were grown up until the 3rd true leaf formed. Seedlings were grown up 7-10 days. For infiltrations, bacteria were cultured on appropriate antibiotic plates two days in advance. Cells were suspended in $MgCl_2$ and brought to an OD_{600} 0.05-0.1. Plant leaves were infiltrated with approximately 100ul

of bacterial inoculum with a needless syringe. After inoculated, plants were maintained in growth chambers (30°C, 80% humidity, 14 h day length) for 3-7 days before imaging.

3.5.3 Biofilm assays

Bacteria strains were diluted to an OD_{600} 0.7-1 in 10mM $MgCl_2$. Cocultures of Ps480 and Xcm were prepared 1:1. 100 ul of each strain and coculture was added to the wells of a round-bottom 96-well plate which was incubated at 30°C. After 48 hours, samples were removed from the wells and 100ul of 0.1% crystal violet was added to each well four times for 20 min increments. Afterwards, 150ul of 30% acetic acid was added to each well to dissolve the crystal violet and was transferred to a flat bottom 96-well plate and read at OD_{550} using a Tecan Microplate Reader M200 PRO. These techniques were modified from the biofilm formation assay created by Mingsheng Qi 2019.

3.5.4 Crude extractions

Ethyl acetate extractions were performed as previously described (Gudesblat, Torres, and Vojnov 2009). Xcm was grown in 5ml cultures (agitated at 250 rpm) with NYG broth overnight at 30°C. For supernatant extractions, 1 ml of cells were transferred to a small tube and spun down for 1 minute at 15000 rpm. The supernatant was removed and filtered using a 0.2um filter. For the ethyl acetate extracts, the remaining overnight culture was spun down at 4000 rpm for 10 min. The supernatant was filtered using a 0.2um filter. Ethyl acetate was mixed with the sample by inverting the samples several times until 52oluteion turned cloudy, then spun down at 4000 rpm for 10 min to separate the aqueous layer. The organic layer was then transferred to a 1.5ml tube and, with the lid open, spun down to evaporate for 40 min. Afterwards, the dried extract was suspended in 50ul

water. For the water samples, a lawn of Xcm was grown over 2 nights and transferred to 1ml of water and vortexed until completely dissolved. The solution was spun down for 1 min at 15000rpm, after which the water was removed and filtered using a 0.2um filter into a new tube. Each type of extract or supernatant was spotted with Ps on the soft agar plates as previously described.

3.5.5 Microscopy

Bacteria were infiltrated into cotton leaves at OD_{600} 0.05. After 3 days, the inoculated sections of the leaves were excised with a razor blade leaving at least 3-5 cm outside the infiltration area. Horizontal sections were layered on top of few drops of water inside a plastic chamber used for viewing from the underside of the leaf, then topped with a weight to keep the section from lifting. Leica TCS SP8 confocal microscope was used to images the leaves and visualize the following fluorophores (excitation/emission): miCy (Midoriishi-Cyan) (472nm/495nm), mCitrine (516nm/529nm), plant autofluorescence (440nm/700nm).

3.5.6 Calculating transformation Efficiency

The transformation efficiency was calculated by first performing electroporation and counting the number of colonies that grew overnight on antibiotic selective plates. For the electroporation, 50-100ul of competent cells were mixed with approximately 10-1000ng of plasmid DNA and electroporated at 1.6 kV, 600 Ω, 25uF. Immediately after, cells were transferred to 1 ml NYG broth to shake for an hour then plated on the appropriate antibiotic selective plates. The number of colonies was multiplied by any dilution factor used to get the total number of cells transformed

then divided by the amount (ng) of plasmid DNA used: total cells transformed (cfu/ml) / pDNA used (ng).

3.5.7 Transposon mutagenesis

For the triparental mating using (miniTn5<KanR/Gus>), 2ml of the recipient strain Ps480 (BLO187), donor strain *E. coli* (BLE416), and helper strain *E. coli* (BLE94) (Table 3.1) were grown for 4 hours after growth overnight on antibiotic selective plates. BLE416 was a gift from the Kunkel lab. Strains were suspended in 10mM $MgCl_2$, combined 2:1:1 and filtered through a 25mm diameter, 0.45 um filter. The filter paper containing the concentrated cells was added to NYG plates overnight at 30°C. The filters were then removed and vortexed in $MgCl_2$ and plated in 250ul aliquots onto NYG-rif/kan plates. Single primer PCR was used to identify transposon insertion sites.

For generating EZ-Tn5 mutants, EZ-Tn5 <R6Kyori/KAN-2> kit (EZ-Tn5 <R6Kyori/KAN-2>Tnp Transposome Kit Cat. No. TSM08KR) was used. Briefly, 1 unit of transposome was mixed into 50ul of competent Ps480 cells and transferred to a chilled 2mm electroporation cuvette. Cells were electroporated at 200Ω, 2.5 kV, 25uF then transferred to 1ml NYG media and shaken for 1h at 30°C. Cells were then plated on NYG plates with kanamycin. Rescue cloning and nanopore sequencing was used to identify transposon insertion sites. Rescue cloning was performed per kit instructions. Briefly, genomic DNA was extracted for selected clones using EZNA DNA Kit (Omega Biotek Inc D339602). Afterwards, 1ug of DNA was digested with 20 units EcoRI for 1 hr at 37°C. Ligation was carried out by combining 0.5ng digested product and 2 units of T4 for 1hr at room temperature, then to 70°C for 10 min to stop the reaction. The ligations were then transformed into pir E. coli at 100Ω, 2.1 kV, 25uF then

transferred to 1ml SOC media to shake for 1h. Transformants were plated on LB agar containing kanamycin. The rapid barcoding kit (SQK-RBK004) was used for nanopore sequencing the using manufacturer's instructions.

3.6 References

Bassett, Carole L., and Wojciech J. Janisiewicz. 2003. "Electroporation and Stable Maintenance of Plasmid DNAs in a Biocontrol Strain of Pseudomonas Syringae." *Biotechnology Letters* 25 (3): 199–203.

Buonaurio, Roberto, Chiaraluce Moretti, Daniel Passos da Silva, Chiara Cortese, Cayo Ramos, and Vittorio Venturi. 2015. "The Olive Knot Disease as a Model to Study the Role of Interspecies Bacterial Communities in Plant Disease." *Frontiers in Plant Science* 6 (June): 434.

Diver, J. M., L. E. Bryan, and P. A. Sokol. 1990. "Transformation of Pseudomonas Aeruginosa by Electroporation." *Analytical Biochemistry* 189 (1): 75–79.

Flemming, Hans-Curt, and Jost Wingender. 2010. "The Biofilm Matrix." *Nature Reviews. Microbiology* 8 (9): 623–33.

Gudesblat, Gustavo E., Pablo S. Torres, and Adrián A. Vojnov. 2009. "Xanthomonas Campestris Overcomes Arabidopsis Stomatal Innate Immunity through a DSF Cell-to-Cell Signal-Regulated Virulence Factor." *Plant Physiology* 149 (2): 1017–27.

Hosni, Taha, Chiaraluce Moretti, Giulia Devescovi, Zulma Rocio Suarez-Moreno, M' Barek Fatmi, Corrado Guarnaccia, Sandor Pongor, Andrea Onofri, Roberto Buonaurio, and Vittorio Venturi. 2011. "Sharing of Quorum-Sensing Signals and Role of Interspecies Communities in a Bacterial Plant Disease." *The ISME Journal* 5 (12): 1857–70.

Kloek, A. P., D. M. Brooks, and B. N. Kunkel. 2000. "A DsbA Mutant of Pseudomonas Syringae Exhibits Reduced Virulence and Partial Impairment of Type III Secretion." *Molecular Plant Pathology* 1 (2): 139–50.

Lorenzo, V. de, M. Herrero, U. Jakubzik, and K. N. Timmis. 1990. "Mini-Tn5 Transposon Derivatives for Insertion Mutagenesis, Promoter Probing, and Chromosomal Insertion of Cloned DNA in Gram-Negative Eubacteria." *Journal of Bacteriology* 172 (11): 6568–72.

Phillips, A. Z., T. Wheeler, J. Woodward, and R. S. Bart. 2018. "Pseudomonas Syringae Pathogen Causes Foliar Disease of Upland Cotton in Texas." *Plant Disease* 102 (6): 1171–1171.

Rentel, Maike C., Lauriebeth Leonelli, Douglas Dahlbeck, Bingyu Zhao, and Brian J. Staskawicz. 2008. "Recognition of the Hyaloperonospora Parasitica Effector ATR13 Triggers Resistance against Oomycete, Bacterial, and Viral Pathogens." *Proceedings of the National Academy of Sciences of the United States of America* 105 (3): 1091–96.

Rigano, Luciano A., Florencia Siciliano, Ramón Enrique, Lorena Sendín, Paula Filippone, Pablo S. Torres, Julia Qüesta, et al. 2007. "Biofilm Formation, Epiphytic Fitness, and Canker Development in Xanthomonas Axonopodis Pv. Citri." *Molecular Plant-Microbe Interactions: MPMI* 20 (10): 1222–30.

Sena-Vélez, M., C. Redondo, I. Gell, E. Ferragud, E. Johnson, J. H. Graham, and J. Cubero. 2015. “Biofilm Formation and Motility of Xanthomonas Strains with Different Citrus Host Range.” *Plant Pathology* 64 (4): 767–75.

Sena-Vélez, Marta, Cristina Redondo, James H. Graham, and Jaime Cubero. 2016. “Presence of Extracellular DNA during Biofilm Formation by Xanthomonas Citri Subsp. Citri Strains with Different Host Range.” *PloS One* 11 (6): e0156695.

Ueda, Akihiro, and Hirofumi Saneoka. 2015. “Characterization of the Ability to Form Biofilms by Plant-Associated Pseudomonas Species.” *Current Microbiology* 70 (4): 506–13.

Von Bodman, Susanne B., W. Dietz Bauer, and David L. Coplin. 2003. “Quorum Sensing in Plant-Pathogenic Bacteria.” *Annual Review of Phytopathology* 41 (April): 455–82.

Wendt-Potthoff, Katrin, Frank Niepold, and Horst Backhaus. 1992. “High-Efficiency Electro-Transformation of the Plant Pathogen Pseudomonas Syringae Pv. Syringae R32.” *Journal of Microbiological Methods* 16 (1): 33–37.

Walker, Travis S., Harsh Pal Bais, Eric Déziel, Herbert P. Schweizer, Laurence G. Rahme, Ray Fall, and Jorge M. Vivanco. 2004. “Pseudomonas Aeruginosa-Plant Root Interactions. Pathogenicity, Biofilm Formation, and Root Exudation.” *Plant Physiology* 134 (1): 320–31.

Chapter 4: Contemporary look at cotton and its pathogens

Parts of this chapter was previously published in *Theoretical and Applied Genetics* as:

Gowda, S.A., Shrestha, N., Harris, T.M. *et al*. Identification and genomic characterization of major effect bacterial blight resistance locus (*BB-13*) in Upland cotton (*Gossypium hirsutum* L.). *Theor Appl Genet* 135, 4421–4436 (2022). https://doi.org/10.1007/s00122-022-04229-2

4.1 Abstract

Cotton bacterial blight (CBB), caused by the bacteria *Xanthomonas citri* pv. *malvacearum* (Xcm), is a major disease of cotton that has reemerged in the US. This disease has historically been controlled by using CBB resistant germplasm, however the precise genes that confer resistance are unknown. In a 2016 outbreak in Lubbock, TX, an additional bacterium, *Pseudomonas syringae* (Ps), was isolated with Xcm. Ps has been isolated multiple times from cotton and there is at least one previous record of Ps infection in cotton. The recent developments in cotton present an opportune time to identify and implement genetic resistance to these bacteria. Here, a straightforward screening method using cotton seedlings was developed to 1) identify resistance to Xcm using GWAS and genetic mapping and 2) identify resistance to Ps. Sixty-one out of 253 diversity accessions were resistant to CBB and only one line, DIV282 was resistant to Ps. A set of recombinant inbred lines were tested separately for resistance against CBB. Approximately 51% of the lines were resistant, suggesting this trait segregates 1:2. This work proves useful in successfully identifying CBB resistance phenotypes in cotton seedlings and can be considered for use in future CBB genetic resistance studies.

4.2 Introduction

Cotton is an important natural fiber crop used to produce textiles, animal feed, and oil. Its textile fiber accounts for 25% of fiber use worldwide (Voora, Larrea, and Bermudez n.d.; "Cotton Sector at a Glance" 2022). Upland Cotton (*Gossypium hirsutum*) makes up approximately 97% of all cotton production in the US, with Texas contributing to about 40% of total production ("Cotton" 2022). Cotton Bacterial Blight (CBB) is a detrimental disease to cotton caused by the bacterial pathogen, *Xanthomonas citri pv. malvacearum* (Xcm). This disease is characterized by black arm rot, boll rot, angular leaf spots, and water-soaking which presents as wet lesions that form on different parts of the plant (Innes 1983). This disease has historically been controlled by acid-delinting seeds and by using CBB-resistant cultivars. Though these methods have worked for the past several decades, several outbreaks have occurred along the US cotton belt because of the use of susceptible cultivars (Anne Z. Phillips et al. 2017).

In 2016, there were reports of CBB-like outbreaks in resistant cotton in Texas. One might speculate that the Xcm pathogen evolved to overcome cotton resistance, but genome sequencing and testing of different Xcm races in CBB-resistant cotton revealed that the pathogen did not evolve to overcome resistance (T. A. Wheeler et al. 2022). Two bacteria were identified in isolations from diseased fields: Xcm and a previously uncharacterized strain of *Pseudomonas syringae* (Ps480) (A. Z. Phillips et al. 2018). Pseudomonads have been isolated from Texas cotton fields multiple times after this first observation. Each time, *Pseudomonas* was co-isolated with Xcm, never alone. *Pseudomonas* has been reported in cotton at least once before 2016 (Lewis 1960). As of 2021, there have been no additional reports or noticeable occurrences of *Pseudomonas* or *Pseudomonas*-like symptoms in Texas (T. Wheeler 2021).

As far as cotton resistance to CBB is concerned, over 20 resistance genes, known as *B* genes, and 20 polygene complexes have been identified in cotton (Zhang et al. 2020). Resistance can manifest as a hypersensitive response (HR) wherein the plant cells undergo a rapid, localized cell death. The precise locations and functions of *B* genes are still being investigated. *Pseudomonas* infection in cotton is a more recent and less-frequent observation, thus its classification as a bona-fide cotton pathogen and any evidence of cotton resistance has not yet been established.

In 2014, Tyagi et al. generated a cotton diversity panel useful genetics studies such as identifying resistance to CBB or *P. syringae* (Tyagi et al. 2014). Here, I present a screening method, done in collaboration with the Kuraparthy lab, using cotton seedlings to test recombinant in bred lines (RILs) and a diversity panel for resistance to Xcm and Ps. The work performed using Xcm was used to map *BB-13* resistance to a 371 kb region on chromosome D02. No lines were resistant to Ps, however, one line, DIV282, yielded the least severe symptoms. This screening method proves useful in identifying resistance and susceptible symptoms of CBB for further CBB genetic resistance studies.

4.3 Results

4.3.1 *Xanthomonas* resistance in RILs

To identify CBB resistance in cotton, Xcm was tested against a diversity panel of 253 accessions and 104 RILs. Infiltrations were first performed to find the most optimal bacteria concentration to use to produce consistent symptoms. Xcm produced clear water-soaking results in susceptible cotton at an optical density of 0.1, compared to an OD 0.05 where water-soaking appeared light and variable. Seedling cotyledons were also examined to see to confirm that symptoms in young plants matched the true leaves of adult plants. It was found that young plants

develop both water soaking and hypersensitive response symptoms like true leaves. I also observed that water-soaking symptoms developed more consistently under growth chamber conditions; when left at ambient conditions susceptible symptoms present as water-soaking only at the perimeter of the inoculation area and as a reflective symptom that develops within the inoculation area.

To test the diversity panel and RILs for CBB-resistance, Xcm were infiltrated into 10-day old cotton seedlings at OD_{600} 0.1 and monitored for symptom development 7 days after infection. Resistance was determined by observing a hypersensitive response (HR) and susceptibility was determined by the presence of water-soaking at the infiltration area. I observed a distinguishable difference between the two phenotypes in seedlings: resistance presented as a brown lesion within the inoculation area while susceptibility presented as dark, wet lesions within the inoculation area. I observed 61 accessions with resistance to CBB and 192 susceptible accessions. A phylogenetic neighbor joining tree was created including each of the lines (Gowda 2022). It is likely that resistance developed on multiple occasions throughout evolution and was lost even in lines that shared resistant common ancestors. There are a few instances where resistance might have been developed spontaneously. For example, CD3HCABCUH 1 89 and BJAGL NECT are two lines that evolved to have resistance though closely related to other lines found to be susceptible. For the RILs, 54 lines were resistant to Xcm, while the remaining 50 lines showed susceptibility. This demonstrates a 1:1 segregation and suggests that, in this case, resistance is controlled at a single locus.

4.3.2 *Pseudomonas* resistance in RILs

To explore cotton resistance to *Pseudomonas*, Ps was infiltrated into the diversity panel of 253 accessions. Bacteria were infiltrated into 10-day old cotton seedlings at OD_{600} 0.05 and monitored for symptom development after 7 days. At this concentration, spreading necrosis symptom develops clearly and spreads beyond the infiltration area. Because I was not sure what resistance looks like in cotton, any severe changes in the spreading necrosis phenotype were reported. No lines appeared to be resistant to Ps. I observed one accession, DIV 282, with less severe spreading necrosis. While the spreading appeared less by eye, dead tissue still formed at the site of inoculation suggesting DIV 282 may be more tolerant to Ps compared to other accessions.

4.4 Discussion

A method was developed to screen cotton seedlings for resistance to *Xanthomonas citri* pv. *malvacearum*, the causal agent of cotton bacterial blight, and *Pseudomonas syringae*, a known crop pathogen whose relevance in cotton is still being investigated. Efficient screening methods feature protocols that allow testing several samples within a short amount of time. Thus, cotton seedlings, rather than adults, were used to allow for a more rapid assessment of disease symptoms and to conserve space.

A previously generated diversity panel of 380 accessions and 104 recombinant inbred lines were used to assay against Xcm. Out of the 380 diversity panel accessions, 253 were tested due to availability. Of these 61 were found to have clear resistance against Xcm. Using cotton seedlings offered a more simplified approach to monitoring disease symptoms: the cotyledons are small yet large enough to infiltrate a substantial amount of inoculum and produce the same symptoms as adult leaves. The hypersensitive response in the cotyledons is very clear by eye in cotyledons and

develop within 7 days of inoculation. Water-soaking is also clearly observable in cotyledons by 7 days.

Since the prevalence of *Pseudomonas* infection in cotton is not yet understood, we decided to screen the diversity panel for resistance to Ps. Ps causes severe spreading necrosis in both CBB-susceptible and CBB-resistance cotton, so we looked for any variations of this phenotype during the screen. No resistance was observed for Ps in the diversity panel. The one line, DIV282, still produced disease symptoms, however the symptoms were less severe. Based on effector analysis, it is hypothesized that the spreading necrosis produced by Ps in cotton is from a toxin (Phillips dissertation 2017). DIV282 may tolerate Ps by suppressing its growth and/or the spread of toxins. The *P. syringae* group of pathovars are known to produce coronatine, a toxin that causes chlorotic symptoms in different plants (Mitchell 1893). This symptom is characterized by yellowing or halo formation around small necrotic lesions and is different than that of cotton-isolated Pseudomonads, which cause dead tissue that spreads beyond the initial infiltration site. To my knowledge there are no other reports of Pseudomonads producing dead tissue symptoms other than chlorosis. Future work might involve screening of more cotton accessions, perhaps from other species, to identify other lines with Ps tolerance. Additionally, growth assays could be considered to monitor Ps growth in DIV282 versus other more disease-burdened lines like the controls C8 (resistant) and Des56 (susceptible), for example.

As of 2021, there have been no observations of *Pseudomonas* in cotton fields of Texas. The occurrence of Pseudomonas in cotton is sporadic and likely due to optimal environmental conditions. It may take several years of being challenged with Pseudomonas for cotton to develop resistance. Given this, methods to prevent future Ps outbreaks in cotton are still to be determined as we learn more about the pathogen.

4.5 Materials and methods

4.5.1 Bacterial strains and culture conditions

Pseudomonas syringae (Ps) and *Xanthomonas citri* pv. *malvacearum* (Xcm) race 18 were used to infiltrate in cotton. Both Ps and Xcm were isolated from leaves from Lubbock, TX (Phillips 2018). Bacteria were routinely grown on nutrient agar (5g bacteriological peptone, 3g yeast extract, 20ml of glycerol) at 30°C with appropriate antibiotics: Ps (rifampicin) and Xcm (streptomycin).

4.5.2 Plant growth conditions

A diversity panel created by Tyagi et al. (2014) and a set of recombinant inbred lines (Arkot 8102 [resistant male] x Acala Maxxa [susceptible female]) by Gowda et al. (2022) were used for screening. The diversity panel was grown individually as one seed in a 2-inch pot, 4 replicates each. The RIL population was grown with 4 seeds in 4-inch pots. Plants were grown in BRK-20 with mycorrhizae in greenhouse conditions (28°C, 50% humidity, 16hr light/8h dark) for 7-10 days. DES56 (CBB-susceptible) and C8 (CBB-resistant) were included as controls. For infiltrations, bacteria were cultured on appropriate antibiotic plates two days in advance. Cells were suspended in $MgCl_2$ and brought to an OD_{600} 0.05-0.1. Plant leaves were infiltrated with approximately 100ul of bacterial inoculum with a needless syringe. After inoculated, plants were maintained in growth chambers (30°C, 80% humidity, 14 h day length) for 3-7 days before imaging.

4.5.3 Bacterial inoculations

For infiltrations, bacteria were cultured on appropriate antibiotic plates two days in advance. Cells were suspended in 10mM $MgCl_2$ and brought to an OD_{600} 0.05 (Ps) and 0.1 (Xcm). Cotyledons of ten-day old plants were infiltrated with approximately 100ul of bacterial inoculum with a needless syringe. Once inoculated, plants were maintained in growth chambers (30°C, 80% humidity, 14 h day length) for 7 days before phenotyping and imaging.

4.5.4 Phenotyping

For Xcm, a susceptible response was characterized by water-soaked lesions, while a resistance response was characterized by the hypersensitive necrotic response. For Ps, necrotic spread was monitored. Mock infections with $MgCl_2$ were also performed to confirm the symptoms of bacterial infections. Cotton varieties C8 (CBB-resistant) and Des56 (CBB-susceptible) were used as controls.

4.6 References

"Cotton." 2022. Agricultral Marketing Resource Center. April 2022. https://www.agmrc.org/commodities-products/fiber/cotton#:~:text=The%20predominant%20type%20of%20cotton,97%20percent%20of%20U.S.%20production.

"Cotton Sector at a Glance." 2022. USDA Economic Research Service. October 2022. https://www.ers.usda.gov/topics/crops/cotton-and-wool/cotton-sector-at-a-glance/.

Innes, N. L. 1983. "Bacterial Blight of Cotton." *Biol. Rev*. 58: 157–76.

Lewis, R. D. 1960. "Pseudomonas Wilt of Cotton."

Phillips, A. Z., T. Wheeler, J. Woodward, and R. S. Bart. 2018. "Pseudomonas Syringae Pathogen Causes Foliar Disease of Upland Cotton in Texas." *Plant Disease* 102 (6): 1171–1171.

Phillips, Anne Z., Jeffrey C. Berry, Mark C. Wilson, Anupama Vijayaraghavan, Jillian Burke, J. Imani Bunn, Tom W. Allen, Terry Wheeler, and Rebecca S. Bart. 2017. "Genomics-Enabled Analysis of the Emergent Disease Cotton Bacterial Blight." *PLoS Genetics* 13 (9): e1007003.

Tyagi, Priyanka, Michael A. Gore, Daryl T. Bowman, B. Todd Campbell, Joshua A. Udall, and Vasu Kuraparthy. 2014. "Genetic Diversity and Population Structure in the US Upland

Cotton (Gossypium Hirsutum L.)." *TAG. Theoretical and Applied Genetics. Theoretische Und Angewandte Genetik* 127 (2): 283–95.
Voora, V., C. Larrea, and S. Bermudez. n.d. "Global Market Report: Cotton." Accessed November 24, 2023. https://www.jstor.org/stable/pdf/resrep26555.pdf.
Wheeler, Terry A., Taylor Harris, Rebecca S. Bart, Thomas Isakeit, Jason Woodward, Tom W. Allen, and Robert C. Kemerait. 2022. "Response of Xanthomonas Citri Pv. Malvacearum Isolates to Cotton Differing in Susceptibility to the Bacterium and Their Predicted Type III Effectors." *Plant Health Progress* 23 (1): 40–44.
Wheeler, Terry. Letter to Taylor Harris. 2021, 2021.
Zhang, Jinfa, Fred Bourland, Terry Wheeler, and Ted Wallace. 2020. "Bacterial Blight Resistance in Cotton: Genetic Basis and Molecular Mapping." *Euphytica/ Netherlands Journal of Plant Breeding* 216 (7). https://doi.org/10.1007/s10681-020-02630-w.

Chapter 5: Discussion and Future Directions

5.1 Introduction

It has become more evident in the last several years that bacteria can coexist in nature and form synergistic relationships. Synergistic relationships can manifest as disease complexes in plants where multiple pathogens work together to cause disease. Understanding how multi-pathogen infections work can help us identify strategies for disease prevention. In 2016, *Pseudomonas syringae* (Ps) and *Xanthomonas citri* pv. *malvacearum* (Xcm) were co-isolated from disease-burdened cotton fields of Texas (A. Z. Phillips et al. 2018). The presence of Xcm was surprising because the outbreak occurred in a cotton variety that was resistant to Xcm, which is the known causal pathogen for cotton bacterial blight (CBB). It was also surprising that *P. syringae* was present because, though it is a prominent pathogen of many important crops, it has not been classified as a pathogen of cotton. In my dissertation, I focused on understanding how the two interact with each other to develop hypotheses on how they may function in a disease complex against cotton. Using *in vitro* I-plate assays and RNA-sequencing, I discovered that Xcm and Ps interact through exchange of a volatile signal, and that iron plays a role in this interaction; however, the signal from Xcm remains unknown. We also learned that although Ps can cause spreading necrosis in CBB-resistant cotton when infiltrated alone and with cotton, a resistance response is effective at blocking its disease if initiated by Xcm first; what remains unknown is whether Ps can actively block the resistance response. Finally, screening a diversity panel for resistance to Xcm led to the identification a more precise location, specifically on cotton chromosome D02, of genes conferring CBB resistance. In contrast, no resistance to Ps was observed. Here, I discuss a

summary of what all we learned as a result of this investigation and highlight remaining questions and possible future directions.

5.2 Investigating disease complexes in plants

The finding that Ps has only been isolated with Xcm on multiple occasions led to the hypothesis that the two form a disease complex to cause disease in CBB-resistant cotton. To investigate this, different experiments were performed to understand their behaviors at different stages of the plant infection cycle: the epiphytic stage where bacteria live on the surfaces of plants and the endophytic stage where bacteria occupy areas inside the plant.

Preliminary growth assays, performed by Anne Phillips, where both Xcm and Ps were syringe-infiltrated at the same time into cotton suggested that Ps outgrows Xcm (Anne Z. Phillips 2018). I used confocal microscopy to see how the bacteria localize inside the plant and found that Xcm and Ps can colocalize together. I also observed that Ps appeared to grow larger microcolonies than Xcm supporting the preliminary findings that Ps outgrows Xcm. These data, although performed using standard plant-bacteria interactions techniques, did not tell us *how* the two collaborate, if at all. The *Pseudomonas* cotton isolates, when infiltrated either alone or with Xcm, produce a severe spreading necrosis in the leaves (A. Z. Phillips et al. 2018) (see Fig. 1.1). This observation is intriguing because we would expect the hypersensitive response elicited by Xcm to also be effective against Ps during coinfection. To understand whether the cotton resistance response can stop Ps disease, I performed sequential infiltrations and learned that an Xcm-induced hypersensitive response can block its disease. A question that remains is how exactly Ps can cause disease when coinfecting with Xcm, if the hypersensitive response is, in fact, effective against it.

Can Ps actively block the hypersensitive response? We know that bacteria utilize Type-3 secreted effector proteins to overcome the plant immune response. For example, the effector HopZ3 of bean pathogen *P. syringae* B728a is effective in suppressing immune responses in both tobacco and Arabidopsis (Jeleńska et al. 2021; Vinatzer et al. 2006). Genomic analyses performed by Anne Phillips revealed several variable and conserved effectors present across multiple *Pseudomonas* cotton isolates. Future work might include generating Type-3 secretion system mutants and Type-3 effector mutants to test for virulence in cotton. In her work, she also identified the presence of several biosynthetic gene clusters for *Pseudomonas* specific toxins in all the cotton isolates. *Pseudomonas syringae* phytotoxins can cause chlorosis (coronatine, phaseolotoxin, tabtoxin) or necrosis (syringomycin and syringopeptin) (Bender, Alarcón-Chaidez, and Gross 1999). For example, *P. syringae* pv. *syringae* mutants deficient in syringomycin and syringopeptin production produce little to no necrotic lesions in cherry fruits compared to its wildtype (Scholz-Schroeder et al. 2001). Coronatine deficient mutants of *P. syringae* pv. *tomato* produce fewer lesions and have reduced fitness in tomato (Bender et al. 1987; Brooks et al. 2004). One hypothesis is that Ps produces phytotoxins that cause the spreading necrotic lesions. Future work could be done to better understand the use of toxins in its virulence. For example, syringafactin, syringomycin, and syringopeptin mutants could be generated and tested for their fitness in cotton.

Alternative inoculation methods like spray inoculation or dip inoculation can be used to mimic the epiphytic stage. These methods allow you to ascertain whether bacteria can move inside the plant. In my preliminary work, I attempted to assess whether Xcm promotes Ps entry into cotton by performing dip inoculations and using fluorescent microscopy to monitor its localization *in planta*. I learned that addressing this question would take more optimization; specifically, more work could be done to 1) identify the best concentration of each bacterium to use, 2) identify what

timepoints to access symptoms and bacterial growth, and 3) identify what locations to monitor growth or localization of the bacteria.

5.3 Volatile signaling between bacteria

Metabolites and volatiles produced by bacteria play an important role in how they interact with the environment and with other bacteria (Farag, Zhang, and Ryu 2013; Westhoff, van Wezel, and Rozen 2017). Studies on the biological roles of volatiles are becoming more prominent as we discover their exchange among microbes is quite common and can have effects both on the producers and the nearby microbial community. I investigated how Ps and Xcm interact outside their plant host to better understand how they may interact in a disease complex. We now know that the two bacteria can interact through volatile-mediated communication; when cultured in an I-plate that separates the media but still allows gas exchange, Ps migrates toward Xcm when cultured together, but does not move when cultured alone. By using RNA-sequencing to monitor gene expression in both bacteria, we learned this movement phenotype in Ps is linked to iron sensing. Whether iron sensing and perception is implicated in their *in planta* interactions is currently unknown. Additionally, the nature of this migration interaction (for example, is it antagonistic or synergistic?) has not been explored fully. Some Gram-negative bacteria utilize the type-6 secretion system (T6SS) in antagonistic interactions to target and kill other competing bacteria (Cianfanelli, Monlezun, and Coulthurst 2016). To test the hypothesis that the movement interaction is antagonistic, one could look for T6SS gene expression in Ps when exposed to Xcm. Two T6SS gene clusters, HSI-I and HSI-II, have been identified in different *P. syringae* pathovars. Expression of the HSI-II gene cluster and *hcp2*, a T6SS marker gene in *P. syringae* pv. *tomato*

DC3000, are necessary for DC3000 interspecies competition several bacteria species including *Xanthomonas euvescatoria* and *E. coli* (Chien et al. 2020). There was at least one gene related to the T6SS upregulated in both Ps183 and Ps236 when exposed to Xcm: in Ps183, "type VI secretion system amidase effector protein Tae4" (pseudo_prokka_04019); and in Ps236, "type VI secretion system amidase immunity protein Tai4 (pseudo_prokk_04066), and "type VI secretion system tube protein hcp" (pseudo_prokka_01557). This suggests that the relationship between both Ps and Xcm is antagonistic, at least *in vitro*. Future work might involve exploring the T6SS gene clusters in Ps and monitoring gene expression of common competition-related genes, like those related to the T6SS, in Ps at earlier timepoints after coculture with Xcm and when coinfected into cotton.

What still remains unknown is the signals exchanged between Ps and Xcm and which signals prompt Ps movement. Future work could involve the use of gas chromatography and mass spectrometry (GC/MS) to identify the volatile signals produced by Xcm, and testing each molecule for its effect on Ps. For instance, GC/MS was used in a previous study to identify volatile emissions, the majority of which were the ketone decan-2-one and its derivatives, from *Xanthomonas citri* pv. *vesicatoria* (Weise et al. 2012). When tested individually, some of the volatiles were shown to inhibit growth of different fungi. In a separate study, the ketone 2,3 butanedione and glyoxylic acid produced by *B. subtilis* were identified as the precise volatiles that prompt motility in *E. coli* (Kim, Lee, and Ryu 2013). A future experiment could be set up as follows: both Ps and Xcm are grown separately and together on agar-slants in bottles or tubes. The containers can be capped with septa lids that contain a rubber portion that can be pierced with a syringe needle to pull out the air that accumulates in the container. This extracted air can be used for gas chromatography. The challenge with this is that proper controls need to be identified. For instance, Ps does not move in response to *E. coli*, so this strain could be used as a negative control.

However, it might be more advantageous to identify a *Xanthomonas* strain that does not cause movement, to keep the strains and their subsequent volatiles as related as possible. However, based on testing multiple strains of *Xanthomonas* for their ability to promote Ps movement, it seems that the effector molecule that promotes Ps movement may be produced widely among Xanthomonads. Ideally, we could look to the RNA-sequencing data of Xcm when exposed to Ps. Perhaps certain biosynthetic gene clusters related to metabolite biosynthesis are upregulated. Oddly, a large portion of Xcm's upregulated genes were "hypothetical proteins". However, there were a few genes with annotations that could provide clues on how it responds to other bacteria (see Fig. S2.4B). The upregulated genes "Response regulator receiver protein *CpdR_2*", and "response regulator *mprA_1*" look interesting. Response regulators function as one of two parts in two-component signal transduction systems that help bacteria sense and response to the environment. Not much is known about these two response regulators other than that *cpdR2* is necessary for cell-cycle progression in rhizobia *Sinorhizobium meliloti* and *mprA1* is linked to multi-drug resistance in *E. coli*. Gaining antibiotic resistance is a common trait among bacteria during interspecies interactions (Westhoff, van Wezel, and Rozen 2017). For example, *Pseudomonas putida* responds to the volatile indole produced *E. coli* by inducing an efflux pump that increases resistance to antibiotics (Molina-Santiago et al. 2014). Perhaps *cpdR2* and *mprA* is expressed in Xcm in response to perceiving a nearby competitor and subsequently influence the volatiles Xcm produces. Could disruptions in any of these genes result in Xcm losing its attractive scent? Do other Xanthomonads express these same genes when exposed to Ps? These questions still remain and could be the key to unlocking how Xcm attracts Ps, and more broadly opening a new door to *Xanthomonas* inter- and intraspecies interactions.

Taken together, my working model of how Xcm and Ps interact to form a disease complex in cotton involves the signaling cue from Xcm which prompts movement in Ps. As an epiphyte Ps is non-motile and therefore unable to enter the plant. Xcm produces volatiles that, through interplay with Ps iron-sensing and signaling mechanisms, prompts Ps movement. This motility induction helps Ps enter the plants where it's then able to block or surpass the cotton resistance response, allowing the increased fitness for both it and Xcm (Fig. 4.1)

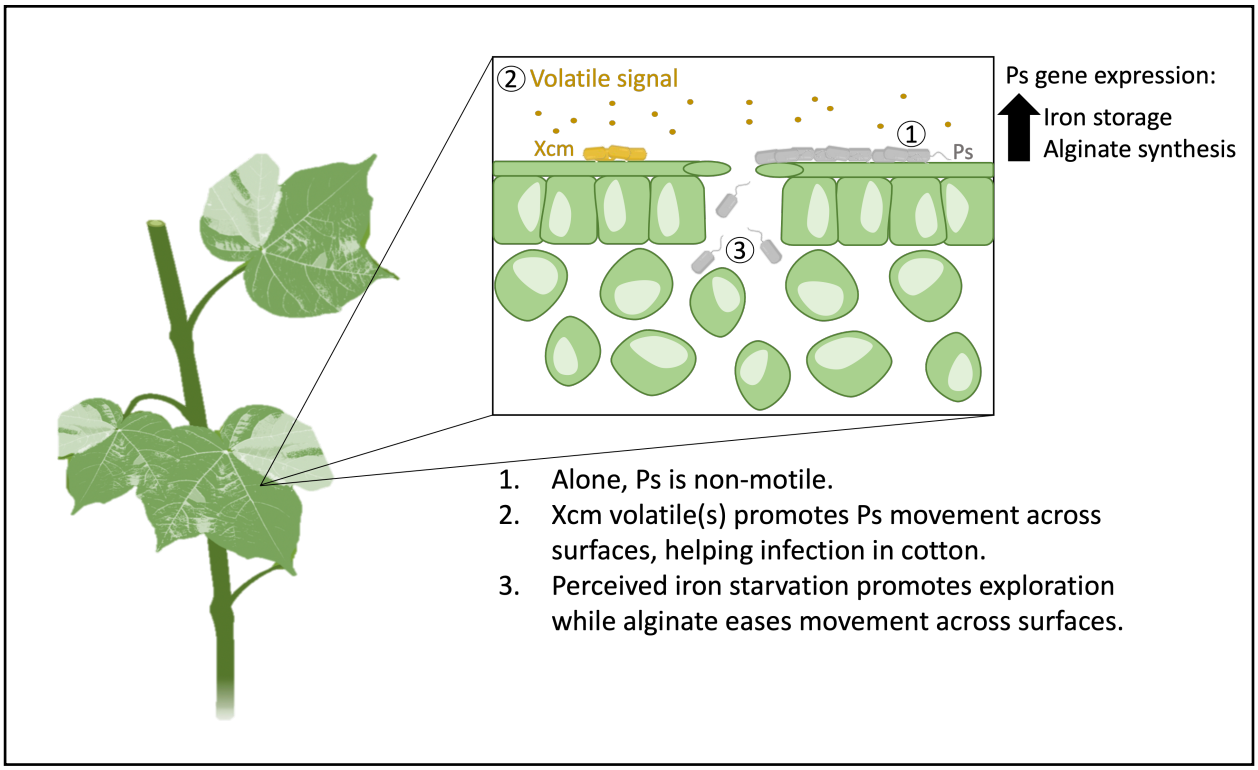

Fig. 4.1 – Working model for how Ps and Xcm interact in a disease complex. 1) Both Xcm and Ps live on the surfaces of cotton. Alone, Ps is non-motile. 2) Xcm produces volatiles that promote Ps movement across the surfaces, aiding its invasion into cotton. These signals influence iron perception in Ps. 3) Perceived iron starvation prompts exploratory movement facilitated by the increased production of alginate, which allows the cells to move more easily.

5.4 The future of cotton bacterial blight resistance

The CBB outbreaks that occurred in the 2010s ignited new efforts to identify sources of resistance in cotton. Though there are more than 20 sources of *B*-gene resistance described, the exact genes and their locations still remain largely unknown. In 2014, a diversity panel of Upland Cotton was created and has since then been used for mapping purposes to identify genes that confer bacterial blight resistance (Tyagi et al. 2014). I collaborated with the Kuraparthy lab to screen this diversity panel and a recombinant inbred line mapping population for resistance to Xcm, the causal agent of CBB, and I identified 61 resistant accessions (Gowda 2022). This screen was used for a genome-wide association study of CBB, which localized the resistance, *BB-13*, to chromosome D02. Several possible gene candidates were identified as a result of this work and will contribute to future studies involving cloning the precise resistance gene and developing robust CBB resistance in cotton.

I also screened the diversity panel for resistance to *Pseudomonas syringae* and found that no accessions had complete resistance. One line exhibited less disease severity compared to all other accessions but was still considered "susceptible". Nonhost resistance, where a plant species that is not a host to a specific pathogen but exhibits resistance towards it, is a common and durable form of plant resistance against many pathogenic microbes (Mysore and Ryu 2004; Heath 2000). This has been demonstrated well regarding the tomato pathogen, *P. syringae* pv. *tomato*. The major resistance gene that confers resistance to race 0 strains in tomatoes, *Pto*, was first found in the wild tomato relative, *Solanum pimpinellifoliium* (Pitblado and Kerr 1980). More recently, *Solanum lycopersicoides*, a distantly relative of tomato, was found to exhibit resistance to race 1 strains (Mazo-Molina et al. 2019). Additionally, model plant *Nicotiana benthamiana*, also part of the tomato family, holds non-host resistance against *P. syringae* pv. *tomato* DC3000 (Wei et al. 2007). Taken together, these observations of the well-studied *P. syringae* tomato pathogen, demonstrates

that plant-relatives may be reliable sources of resistance. Future work might focus on screening other species of *Gossypium* and other plants in the Malvaceae family for resistance. Though it is concerning that there is no known resistance to this pathogen currently, *Pseudomonas* outbreaks in cotton are not frequent. In nature, *P. syringae* is spread by aerosols, wind, rainfall, and rain splash (Morris, Monteil, and Berge 2013; Lamichhane, Messéan, and Morris 2015; Hirano and Upper 2000). Its occurrence in Texan cotton fields is likely due to favorable environmental conditions that support its growth and spread in fields. Thus, it may be helpful to analyze weather patterns at the time of outbreaks to understand its occurrence.

5.5 Conclusion of the thesis

As pathogens and pests continue to threaten agriculture worldwide, it is of upmost importance to understand the interactions among plants and their pathogens to create durable crops for the future. Though most plant-pathogen studies focus on one pathogen and its host, it has become more evident that microbes coexist with others in nature. Such is the case for disease complexes in plants wherein multiple microbes coexist and contribute to disease. By investigating interactions among different microbes, we can better understand their implications on agriculture. In this thesis, I investigated the interactions between *Xanthomonas citri* pv. *malvacearum* (Xcm) and *Pseudomonas syringae* (Ps) isolated from disease burdened cotton. Through *in vitro* plate assays, genetic studies, and RNA-sequencing, we now know that Xcm and Ps interact by communicating through volatiles that prompt directional movement of Ps toward Xcm. Furthermore, screening of a cotton diversity panel identified a more precise location of genetic resistance to Xcm, putting us a step closer to creating durable bacterial blight resistance in cotton. The data discussed here

demonstrates how two common phytopathogenic genera interact with each other directly and provides clues as to how they could function in a disease complex in one of the world's leading fiber crops.

5.6 References

Bender, C. L., F. Alarcón-Chaidez, and D. C. Gross. 1999. "Pseudomonas Syringae Phytotoxins: Mode of Action, Regulation, and Biosynthesis by Peptide and Polyketide Synthetases." *Microbiology and Molecular Biology Reviews: MMBR* 63 (2): 266–92.

Bender, C. L., H. E. Stone, J. J. Sims, and D. A. Cooksey. 1987. "Reduced Pathogen Fitness of Pseudomonas Syringae Pv. Tomato Tn5 Mutants Defective in Coronatine Production." *Physiological and Molecular Plant Pathology* 30 (2): 273–83.

Brooks, David M., Gustavo Hernández-Guzmán, Andrew P. Kloek, Francisco Alarcón-Chaidez, Aswathy Sreedharan, Vidhya Rangaswamy, Alejandro Peñaloza-Vázquez, Carol L. Bender, and Barbara N. Kunkel. 2004. "Identification and Characterization of a Well-Defined Series of Coronatine Biosynthetic Mutants of Pseudomonas Syringae Pv. Tomato DC3000." *Molecular Plant-Microbe Interactions: MPMI* 17 (2): 162–74.

Chien, Ching-Fang, Cheng-Ying Liu, Yew-Yee Lu, You-Hsing Sung, Kuo-Yau Chen, and Nai-Chun Lin. 2020. "HSI-II Gene Cluster of Pseudomonas Syringae Pv. Tomato DC3000 Encodes a Functional Type VI Secretion System Required for Interbacterial Competition." *Frontiers in Microbiology* 11 (June): 1118.

Cianfanelli, Francesca R., Laura Monlezun, and Sarah J. Coulthurst. 2016. "Aim, Load, Fire: The Type VI Secretion System, a Bacterial Nanoweapon." *Trends in Microbiology* 24 (1): 51–62.

Farag, Mohamed A., Huiming Zhang, and Choong-Min Ryu. 2013. "Dynamic Chemical Communication between Plants and Bacteria through Airborne Signals: Induced Resistance by Bacterial Volatiles." *Journal of Chemical Ecology* 39 (7): 1007–18.

Heath, M. C. 2000. "Nonhost Resistance and Nonspecific Plant Defenses." *Current Opinion in Plant Biology* 3 (4): 315–19.

Hirano, S. S., and C. D. Upper. 2000. "Bacteria in the Leaf Ecosystem with Emphasis on Pseudomonas Syringae-a Pathogen, Ice Nucleus, and Epiphyte." *Microbiology and Molecular Biology Reviews: MMBR* 64 (3): 624–53.

Jeleńska, Joanna, Jiyoung Lee, Andrew J. Manning, Donald J. Wolfgeher, Youngjoo Ahn, George Walters-Marrah, Ivan E. Lopez, et al. 2021. "Pseudomonas Syringae Effector HopZ3 Suppresses the Bacterial AvrPto1-Tomato PTO Immune Complex via Acetylation." *PLoS Pathogens* 17 (11): e1010017.

Kim, Kwang-Sun, Soohyun Lee, and Choong-Min Ryu. 2013. "Interspecific Bacterial Sensing through Airborne Signals Modulates Locomotion and Drug Resistance." *Nature Communications* 4: 1809.

Lamichhane, Jay Ram, Antoine Messéan, and Cindy E. Morris. 2015. "Insights into Epidemiology and Control of Diseases of Annual Plants Caused by the Pseudomonas Syringae Species Complex." *Journal of General Plant Pathology: JGPP* 81 (5): 331–50.

Mazo-Molina, Carolina, Samantha Mainiero, Sarah R. Hind, Christine M. Kraus, Mishi Vachev, Felicia Maviane-Macia, Magdalen Lindeberg, et al. 2019. "The Ptr1 Locus of Solanum Lycopersicoides Confers Resistance to Race 1 Strains of Pseudomonas Syringae Pv. Tomato and to Ralstonia Pseudosolanacearum by Recognizing the Type III Effectors AvrRpt2 and RipBN." *Molecular Plant-Microbe Interactions: MPMI* 32 (8): 949–60.

Molina-Santiago, Carlos, Abdelali Daddaoua, Sandy Fillet, Estrella Duque, and Juan-Luis Ramos. 2014. "Interspecies Signalling: Pseudomonas Putida Efflux Pump TtgGHI Is Activated by Indole to Increase Antibiotic Resistance." *Environmental Microbiology* 16 (5): 1267–81.

Morris, Cindy E., Caroline L. Monteil, and Odile Berge. 2013. "The Life History of Pseudomonas Syringae: Linking Agriculture to Earth System Processes." *Annual Review of Phytopathology* 51 (May): 85–104.

Mysore, Kirankumar S., and Choong-Min Ryu. 2004. "Nonhost Resistance: How Much Do We Know?" *Trends in Plant Science* 9 (2): 97–104.

Phillips, A. Z., T. Wheeler, J. Woodward, and R. S. Bart. 2018. "Pseudomonas Syringae Pathogen Causes Foliar Disease of Upland Cotton in Texas." *Plant Disease* 102 (6): 1171–1171.

Phillips, Anne Z. 2018. "Phylogenetic and Genomic Characterization of the Host-Pathogen Arms Race Between Bacterial Pathogens and Gossypium Hirsutum." Edited by Rebecca Bart. Plant & Microbial Biosciences, Washington University in St. Louis.

Pitblado, R. E., and E. A. Kerr. 1980. "Resistance to Bacterial Speck (Pseudomonas Tomato) in Tomato." *Acta Horticulturae*, no. 100 (December): 379–82.

Scholz-Schroeder, B. K., M. L. Hutchison, I. Grgurina, and D. C. Gross. 2001. "The Contribution of Syringopeptin and Syringomycin to Virulence of Pseudomonas Syringae Pv. Syringae Strain B301D on the Basis of SypA and SyrB1 Biosynthesis Mutant Analysis." *Molecular Plant-Microbe Interactions: MPMI* 14 (3): 336–48.

Tyagi, Priyanka, Michael A. Gore, Daryl T. Bowman, B. Todd Campbell, Joshua A. Udall, and Vasu Kuraparthy. 2014. "Genetic Diversity and Population Structure in the US Upland Cotton (Gossypium Hirsutum L.)." *TAG. Theoretical and Applied Genetics. Theoretische Und Angewandte Genetik* 127 (2): 283–95.

Vinatzer, Boris A., Gail M. Teitzel, Min-Woo Lee, Joanna Jelenska, Sara Hotton, Keke Fairfax, Jenny Jenrette, and Jean T. Greenberg. 2006. "The Type III Effector Repertoire of Pseudomonas Syringae Pv. Syringae B728a and Its Role in Survival and Disease on Host and Non-Host Plants." *Molecular Microbiology* 62 (1): 26–44.

Wei, Chia-Fong, Brian H. Kvitko, Rena Shimizu, Emerson Crabill, James R. Alfano, Nai-Chun Lin, Gregory B. Martin, Hsiou-Chen Huang, and Alan Collmer. 2007. "A Pseudomonas Syringae Pv. Tomato DC3000 Mutant Lacking the Type III Effector HopQ1-1 Is Able to Cause Disease in the Model Plant Nicotiana Benthamiana." *The Plant Journal: For Cell and Molecular Biology* 51 (1): 32–46.

Weise, Teresa, Marco Kai, Anja Gummesson, Armin Troeger, Stephan von Reuß, Silvia Piepenborn, Francine Kosterka, et al. 2012. "Volatile Organic Compounds Produced by the Phytopathogenic Bacterium Xanthomonas Campestris Pv. Vesicatoria 85-10." *Beilstein Journal of Organic Chemistry* 8 (April): 579–96.

Westhoff, Sanne, Gilles P. van Wezel, and Daniel E. Rozen. 2017. “Distance-Dependent Danger Responses in Bacteria.” *Current Opinion in Microbiology* 36 (April): 95–101.

Appendix 1: Supplemental figures for *Pseudomonas syringae* strains isolated from cotton, migrate towards *Xanthomonas* strains in vitro and this response is negatively regulated by iron.

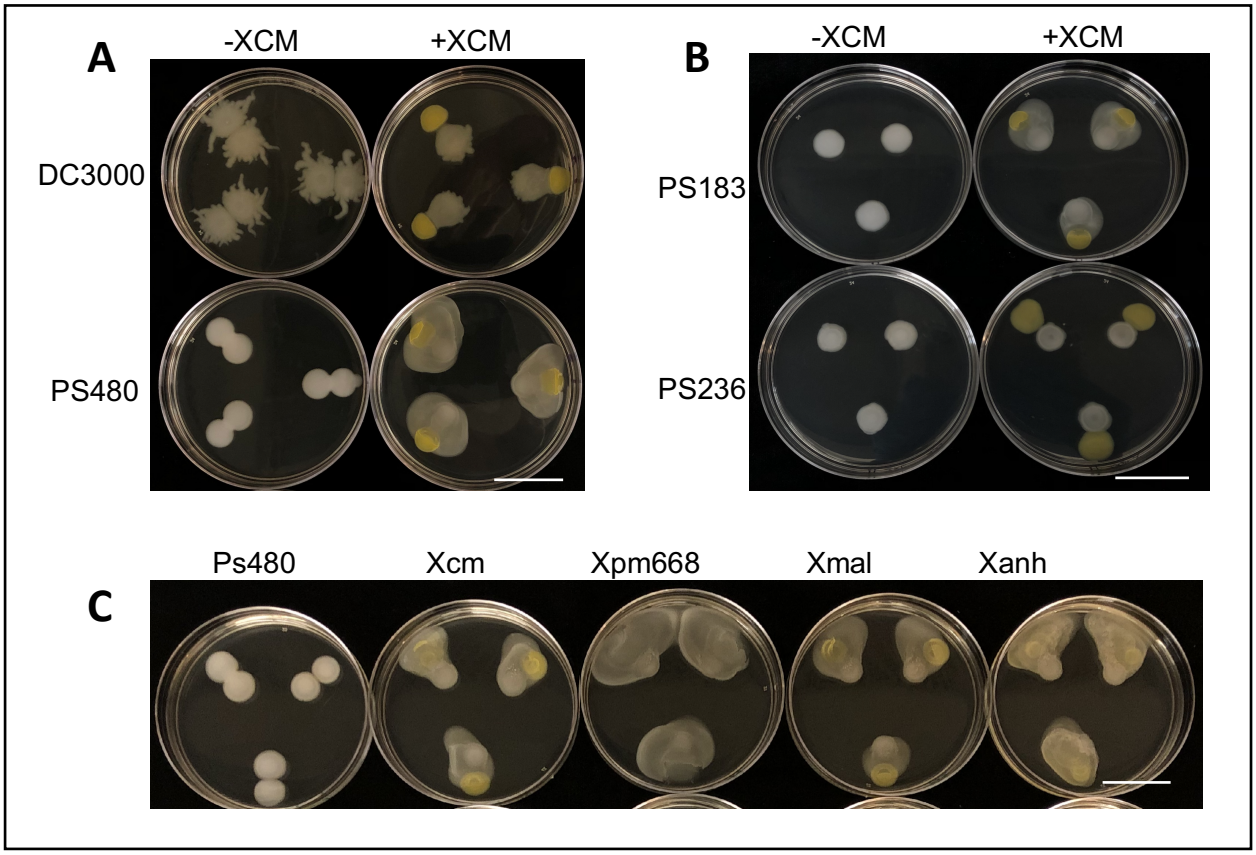

Fig S2.1. Cotton isolates Ps183 and Ps480 migrate toward Xcm, while cotton isolate Ps236 and model strain DC3000 do not. A) Ps480 (bottom) and DC3000 (top) cultured with (right) and without (left) Xcm on NYG soft agar (0.4% agar). B) Ps183 and Ps236 on NYG soft agar (0.4%) cultured with (right) and without (left) Xcm. C) Ps480 cultured with Xcm, Xpm668 (BLX38), Xmal (BLX722), and Xanh (BLX791). Bacteria were cultured 5 days at 30°C. 3cm scale.

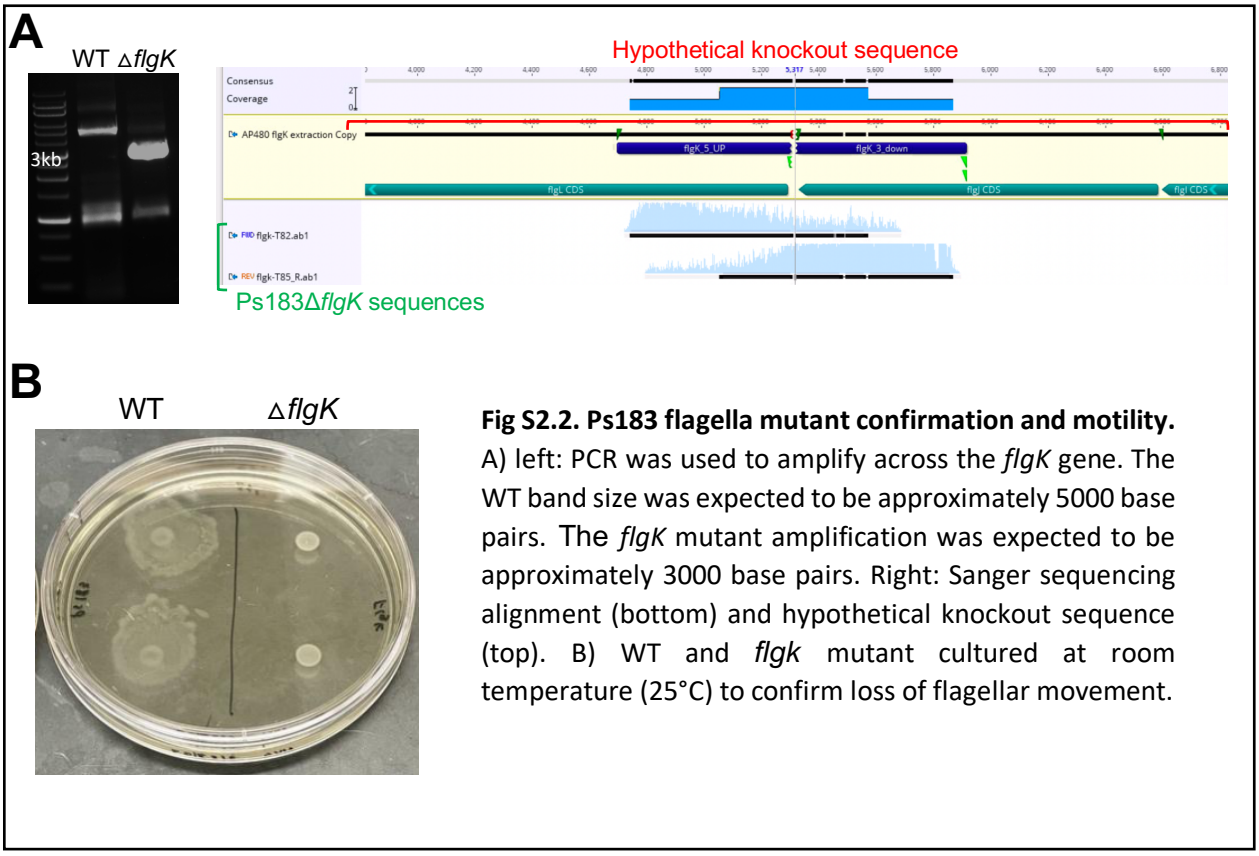

Fig S2.2. Ps183 flagella mutant confirmation and motility. A) left: PCR was used to amplify across the *flgK* gene. The WT band size was expected to be approximately 5000 base pairs. The *flgK* mutant amplification was expected to be approximately 3000 base pairs. Right: Sanger sequencing alignment (bottom) and hypothetical knockout sequence (top). B) WT and *flgk* mutant cultured at room temperature (25°C) to confirm loss of flagellar movement.

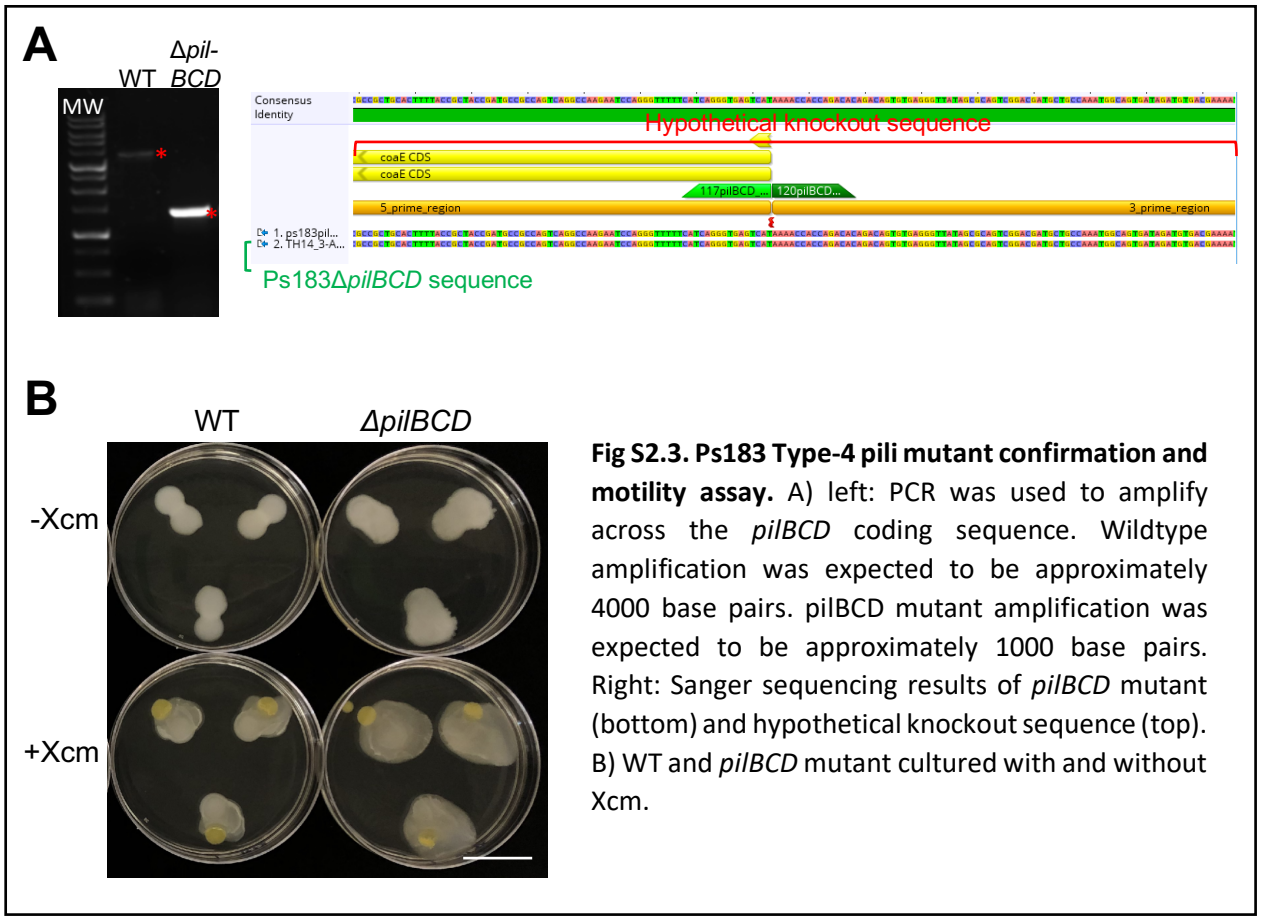

Fig S2.3. Ps183 Type-4 pili mutant confirmation and motility assay. A) left: PCR was used to amplify across the *pilBCD* coding sequence. Wildtype amplification was expected to be approximately 4000 base pairs. pilBCD mutant amplification was expected to be approximately 1000 base pairs. Right: Sanger sequencing results of *pilBCD* mutant (bottom) and hypothetical knockout sequence (top). B) WT and *pilBCD* mutant cultured with and without Xcm.

A

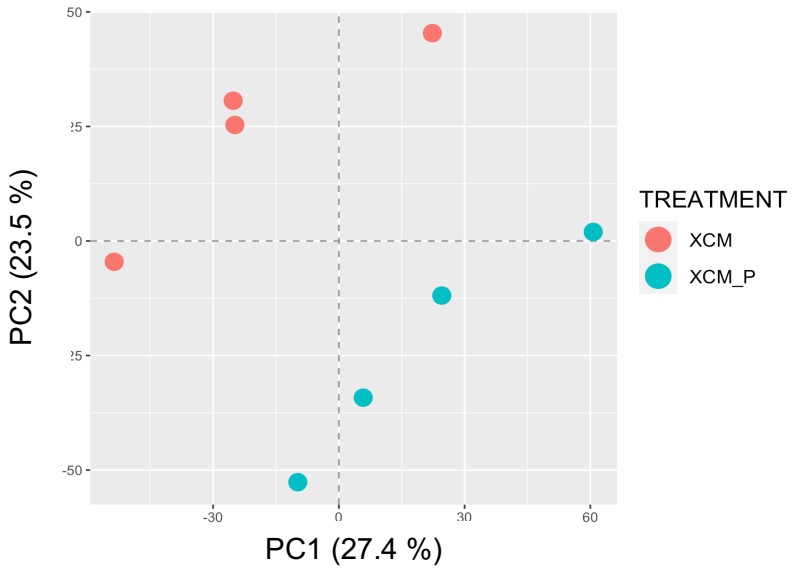

B

Annotated upregulated genes in Xcm		
Name	Log_2 fold change	function
protein kinase UbiB	1.20892768	First monooxygenase step in CoQ biosynthesis
Blue-light-activated protein_1	1.1468644	BLAST: putative two-component system response regulator
O-acetyl-ADP-ribose deacetylase (ymbD)	1.08082932	Deacetylates O-acetyl-ADP ribose to yield ADP-ribose and free acetate
Response regulator receiver protein CpdR_2	1.02916356	Cell cycle progression
Response regulator MprA_1	1.0032123	Negative regulator of the multidrug operon emrAB in E. coli
Murein DD-endopeptidase MepH_1	-1.1262201	Cell wall hydrolase
Flagellar basal body rod protein FlgB	-1.2209681	Flagellar basal body rod protein

Fig. S2.4 Xcm principal component analysis and upregulated genes when exposed to Ps183. A) Principal component analysis (PCA) of Xcm RNA-seq data. Each dot represents individual replicates of Xcm with or without Ps183. Reads were mapped to the Xcm genome. B) Table of upregulated Xcm genes with annotations. Putative functions are proposed based on NCBI BLAST analysis.

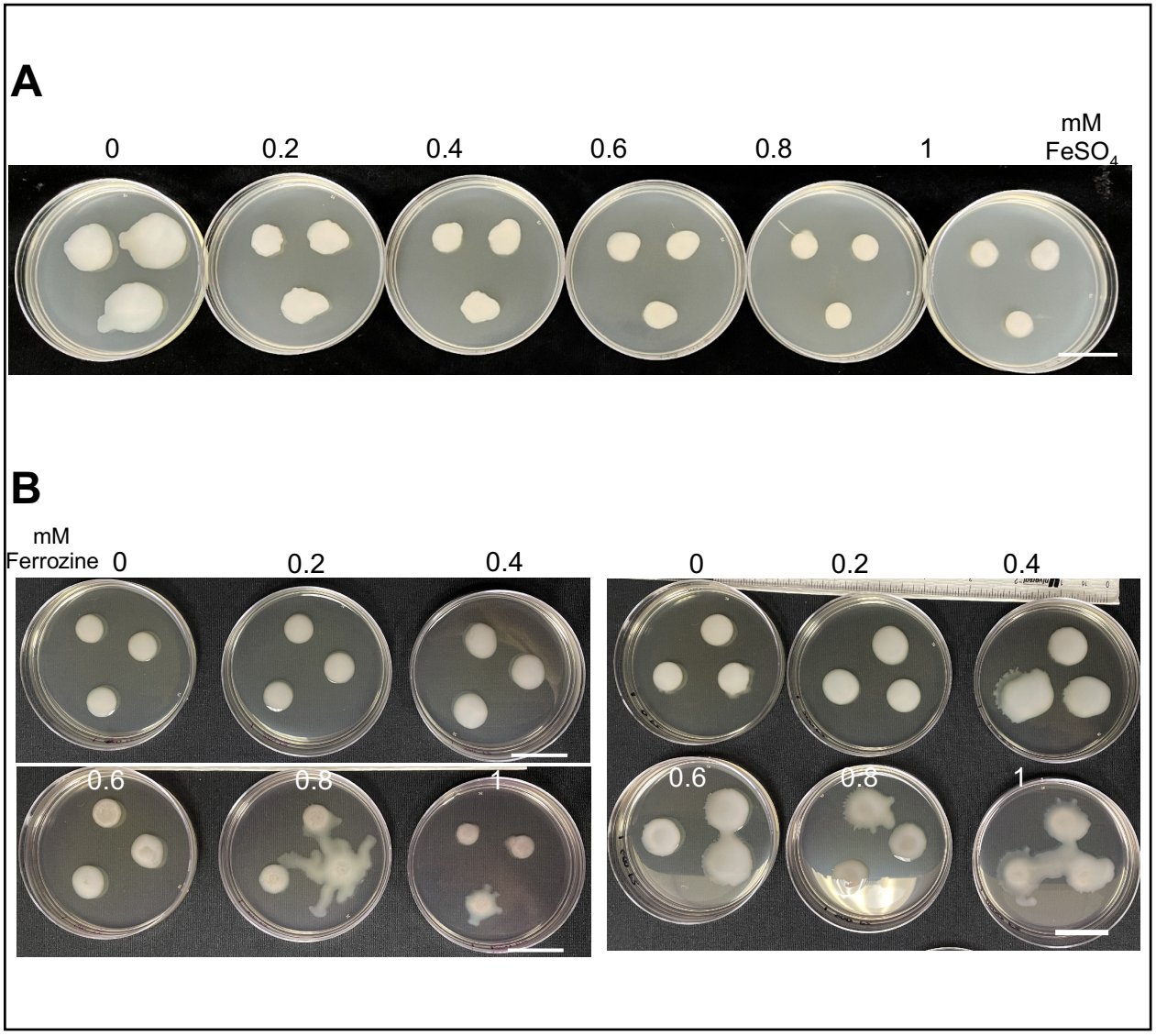

Fig S2.5. Additional iron tests. A) Ps183 was cultured on KB media with soft agar (0.4%) plates with increasing concentrations of $FeSO_4$. B) Ps183 was cultured on NYG soft agar (0.4%) with increasing concentrations of ferrozine. Left and right images represent two separate replicates. Bacteria were cultured 5 days at 30°C. 3cm scale.

Strain	Strain Name and ID	Location	Variety	Year	Sequencing
Ps183	Psuedomonas 444; BLO183	Donley Co, TX	NEXGEN 3406B2XF	2016	Nanopore and Illumina; Prokka annotation
Ps236	*P. syringae* ATCC 51506; BLO179	Lubbock, TX	---	1994	Nanopore and Illumina; Prokka annotation
Ps480	Pseudomonas 480; BLO187	Plains, TX	FM2007-GLT	2015	PacBio; Prokka annotation
Xcm	Xcm Fm2007-GLT; BLX910	Plains, TX	FM2007-GLT	2015	Illumina; Kbase annotation

Table S2.1. Strains used in this study.

Strain	# Raw Reads	Mean Read Length (bp)	Contig Type	Nanopore Reads	Nanopore Coverage	Contig Length (bp)	Illumina Coverage
Ps183	228,000	14,590	Chromosome	56,234	149.16	6,087,715	135
Ps236	244,313	8,474	Chromosome	20,607	48	5,936,430	141
-	-	-	Plasmid	164	46.37	67,923	132
Ps480	31,554	18,652	Chromosome	-	-	5,965,816	--
-	-	-	Plasmid	-	-	68,280	--

Table S2.2: Genome assembly statistics of *P. syringae* cotton pathogens. All genomes were sequenced with nanopore technology, assembled with Canu, polished with Nanopolish, circularized, and further polished with Illumina reads using Pilon, except Ps480, which was sequenced using PacBio technology, assembled with Falcon, polished with Quiver, and circularized.

Table S2.3 – Ps183 day 3 upregulated differentially expressed genes.

Name	Log_2 fold change	FDR p-value	BLAST/function
pseudo_prokka_03743	3.13314371	5.08E-66	protein of unknown function (DUF3309)
pseudo_prokka_03019	3.03435777	8.26E-06	hypothetical protein
pseudo_prokka_01284	2.73495745	6.70E-50	hypothetical protein / effector protein
pseudo_prokka_03756	2.67127416	6.70E-50	PepSY domain-containing protein
bfr	2.64244197	5.28E-41	bacterioferritin
pseudo_prokka_04427	2.4089869	2.58E-48	bacterioferritin
pseudo_prokka_04798	2.38921569	0.01070145	IS5/IS1182 family transposase
algD	2.30910315	1.58E-48	GDP-mannose 6-deyhdrogenase
pseudo_prokka_00495	2.20319659	0.0423638	hypothetical protein
pseudo_prokka_03106	2.16086123	1.98E-17	hypothetical protein
pseudo_prokka_02479	2.09171051	5.57E-12	hypothetical protein / lipoprotein
gcvH-2	2.03782164	1.58E-33	glycine cleavage system H protein
pseudo_prokka_05058	2.00522684	3.57E-12	hypothetical protein
pseudo_prokka_01593	1.99932692	0.000636	site-specific integrase
pseudo_prokka_01545	1.94964652	2.43E-34	ferritin-like domain-containing protein
pseudo_prokka_03700	1.86680947	1.31E-20	hypothetical protein
rpmE-2	1.86336743	3.24E-22	50S ribosomal protein L31
pseudo_prokka_02442	1.81014244	1.10E-31	hypothetical protein
csbD	1.80503024	2.25E-17	CsbD-like proteinral stress response protein
pseudo_prokka_04207	1.78060628	5.10E-18	pLDc N-terminal domain-containing protein
aspA	1.77539509	3.64E-30	aspartate ammonia-lyase
pseudo_prokka_02077	1.76857814	7.14E-22	lipoprotein
pseudo_prokka_00098	1.74319986	1.57E-23	helix-turn-helix domain-containing protein
pseudo_prokka_03020	1.72534413	4.32E-08	hypothetical protein DA456_03705
pseudo_prokka_03742	1.71010744	3.25E-21	DUF2784 domain-containing protein
pseudo_prokka_01222	1.70761236	2.02E-27	hypothetical protein CCL23_12580
pseudo_prokka_05128	1.68132433	1.85E-29	GlsB/YeaQ/YmgE family stress response membrane protein
yraA	1.67376425	2.36E-28	type 1 glutamine amidotransferase
pseudo_prokka_04938	1.66420261	0.00577043	TraR/DksA C4-type zinc finger protein
pseudo_prokka_02969	1.66187832	9.05E-21	DUF883 family protein
ppiC-1	1.65851049	3.26E-24	peptidylprolyl isomerase
pseudo_prokka_01909	1.65314886	8.94E-12	pLDc N-terminal domain-containing protein
pseudo_prokka_03712	1.64536493	4.65E-08	hypothetical protein
pseudo_prokka_01830	1.63879921	8.81E-22	membrane protein
pseudo_prokka_01536	1.63705877	2.80E-19	general stress protein
pseudo_prokka_03502	1.62402113	7.83E-20	Yqcl/YcgG family protein
pseudo_prokka_02964	1.61823345	7.44E-09	hypothetical protein PssSM_3057
pseudo_prokka_01831	1.58317144	1.53E-28	sorbosone dehydrogenase family protein
pseudo_prokka_04153	1.57833281	5.68E-23	BON domain-containing protein
pseudo_prokka_03321	1.56849034	2.14E-11	multidrug/biocide efflux PACE transporter
pseudo_prokka_03224	1.56648649	1.32E-21	hypothetical protein ALQ81_05182
sodB	1.56430356	9.39E-26	superoxide dismutase [Fe]
pseudo_prokka_04491	1.55810052	9.17E-26	bacterioferritin
algK	1.54533862	5.08E-21	alginate biosynthesis TPR repeat lipoprotein algK
pseudo_prokka_05074	1.5318972	3.29E-13	hypothetical protein
ilvA-2_1	1.52439621	2.36E-28	L-threonine ammonia-lyase
pseudo_prokka_00253	1.5242293	2.62E-20	hypothetical protein
rpsT	1.5150907	9.63E-15	30S ribosomal protein S20
pseudo_prokka_01772	1.50834582	5.17E-08	MarR family transcriptional regulator

Table S2.3 continued

Name	Log_2 fold change	FDR p-value	BLAST/function
infA	1.49183601	3.02E-14	translation initation factor IF-1
pseudo_prokka_04619	1.48862503	0.00360343	hypothetical protein
pseudo_prokka_05178	1.46895054	1.53E-19	hypothetical protein
pseudo_prokka_04264	1.45431836	2.76E-20	xanthine dehydrogenase family protein molybdopterin-binding subunit
pseudo_prokka_02647	1.45132499	2.59E-17	helix-turn-helix transcriptional regulator
pseudo_prokka_03017	1.41866354	8.91E-09	hypothetical protein DA456_03720
pseudo_prokka_03795	1.40528657	6.02E-07	DUF3757 domain-containing protein
pseudo_prokka_00748	1.40443656	2.66E-07	hypothetical protein
pseudo_prokka_02724	1.38776485	3.42E-19	hypothetical protein
pseudo_prokka_05195	1.38392173	1.39E-19	DeoR family transcriptional regulator
pseudo_prokka_01164	1.38195983	8.21E-20	alginate biosynthesis protein alg44
pseudo_prokka_05059	1.37877689	9.05E-12	polymorphic toxin type 46 domain-containing protein
pseudo_prokka_03174	1.36776206	2.32E-12	PepSY domain-containing protein
dehII_1	1.36655779	1.43E-21	haloacid dehalogenase type II
pseudo_prokka_03749	1.36555093	3.33E-20	uncharacterized protein ALO80_04383
katE	1.36547358	1.11E-22	catalase
rnk	1.36285088	4.22E-13	nucleoside diphosphate kinase regulator
pseudo_prokka_04785	1.36211242	0.00011535	hypothetical protein / RHS repeat protein
rnhA	1.36133556	3.71E-24	ribonuclease HI
pseudo_prokka_05057	1.35594334	0.00034072	hypothetical protein PsyrH_25510
cynT	1.33096708	2.41E-18	carbonic anhydrase
pseudo_prokka_02225	1.33028686	2.05E-06	cold-shock protein
pseudo_prokka_01952	1.3231616	0.00073448	hypothetical protein
pseudo_prokka_01187	1.31727574	3.29E-15	HU family DNA-binding protein
pseudo_prokka_00794	1.31276216	7.59E-14	hypothetical protein
rpmG	1.3077753	0.0224757	50S ribosomal protein L33
pseudo_prokka_03814	1.30465144	1.00E-11	hypothetical protein
pseudo_prokka_04786	1.30203922	6.47E-14	SMI1/KNR4 family protein
pseudo_prokka_01165	1.29815023	1.39E-18	mannuronan synthase
pseudo_prokka_05181	1.29080567	3.83E-16	DUF4142 domain-containing protein
pseudo_prokka_01905	1.27475051	2.58E-12	DUF3509 domain-containg protein
algI	1.26610593	3.52E-15	MBOAT family protein
capB	1.2522877	2.53E-08	cold-shock protein
pseudo_prokka_00768	1.24697115	0.00012134	hypothetical protein
pseudo_prokka_00093	1.24355579	0.00245731	hypothetical protein CCL18_08585
pseudo_prokka_00941	1.23443824	3.99E-17	zinc ribbon domain-containing protein YjdM
pseudo_prokka_04087	1.21380733	3.12E-17	16S rRNA (cytosine(1402)-N(4))-methyltransferase RsmH
pseudo_prokka_03657	1.21300719	1.84E-10	uncharacterized protein ALO80_03883
pseudo_prokka_01137	1.20523753	3.05E-12	HPF/RaiA family ribosome-associated protein
pseudo_prokka_03211	1.177237	2.18E-22	Ku protein
pseudo_prokka_04859	1.17632008	1.52E-05	hypothetical protein
pseudo_prokka_00117	1.17039037	0.00038147	hypothetical protein
pseudo_prokka_02155	1.15308096	8.69E-08	ribonuclease E activity regulator RraA
pseudo_prokka_00081	1.15261891	0.0270045	sulfur starvation response protein OscA
pseudo_prokka_00489	1.15064355	2.38E-11	Imm5 family immunity protein
pseudo_prokka_04889	1.15052641	2.79E-09	hypothetical protein
pseudo_prokka_03018	1.13917244	3.62E-09	DUF637 domain-containing protein
yjcH	1.13539348	1.94E-12	DUF485 domain-containing protein
pseudo_prokka_05056	1.13478648	1.33E-05	hypothetical protein
pseudo_prokka_04913	1.13216362	0.0008411	phage major tail tube protein

Table S2.3 continued

Name	Log_2 fold change	FDR p-value	BLAST/function
algJ	1.13023092	7.28E-13	alginate O-acetyltransferase
hyuE	1.12917839	1.43E-09	aspartate/glutamate racemase family protein
anr	1.12810814	1.33E-06	transcriptional activator protein Anr / fumarate/nitrate reduction transcriptional regulator Fnr
pseudo_prokka_01811	1.12766157	1.02E-10	hypothetical protein
pseudo_prokka_02055	1.12232455	1.36E-12	electron transfer flavoprotein-ubiquinone oxidoreductase
pseudo_prokka_00307	1.11851205	0.00024635	hypothetical protein
dgoK	1.11778058	5.59E-14	2-dehydro-3-deoxygealactonokinase
acnA	1.11648824	1.31E-16	aconitate hydratase AcnA
pseudo_prokka_02269	1.11415912	2.75E-08	hypothetical protein ALQ96_01777
pseudo_prokka_01036	1.10955202	1.23E-14	hypothetical protein DA456_14085
pseudo_prokka_02436	1.10201342	0.00090084	hypothetical protein
pseudo_prokka_04677	1.10120511	2.91E-12	putative cAMP-binding/CBS domain signal-transduction protein
pseudo_prokka_04265	1.10060088	1.33E-10	xanthine dehydrogenase family protein subunit M
pseudo_prokka_00252	1.09812695	2.36E-09	DUF1328 domain-containing protein
pseudo_prokka_02224	1.09529192	1.97E-11	I78 family peptidase inhibitor
pseudo_prokka_04290	1.09313968	1.08E-08	No Hits
pseudo_prokka_03304	1.08580139	5.35E-10	hypothetical protein / pyridine nucleotide-disulfide oxidoreductase
pseudo_prokka_00097	1.08563203	5.48E-09	AAA family ATPase
pseudo_prokka_03004	1.07475332	0.00078426	ISPssy, transposase
pseudo_prokka_03006	1.07462051	0.00017238	hypothetical protein
pseudo_prokka_00818	1.07327587	1.30E-10	hypothetical protein
algE	1.0719919	4.61E-13	alginate biosynthesis protein algE
pseudo_prokka_04053	1.05995366	3.66E-12	phage T7 F-exclusion suppressor FxsA-like protein / membrane protein FxsA
pseudo_prokka_00163	1.05871326	8.58E-08	ATP-dependent zinc protease
pseudo_prokka_01594	1.05848899	3.43E-08	hypothetical protein
pseudo_prokka_04086	1.05507405	3.13E-12	cell division protein FtsL
fdH_2	1.05274874	2.23E-11	glutathione-dependent formaldehyde dehydrogenase
htpX_1	1.05015164	1.62E-11	protease HtpX
pseudo_prokka_02331	1.04883658	1.07E-14	SCO family protein
pseudo_prokka_00237	1.04423227	4.79E-09	DUF2388 domain-containing protein
pseudo_prokka_01535	1.04016702	4.48E-10	No Hits
pseudo_prokka_01912	1.03946064	8.49E-10	hypothetical protein
pseudo_prokka_04085	1.03538657	2.66E-12	peptidoglycan glycosyltransferase / cell division protein
pseudo_prokka_03172	1.03245644	1.44E-10	response regulator transcription factor
pseudo_prokka_00152	1.0308515	6.49E-12	FAD-binding oxidoreductase
pseudo_prokka_04019	1.02700837	0.00073305	type VI secretion system amidase effector protein Tae4
pseudo_prokka_00637	1.02659665	5.17E-12	3-oxoacyl-ACP reductase
trpG	1.02388622	1.84E-11	aminodeoxychorismate/anthranilate synthase component II
hrcT	1.01309484	0.02191764	type III secretion system export apparatus subunit SctT
pseudo_prokka_03016	1.01290445	2.46E-07	hypothetical protein / filamentous hemagglutinin N-terminal domain-containing protein
pseudo_prokka_02488	1.01159409	4.10E-11	SDR family oxidoreductase
pseudo_prokka_02369	1.01076047	0.00014794	hypothetical protein
pseudo_prokka_00351	1.01060814	7.80E-11	DUF3455 domain-containing protein
galE	1.00925144	3.78E-10	UDP-glucose 4-epimerase GalE
pseudo_prokka_01624	1.00249684	5.43E-12	hybrid sensor histidine kinase/response regulator

Table S2.4 – Ps236 day 3 upregulated differentially expressed genes.

Name	Log2 fold change	FDR.p.value	BLAST / FUNCTION
pseudo_prokka_03812	3.22584532	0	PepSY domain-containing protein
pseudo_prokka_05266	2.47006969	6.69E-06	conjugal transfer protein
pseudo_prokka_04066	2.33625424	0.02497127	type VI secretion system amidase immunity protein Tai4
pseudo_prokka_01164	2.04387192	0	effector protein
ggt_2	1.98788016	0	gamma-glutamyl transpeptidase
pseudo_prokka_00367	1.95761275	0	hypothetical protein
virB1	1.91620953	0.0002035	virulence plasmid transcriptional regulator
topB_3	1.85562045	4.98E-05	DNA topoisomerase 3
fni	1.84964204	8.90E-06	isopentenyl diphosphate
pseudo_prokka_03694	1.83246998	4.26E-05	hypothetical protein
pseudo_prokka_05279	1.77682716	2.38E-06	hypothetical protein
cynT	1.71880019	0	carbonic anhydrase
pseudo_prokka_05269	1.64527654	0.0008906	conjugal transfer protein
pseudo_prokka_04996	1.58091328	0.007892	phage terminase small subunit
pseudo_prokka_02723	1.53993759	4.42E-14	methyl-accepting chemotaxis protein
pseudo_prokka_01388	1.47090822	1.12E-11	phage terminase small subunit
pseudo_prokka_05275	1.45450446	0.0003941	TrbM/KikA/MpfK family conjugal transfer protein
pseudo_prokka_05260	1.44480195	0.009308	conjugal transfer protein
pseudo_prokka_05271	1.43438166	0.0006983	hypothetical protein
pseudo_prokka_00297	1.42571979	1.23E-13	sulfate transporter protein
pseudo_prokka_01557	1.41784212	1.66E-09	type VI secretion system tube protein Hcp
pseudo_prokka_01492	1.41275465	1.65E-05	hypothetical protein
pseudo_prokka_05283	1.3991661	0.00146	relaxase/mobilization nuclease domain-contain protein
pseudo_prokka_04699	1.37326617	2.60E-08	integrase
dppC_1	1.37003589	8.68E-05	dipeptide transport system permease
pseudo_prokka_02214	1.36428037	0.0007004	hypothetical protein
pseudo_prokka_02757	1.33425974	2.30E-05	glucarate dehydratase family protein
pseudo_prokka_05280	1.32103611	0.0004163	hypothetical protein
pseudo_prokka_00992	1.31081232	1.51E-05	glycosyltransferase family 1 protein
pseudo_prokka_01010	1.30517013	2.24E-05	cellulose biosynthesis cyclic di-GMP binding regulatory protein bcsB
aspA	1.29401805	4.49E-10	aspartate lyase
pseudo_prokka_02266	1.27683816	0.0006612	polymorphic toxin type 15 domain-containing protein
phnG	1.26698221	0.02216194	Phosphonate C-P lyase system protein
pseudo_prokka_04855	1.25723006	0.0001348	SMI1/KNR4 family protein
pseudo_prokka_02719	1.25714513	0.001509	ABC transporter substrate-binding protein
pseudo_prokka_05270	1.25700537	0.001756	P-type DNA transferase ATPase VirB11
phaG-2	1.25455965	0.002473	(R)-3-hydroxydecanoyl-ACP:CoA transacylase
exsB	1.2329835	4.72E-07	exosporium protein
pseudo_prokka_01832	1.22978427	0.007626	hypothetical protein
pseudo_prokka_04237	1.2130392	0.03565194	SGNH/GDSL hydrolase family protein
pseudo_prokka_05231	1.20175064	0.005248	lycopene beta-cyclase CrtY
pseudo_prokka_05215	1.1711861	0.003794	replication initiation protein
pseudo_prokka_05254	1.16653516	3.79E-05	helix-turn-helix transcriptional regulator
pseudo_prokka_04698	1.16481663	1.24E-06	site-specific integrase
pseudo_prokka_01556	1.15403416	2.24E-08	DUF2778 domain-containing protein
greA_2	1.13493648	2.54E-05	transcription elongation facor
pseudo_prokka_02273	1.13399814	0.04039059	DUF1289 domain-containing protein
pseudo_prokka_02186	1.12061523	0.0434796	hypothetical protein
mucB	1.11498994	2.43E-07	negative regulator for alginate biosynthesis
galM_1	1.11112699	0.00164	galactomutarotase
pseudo_prokka_05017	1.1107105	0.002842	sce7726 family protein
pseudo_prokka_02196	1.10346156	0.0001735	hypothetical protein
dapB	1.0927785	9.43E-07	dihydrodipicolinate reductase
pseudo_prokka_00031	1.08514063	1.90E-05	hypothetical protein
galE	1.06897544	5.52E-05	UDP-glucose 4-epimerase
pseudo_prokka_00028	1.06748348	4.39E-06	Yd repeat protein
pseudo_prokka_04850	1.04963217	0.01009685	hypothetical protein
pseudo_prokka_03848	1.03020473	0.01158613	DUF3757 domain-containing protein
pseudo_prokka_05253	1.0271268	0.0001084	hypothetical protein
pseudo_prokka_04974	1.02202464	0.0003337	hypothetical protein
pseudo_prokka_02003	1.00850796	3.31E-05	hypothetical protein

Table S2.5 – Xcm differentially expressed genes with annotations.

Functions of Genes with Annotations		
Name	Log^2 fold change	function
protein kinase UbiB	1.20892768	First monooxygenase step in CoQ biosynthesis
Blue-light-activated protein_1	1.1468644	BLAST: putative two-component system response regulator [Xanthomonas campestris pv. vesicatoria str. 85-10]
O-acetyl-ADP-ribose deacetylase (ymbD)	1.08082932	Deacetylates O-acetyl-ADP ribose to yield ADP-ribose and free acetate
Response regulator receiver protein CpdR_2	1.02916356	Cell cycle progression
Response regulator MprA_1	1.0032123	Negative regulator of the multidrug operon emrAB in E. coli
Murein DD-endopeptidase MepH_1	-1.1262201	Cell wall hydrolase
Flagellar basal body rod protein FlgB	-1.2209681	Flagellar basal body rod protein

GO.ID	Term Annotated	Significant	Expected	Fisher.weight01
Upregulated terms				
GO:0034645 cellular macromolecule biosynthetic process	132	8	2.04	0.00031
GO:0046394 carboxylic acid biosynthetic process	134	5	2.07	0.00038
GO:0044262 cellular carbohydrate metabolic process	26	4	0.40	0.00057
GO:0006826 iron ion transport	25	3	0.39	0.00620
GO:0016051 carbohydrate biosynthetic process	30	3	0.46	0.01038
GO:0019725 cellular homeostasis	32	3	0.50	0.01241
GO:0051252 regulation of RNA metabolic process	362	8	5.60	0.01476
Downregulated Terms				
GO:0006935 chemotaxis	86	39	5.51	7.800e-26
GO:0007165 signal transduction	242	44	15.50	7.200e-16
GO:0071973 bacterial-type flagellum-dependent cell ...	22	13	1.41	5.500e-11
GO:0009058 biosynthetic process	897	53	57.46	2.400e-05
GO:0006826 iron ion transport	25	8	1.60	1.000e-04
GO:0030030 cell projection organization	20	7	1.28	1.500e-04
GO:0009448 gamma-aminobutyric acid metabolic proces...	24	7	1.54	5.300e-04
GO:0006820 anion transport	116	7	7.43	1.050e-03
GO:0006996 organelle organization	28	7	1.79	1.450e-03
GO:0006760 folic acid-containing compound metabolic...	20	4	1.28	3.503e-02

Table S2.6. Ps183 GO Enrichment Analysis Results. Upregulated and downregulated GO results of Ps183+Xcm vs Ps183.

GO.ID	Term Annotated	Significant	Expected	Fisher.weight01
Upregulated Terms				
GO:0015074 DNA integration	22	2	0.14	0.0083
GO:0043648 dicarboxylic acid metabolic process	23	2	0.15	0.0091
GO:0009066 aspartate family amino acid metabolic proc	22	2	0.14	0.0121
GO:0006310 DNA recombination	44	2	0.28	0.0314
Downregulated Terms				
GO:0006935 Chemotaxis	86	11	1.03	1.20e-09
GO:0007165 signal transduction	242	12	2.91	1.00e-07
GO:0071973 bacterial-type flagellum-dependent cell ...	23	3	0.28	2.40e-03
GO:0006082 organic acid metabolic process	295	3	3.55	2.54e-02

Table S2.7. Ps236 GO Enrichment Analysis Results. Upregulated and downregulated GO results of Ps236+Xcm vs Ps236.

Appendix II: Supplemental figures for Assessment of Xcm and Ps in cotton and in the laboratory

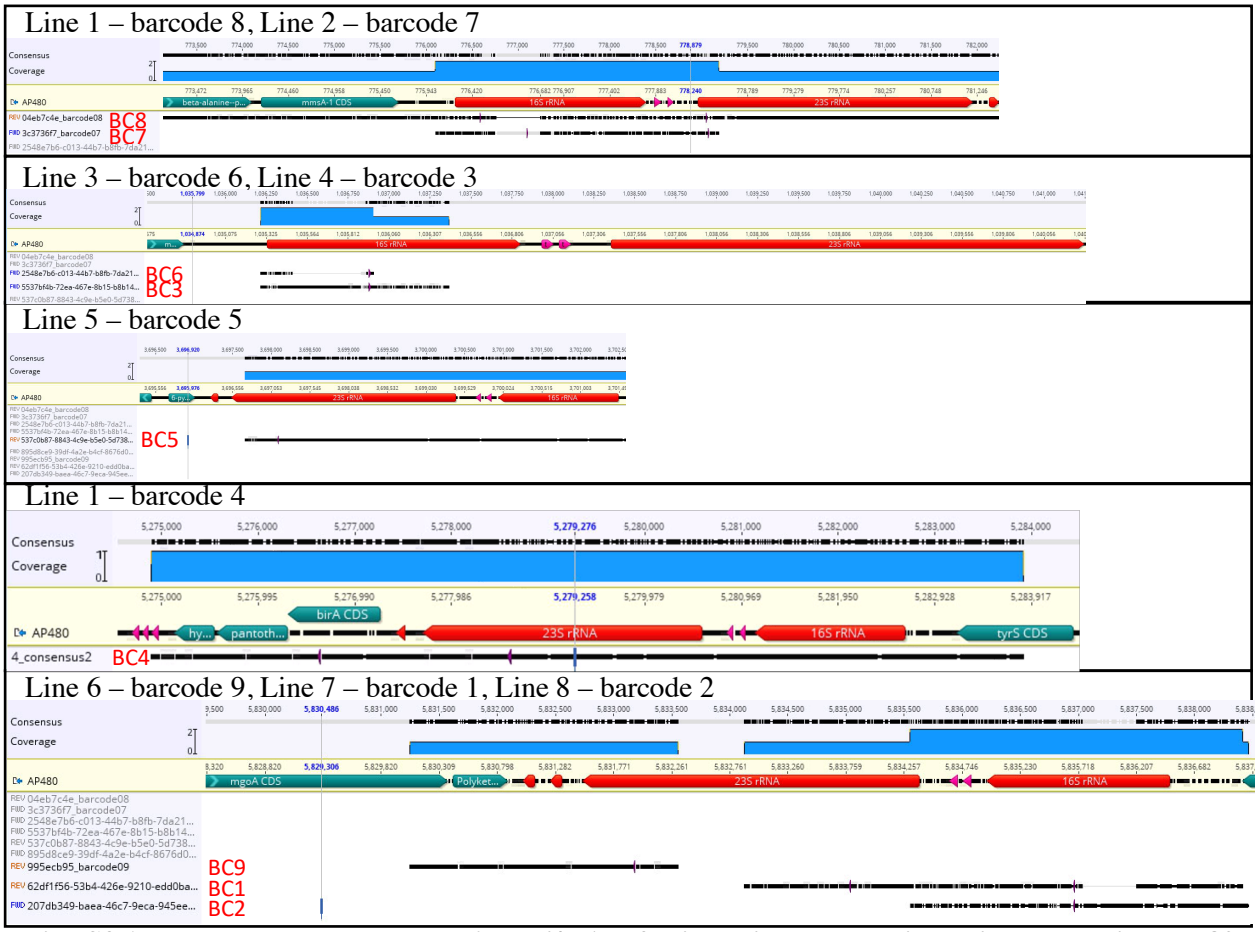

Fig. S3.1 – Nanopore EZ-Tn5 <R6Kyori/KAN-2> insertion sequencing alignment with Ps480 genome. Each panel is a screenshot of each barcode sequence (indicated as BC in red) mapped to Ps480 genome. The portion highlighted in light yellow represents the part of the genome that each sequence best mapped to. The black lines that fall beneath the genome sequence represent the entire barcode sequence from each mutant.

Fig. S3.2 – EZ-Tn5 <R6Kyori/KAN-2> alignment with Ps480 23S sequence. Top panel: alignment with EZ-Tn5 sequence (sequence 1) and Ps480 23S sequence. Bottom panel is zoomed in.

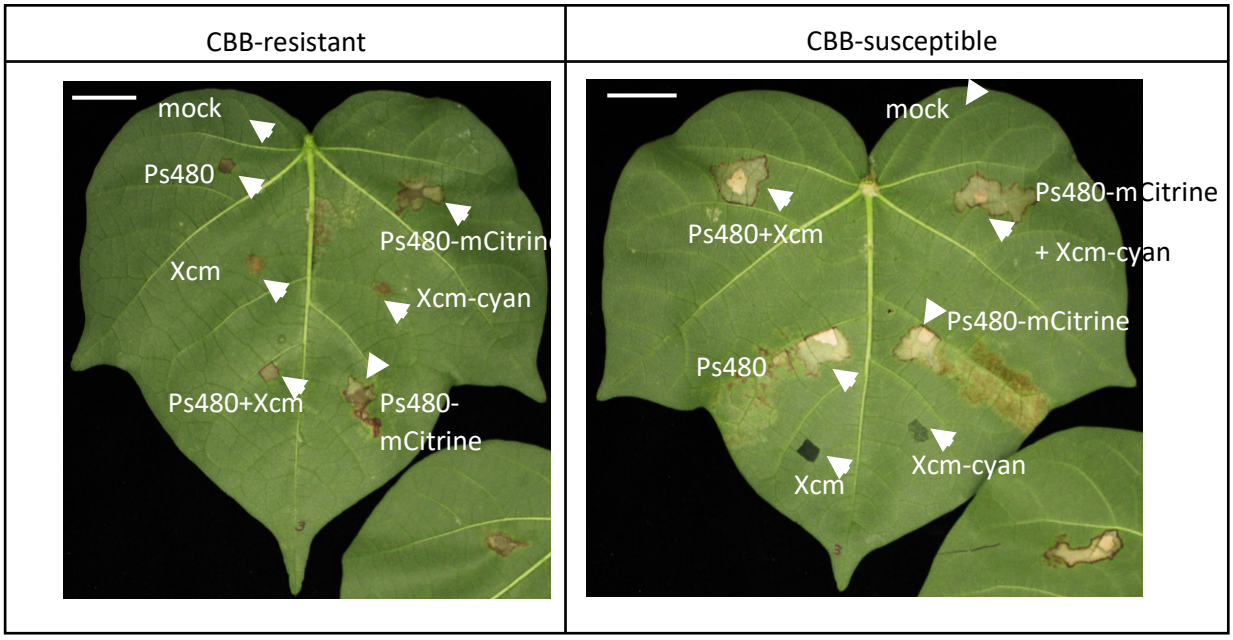

Fig. S3.3 – Symptoms of Ps480-mCitrine and Xcm-cyan. 2mm scale.

Strain ID	Strain Name	Added plasmids
BLO187	Ps480	none
BLE910	Xcm	none
TH6 / AP156	Ps480-mCitrine	pDGW4M-mCitrine
TH8/ AP159	Xcm-miCyan	pDGW4M-mCitrine
BLO402	Arthrobacter sp. UNCCL28	none
BLE416	E. Coli KEC569	pGP704-mini-Tn5-gus/kan
BLE94	E. Coli helper	none

Table S3.1 – List of strains used in this study.

[DNA]	Total colonies (estimate)	Efficiency (CFU/ng)
pHC60 – IncP plasmid		
10ng	867	87
100ng	3952	40
1000ng	5524	6
pDGW4M – IncQ plasmid		
10ng	84	8
100ng	641	6
1000ng	859	1

Table S3.2 – Transformation efficiency of Ps480.

Mutant	BLAST in Ps480 genome	NCBI BLAST top hit
1[a]	none	P. Syringae pv atrofaciens LMG5095; 99.54%
2[a]	none	P. Syringae pv atrofaciens LMG5095; 99.52%
3	none	Reporter vector pFAJ1819; 100%
4	Hypothetical CDS	
5	dadA/lrp	
6[b]	none	Cloning vector pFTarget3-Tn7; 100%
7	dadA/lrp	
8	tRNA-Ala/tRNA-ILW	
9	No CDS region	
10[b]	none	Cloning vector pFTarget3-Tn7; 100%

Table S3.3 – BLAST results of mini-Tn5 insertion mutants. Insertion locations were identified using single-colony PCR. Sequencing was BLASTed in Ps480 genome first. If no hits were identified, sequences were used to BLAST in NCBI.

Ps480 mutant	BLAST hit in Ps480 Genome
1st Transformation	
1	16S rRNA
2	16S rRNA
3	16S rRNA
4	23S rRNA
5	23S rRNA
6	23S rRNA
7	23S rRNA
8	23S rRNA
9	23S rRNA
2nd and 3rd transformation	
10	23S rRNA
11	23S rRNA
13	16S rRNA
14	scpA
15	23S rRNA

Table S3.4 – Blast results of EZ-Tn5 <R6Kyori/KAN-2> insertion mutants in Ps480 genome.